Investigation of the Impact of Dual-Lane Axle Spacing on Lateral Load Distribution

Final Report
May 2016

BRIDGE ENGINEERING CENTER

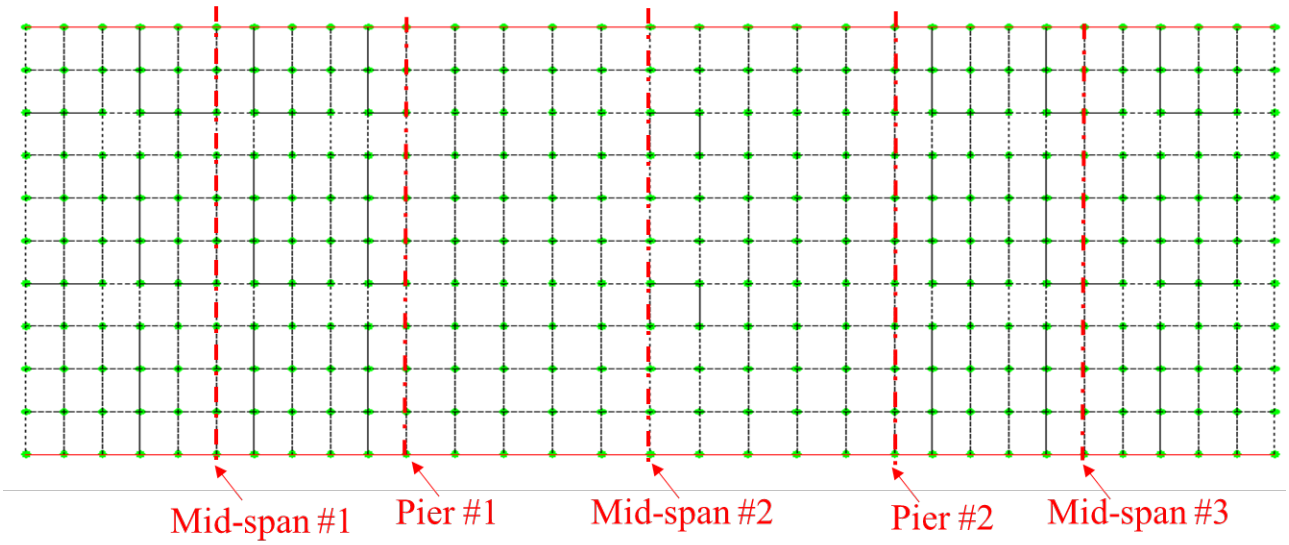

IOWA STATE UNIVERSITY
Institute for Transportation

Sponsored by
Federal Highway Administration
Iowa Department of Transportation
(InTrans Project 14-522)

About the Bridge Engineering Center

The mission of the Bridge Engineering Center (BEC) at Iowa State University is to conduct research on bridge technologies to help bridge designers/owners design, build, and maintain long-lasting bridges.

Disclaimer Notice

The contents of this report reflect the views of the authors, who are responsible for the facts and the accuracy of the information presented herein. The opinions, findings and conclusions expressed in this publication are those of the authors and not necessarily those of the sponsors.

The sponsors assume no liability for the contents or use of the information contained in this document. This report does not constitute a standard, specification, or regulation.

The sponsors do not endorse products or manufacturers. Trademarks or manufacturers' names appear in this report only because they are considered essential to the objective of the document.

Non-Discrimination Statement

Iowa State University does not discriminate on the basis of race, color, age, ethnicity, religion, national origin, pregnancy, sexual orientation, gender identity, genetic information, sex, marital status, disability, or status as a U.S. veteran. Inquiries regarding non-discrimination policies may be directed to Office of Equal Opportunity, Title IX/ADA Coordinator, and Affirmative Action Officer, 3350 Beardshear Hall, Ames, Iowa 50011, 515-294-7612, email eooffice@iastate.edu.

Iowa Department of Transportation Statements

Federal and state laws prohibit employment and/or public accommodation discrimination on the basis of age, color, creed, disability, gender identity, national origin, pregnancy, race, religion, sex, sexual orientation or veteran's status. If you believe you have been discriminated against, please contact the Iowa Civil Rights Commission at 800-457-4416 or Iowa Department of Transportation's affirmative action officer. If you need accommodations because of a disability to access the Iowa Department of Transportation's services, contact the agency's affirmative action officer at 800-262-0003.

The preparation of this report was financed in part through funds provided by the Iowa Department of Transportation through its "Second Revised Agreement for the Management of Research Conducted by Iowa State University for the Iowa Department of Transportation" and its amendments.

The opinions, findings, and conclusions expressed in this publication are those of the authors and not necessarily those of the Iowa Department of Transportation or the U.S. Department of Transportation Federal Highway Administration.

Technical Report Documentation Page

1. Report No.	2. Government Accession No.	3. Recipient's Catalog No.
InTrans Project 14-522		

4. Title	5. Report Date
Investigation of the Impact of Dual-Lane Axle Spacing on Lateral Load Distribution	May 2016
	6. Performing Organization Code

7. Author(s)	8. Performing Organization Report No.
Yaohua Deng and Brent M. Phares (orcid.org/0000-0003-0779-6112 and orcid.org/0000-0001-5894-4774)	InTrans Project 14-522

9. Performing Organization Name and Address	10. Work Unit No. (TRAIS)
Bridge Engineering Center Iowa State University 2711 South Loop Drive, Suite 4700 Ames, IA 50010-8664	**11. Contract or Grant No.**

12. Sponsoring Organization Name and Address	13. Type of Report and Period Covered
Iowa Highway Research Board Iowa Department of Transportation 800 Lincoln Way Ames, Iowa 50010	Final Report
	14. Sponsoring Agency Code SPR RB10-015

15. Supplementary Notes

Visit www.intrans.iastate.edu for color pdfs of this and other research reports.

16. Abstract

The spacing of adjacent wheel lines of dual-lane loads induces different lateral live load distributions on bridges, which cannot be determined using the current American Association of State Highway and Transportation Officials (AASHTO) Load and Resistance Factor Design (LRFD) or Load Factor Design (LFD) equations for vehicles with standard axle configurations. Current Iowa law requires dual-lane loads to meet a five-foot requirement, the adequacy of which needs to be verified. To improve the state policy and AASHTO code specifications, it is necessary to understand the actual effects of wheel-line spacing on lateral load distribution.

The main objective of this research was to investigate the impact of the wheel-line spacing of dual-lane loads on the lateral load distribution on bridges. To achieve this objective, a numerical evaluation using two-dimensional linear elastic finite element (FE) models was performed. For simulation purposes, 20 prestressed-concrete bridges, 20 steel bridges, and 20 slab bridges were randomly sampled from the Iowa bridge database. Based on the FE results, the load distribution factors (LDFs) of the concrete and steel bridges and the equivalent lengths of the slab bridges were derived.

To investigate the variations of LDFs, a total of 22 types of single-axle four-wheel-line dual-lane loads were taken into account with configurations consisting of combinations of various interior and exterior wheel-line spacing. The corresponding moment and shear LDFs and equivalent widths were also derived using the AASHTO equations and the adequacy of the Iowa DOT five-foot requirement was evaluated. Finally, the axle weight limits per lane for different dual-lane load types were further calculated and recommended to complement the current Iowa Department of Transportation (DOT) policy and AASHTO code specifications.

17. Key Words	18. Distribution Statement
axle weight limits—bridge loads—dual-lane axle spacing—lateral load distributions—load distribution factors—oversize permits—overweight permits	**No restrictions.**

19. Security Classification (of this report)	20. Security Classification (of this page)	21. No. of Pages	22. Price
Unclassified.	Unclassified.	85	NA

Form DOT F 1700.7 (8-72) **Reproduction of completed page authorized**

INVESTIGATION OF THE IMPACT OF DUAL-LANE AXLE SPACING ON LATERAL LOAD DISTRIBUTION

Final Report
May 2016

Principal Investigator
Brent M. Phares, Director
Bridge Engineering Center, Iowa State University

Co-Principal Investigator
Yaohua Deng, Research Scientist
Bridge Engineering Center, Iowa State University

Authors
Yaohua Deng and Brent M. Phares

Sponsored by
the Iowa Department of Transportation and
the Federal Highway Administration
(InTrans Project 14-522)

Preparation of this report was financed in part
through funds provided by the Iowa Department of Transportation
through its Research Management Agreement
with the Institute for Transportation

A report from
Bridge Engineering Center
Iowa State University
2711 South Loop Drive, Suite 4700
Ames, IA 50010-8664
Phone: 515-294-8103 / Fax: 515-294-0467
www.bec.iastate.edu

TABLE OF CONTENTS

LIST OF FIGURES

LIST OF TABLES

ACKNOWLEDGMENTS

The research team would like to acknowledge the Iowa Department of Transportation (DOT) for sponsoring this research and the Federal Highway Administration (FHWA) for state planning and research funding. In addition, the authors would like to acknowledge the support of the Iowa DOT Office of Bridges and Structures staff, who continually provide great insight, guidance, and motivation for practical and implementable research like this.

EXECUTIVE SUMMARY

With ever-increasing numbers and sizes of permitted vehicles and loads crossing Iowa's highways and bridges, it has become more and more common for oversized, overweight vehicles to travel on at least four wheel lines that are evenly or unevenly spaced. The spacing of the adjacent wheel lines of dual-lane loads induces different lateral live load distributions on bridges, which cannot be determined using the current American Association of State Highway and Transportation Officials (AASHTO) Load and Resistance Factor Design (LRFD) or Load Factor Design (LFD) equations, which are only applicable for vehicles with standard axle configurations.

Current Iowa law requires dual-lane loads to meet a five-foot requirement (i.e., interior wheel-line spacing no less than five feet) or the maximum weight of each axle cannot exceed 20,000 pounds (20 kips). It is necessary to understand the actual effects of wheel-line spacing on lateral load distribution, such that the five-foot requirement of the Iowa Department of Transportation (DOT) policy can be justified or improved and the applicability of the AASHTO LRFD or LFD equations to dual-lane loads can be determined.

The main objective of this research was to investigate the impact of the wheel-line spacing of dual-lane loads on the lateral load distribution on bridges. To achieve this objective, a numerical evaluation using finite element (FE) models was performed.

For simulation purposes, 20 prestressed-concrete bridges, 20 steel bridges, and 20 slab bridges were randomly sampled from the Iowa bridge database and used in the evaluation program. Two-dimensional linear elastic FE models of the selected bridges were established to derive the load distribution factors (LDFs) for the concrete and steel bridges and the equivalent lengths of the slab bridges. To study the variations of LDFs with respect to wheel-line spacing, 22 types of single-axle four-wheel-line dual-lane loads were taken into account with load configurations consisting of combinations of various interior and exterior wheel-line spacing.

Based on the FE results, a similar procedure was used to derive the moment LDFs for the 20 steel bridges and 20 concrete bridges, the shear LDFs for the 20 steel bridges, and the equivalent widths of the 20 slab bridges. The moment and shear LDFs were determined based on the internal forces in girders at critical cross-sections. The equivalent widths of the slab bridges were calculated based on the strain distributions in the deck at critical bridge cross-sections. For comparison purposes, the corresponding moment and shear LDFs and equivalent widths were also derived using the AASHTO equations.

The adequacy of the Iowa DOT five-foot requirement was evaluated by comparing the LDFs and equivalent widths obtained using the FE models to those obtained using the AASHTO equations. Based on the derived LDFs and equivalent lengths, the axle weight limits per lane for different types of dual-lane loads were further determined and recommended to complement the current Iowa DOT policy and AASHTO code specifications. Conclusions were as follows:

- The moment LDFs in the negative moment regions were almost the same as those in the positive moment regions for both exterior and interior girders of the steel and concrete bridges.

- The AASHTO LRFD and LFD equations either overestimated or underestimated moment LDFs based on the FE results. For the interior girders of the concrete bridges, the LRFD equations provided good estimations on the moment LDFs and the LFD equations underestimated the moment LDFs. For the exterior girders of the concrete bridges, both the LRFD and LFD equations overestimated the moment LDFs. For the interior girders of the steel bridges, the LRFD equations underestimated the moment LDFs and the LFD equations overestimated the moment LDFs. For the exterior girders of the steel bridges, the LRFD equations underestimated the moment LDFs and the LFD equations overestimated the moment LDFs.

- The AASHTO LRFD and LFD equations also either overestimated or underestimated the shear LDFs based on the FE results. For the interior girders of the steel bridges, both the LRFD and LFD equations underestimated the shear LDFs. For the exterior girders of the steel bridges, both LRFD and LFD equations overestimated the shear LDFs.

- For slab bridges, the LRFD equations slightly overestimated the equivalent widths in the positive moment regions and slightly underestimated the equivalent widths in the negative moment regions.

- The LRFD equations gave more consistent predictions than the LFD equations. For the most part, no significant relationships were found between the important bridge parameters and the accuracy of the AASHTO equations in the prediction of LDFs and equivalent widths, although certain trends were found. For instance, the LRFD equations were less conservative for both moment and shear LDFs when the number of girders was no more than five, and the equivalent widths predicted using LRFD equations were less conservative when the modified span length was longer than 30 ft.

- The Iowa DOT current practice on the moment and shear LDFs and equivalent widths for dual-lane loads is reasonable and adequate.

- A lighter axle weight limit should be used for dual-lane loads with narrower wheel-line spacing.

CHAPTER 1 INTRODUCTION

1.1 Background

With ever increasing numbers and sizes of permitted vehicles and loads crossing Iowa's highways and bridges, it has become more and more common for oversized, overweight vehicles to travel on at least four wheel lines. Commonly, these vehicles have nonstandard axle configurations that result in the wheel lines being non-uniformly spaced. It is widely accepted that the spacing of adjacent wheel lines has an influence on the lateral distribution of the wheel loads on bridges. However, current American Association of State Highway and Transportation Officials (AASHTO) Load and Resistance Factor Design (LRFD) or Load Factor Design (LFD) equations for lateral live load distribution on bridges are only applicable for vehicles having standard axle configurations with a six-foot axle and adjacent vehicles spaced no closer than 4 feet apart.

Current Iowa law specifies that trucks with four wheels will qualify as a dual-lane load only if the distance between the exterior-pair of wheel lines is equal to or larger than five feet. When considered a dual-lane load, the truck is then assumed to be the equivalent, in terms of lateral live load distribution, to two standard side-by-side trucks. However, if the gauge distance does not meet the five-foot requirement, the maximum weight of each axle cannot exceed 20,000 pounds (20 kips. Clearly, it is important to understand the actual effects of non-standard wheel-line spacing on lateral live load distribution. With such an understanding, the current five-foot spacing can be either justified or modified.

1.2 Objective and Scope

The main objective of this research was to investigate the impact of the wheel-line spacing of dual-lane loads on lateral live load distribution. To achieve this objective, a numerical evaluation using finite element (FE) models was performed to investigate the lateral load distribution of dual-lane loads on three types of common Iowa bridges: steel girder, pre-stressed concrete girder, and slab. To accomplish the evaluation, different wheel-line spacing for both the interior-pair and exterior-pair were investigated to allow us to study a number of different types of dual-lane loads on these bridges. Recommendations on the lateral distribution of dual-lane loads were given to improve current Iowa Department of Transportation (DOT) policies (e.g., five-foot requirement) and to also complement the current AASHTO LRFD or LFD specifications.

1.3 Research Plan

Task 1 – Literature Review

During Task 1, a brief literature search and review was conducted to investigate other work related to the impact of gauge width and adjacent axle spacing on lateral load distribution. Of special interest was previous work related to steel girder bridges, pre-stressed concrete girder

bridges, and slab bridges, with a particular interest in the application of results to oversized, overweight vehicles.

Task 2 – Analysis of the Impact of Wheel Line Spacing on Lateral Load Distribution

To investigate the impact of wheel-line spacing on lateral load distribution a rigorous, two-dimensional FE analysis study was conducted. After consultation with Iowa DOT Office of Bridges and Structures staff, it appeared that the most benefit will be derived by studying three types of common Iowa bridges: steel girder, pre-stressed concrete girder, and slab. Thus, the first step was to work with the Office to obtain plans for a representative group of approximately 20 of each type of bridge.

To facilitate the correct computation of the lateral live load distribution factors (LDFs), only bridges with less than 10 degrees of skew were utilized in the analytical study. Once the needed information on the bridges was collected, the research team constructed a database of the important bridge information (span length, number of girders, etc.). With this information, two-dimensional analytical models of the bridges were created.

For the purposes of this study, it is clear that the primary factor of interest is the gauge spacing for situations involving four wheel lines in which the spacing between each exterior pair can vary from 4 to 6 ft with the spacing between each exterior pair also variable. To study the impact of adjacent axle spacing, the spacing between each axle pair was systematically varied from 2 ft to 5 ft (in 6 in. increments) for exterior pair spacing of 4, 5, and 6 ft and the resulting distribution factors for each combination were calculated. In addition, a special case where the spacing between all four wheel lines was 3 ft was investigated. At the same time, the current AASHTO multiple-lane live load distribution factor was calculated.

The final steps were to then determine for which spacing combinations the codified AASHTO equations are no longer valid and to validate the five-foot Iowa DOT requirement (or relax the restriction if possible).

Task 3 – Documentation and Information Dissemination

The researchers summarized the work completed during this project in this final report, which consists of four chapters.

CHAPTER 2 LITERATURE REVIEW

Due to the increasing number and size of permit loads on highways and bridges, allowable truck sizes and weights of oversized, overweight vehicles need to be established using information that was not necessarily intended to be used as such. This is mainly due to the fact that the gauge spacing of these vehicles can be different from that of the notional HS-20 truck, which can have an impact on how live loads are resisted by the primary bridge elements.

Several studies have been conducted to quantify the influence of truck wheel-line spacing on lateral load distribution on bridges. A review of pertinent information from these studies is presented in this chapter.

Tabsh and Tabatabai (2001) performed FE simulations of oversized trucks with non-standard-gauge widths on slab-on-girder bridges and developed modification factors to complement the AASHTO equations for LDFs. The researchers found that the first interior girder has the greatest LDFs of all interior girders, and that a gauge width wider than 6 ft results in a lower LDF compared to that predicted by the AASHTO equations. The researchers also found that the gauge width has greater influences on shear LDFs than moment LDFs.

Goodrich and Puckett (2000) established FE models using the finite strip method to investigate LDFs for oversized vehicles on slab-on-girder bridges. Specific vehicles with four-wheel axles, which were either evenly or unevenly spaced, were also utilized for several parametric studies. Based on their FE results, simplified equations were developed to calculate LDFs for vehicles with nonstandard axle gauges. The simplified equations were in a form that incorporated the AASHTO equations for LDFs. However, due to the limited cases that they studied, these equations need to be further improved for estimating LDFs for four-wheel vehicles with unevenly spaced wheels.

Bae and Oliva (2012) established various three-dimensional FE models of slab-on-girder bridges to investigate the moment and shear LDFs for oversized/overload vehicles. The dual-lane loads with variable spacing between the interior wheels were utilized for parametric studies. Through regression analysis of the FE results, equations were developed to calculate moment and shear LDFs taking into account variables including wheel-line spacing, number of spans, bridge skew, and diaphragms. The researchers also found that the positive moment LDFs were almost identical for single- and two-span bridges. However, the negative moment LDFs of two-span bridges were different from the positive moment LDFs of single-span bridges.

Equivalent widths of concrete slab bridges were evaluated using numerical simulations and field testing by two research teams (Mabsout et al. 2004 and Jones and Shenton 2012). However, no publications were found to study the load distribution characteristics of oversized vehicles on slab bridges.

Mabsout et al. (2004) conducted FE simulations of single-span concrete slab bridges to investigate the influence of span length, slab width, and loading conditions on lateral load distribution. The FE results were compared with the AASHTO equations.

Jones and Shenton (2012) conducted field tests on six concrete slab bridges to obtain the actual equivalent widths of the bridges. The results were compared with those calculated using the AAHSTO LRFD equations and showed that the AASHTO equations were conservative compared to the test results.

CHAPTER 3 FINITE ELEMENT ANALYSIS AND RESULTS

3.1 Bridge Selection

A database containing 1,721 prestressed-concrete bridges, 979 steel bridges, and 556 slab bridges was provided by the Iowa DOT staff. A sub-database consisting of the bridges with skew angles less than 10 degrees and no more than three spans was further extracted from the database. From the sub-database, 20 prestressed-concrete bridges, 20 steel bridges, and 20 slab bridges were randomly sampled and then utilized to establish FE models for this investigation of lateral load distribution on bridges.

Note that, because it is well accepted that the LDF decreases with an increase of bridge skew angle, conservative LDFs are commonly obtained from bridges with skew angles less than 10 degrees. In addition, given that the number of spans has little effect on lateral load distribution, the number of spans was limited to three to simplify the analysis and reduce total computational time. The attributes of the selected prestressed-concrete bridges, steel bridges, and slab bridges are summarized in Table 3.1, Table 3.2, and Table 3.3, respectively.

Table 3.1 Attributes of selected prestressed-concrete bridges

Structure Number	Skew (degree)	Number of Spans	Length of Maximum Span (ft)	Structure Length (ft)	Bridge Roadway Width (ft)	Deck Width (ft)	Girder Spacing (ft)	Deck Depth (in.)	Number of Girders
24171	0	3	61	158	40	43	6.2	8.00	7
604250	6	3	77	171	56	59	6.8	8.00	9
51111	0	3	96	261	40	43	7.4	8.25	6
13040	0	3	65	191	30	36	5.0	6.25	7
608435	7	3	107	213	39	42	7.2	7.87	6
16611	0	1	177	177	121	131	7.4	8.75	6
17301	0	3	250	597	134	144	6.9	6.50	7
41430	0	3	44	125	62	67	4.3	6.00	10
22451	0	3	65	171	44	47	6.9	7.50	7
19811	0	3	69	175	40	43	9.3	8.00	5
47851	0	3	77	200	36	39	6.8	8.00	6
31190	5	3	48	128	40	46	5.0	6.00	9
605525	0	3	44	133	40	43	7.4	8.00	6
41231	0	3	91	222	70	73	7.5	8.00	10
601925	6	3	101	215	39	43	7.2	7.87	6
608560	3	3	95	174	39	43	7.2	7.87	6
45430	0	3	69	200	39	42	4.8	6.06	9
17571	0	3	210	533	134	144	6.8	8.00	7
609185	0	3	77	223	39	42	7.2	7.87	6
13170	5	3	134	378	123	141	4.0	6.00	11

Table 3.2 Attributes of selected steel bridges

Structure Number	Skew (degree)	Number of Spans	Length of Maximum Span (ft)	Structure Length (ft)	Bridge Roadway Width (ft)	Deck Width (ft)	Girder Spacing (ft)	Deck Depth (in.)	Number of Girders
364700	0	2	448	838	168	179	10.3	8	6
19011	0	3	88	223	40	43	7.4	8	6
22520	0	3	82	215	26	32	8.3	7.75	4
606320	0	3	192	506	38	46	9.8	8	5
16220	0	3	47	123	26	32	8.3	7.75	4
46730	0	2	244	500	79	98	8.3	7.75	4
46750	0	3	94	243	26	32	8.3	7.75	4
37570	0	3	105	274	30	36	9.7	7.5	4
40521	0	2	135	270	41	57	9.3	7.87	7
25140	0	3	70	183	28	34	8.9	7.06	4
13330	0	1	50	52	30	34	5.0	6	7
50995	0	3	150	388	39	43	8.9	7.87	5
601356	0	3	86	179	71	73	9.7	8.27	8
29110	0	3	44	125	26	32	8.3	7.75	4
15750	0	3	94	242	26	32	8.3	7.75	4
609280	0	2	144	284	60	69	9.0	8	8
22930	8	3	140	365	40	43	9.6	8	5
43370	0	1	32	36	30	35	9.9	8.25	4
50910	0	3	161	357	28	34	8.9	8	4
43880	0	3	59	153	28	34	8.9	7.25	4

Table 3.3 Attributes of selected slab bridges

Structure Number	Skew (degree)	Number of Spans	Length of Maximum Span (ft)	Structure Length (ft)	Bridge Roadway Width (ft)	Deck Width (ft)	Girder Spacing (ft)
15280	0	1	30	34	40	43	18.75
46391	0	3	51	133	40	43	21.5
36210	0	3	31	83	40	43	15
53360	0	3	46	122	26	30	20.25
28670	0	3	30	93	44	47	15.5
14070	0	3	31	84	30	34	16
26780	0	3	31	82	30	33	15.375
36541	0	3	47	123	44	47	19
605755	0	3	45	118	40	43	18.938
23710	0	3	47	123	44	47	18.25
39441	0	1	23	27	40	43	15
49980	0	3	51	132	30	33	21
26860	0	1	19	21	24	26	17
29571	0	3	35	91	44	47	16.25
14371	0	3	39	104	40	43	17.75
608740	0	3	43	113	44	47	18.5
17990	5	3	39	115	39	42	22
39501	0	1	32	32	40	43	17.5
44290	0	2	31	63	39	42	16.25
28760	0	3	29	77	28	32	15

3.2 Finite Element Modeling

Linear elastic FE models were established for each prestressed-concrete girder, steel girder, and slab bridge; examples are shown in Figure 3.1(a) and Figure 3.1(b).

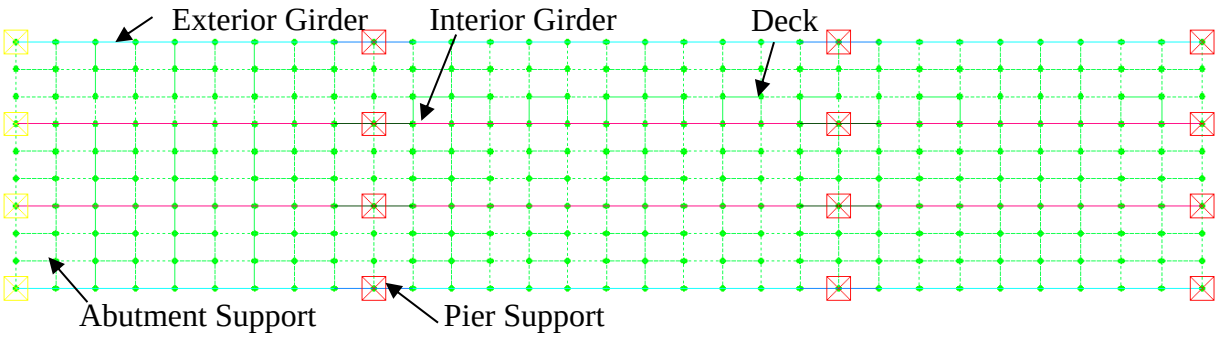

(a) Typical FE model of concrete or steel bridge

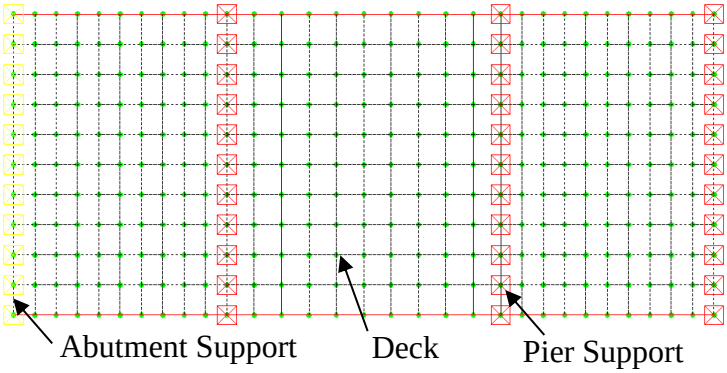

(b) Typical FE model of slab bridge

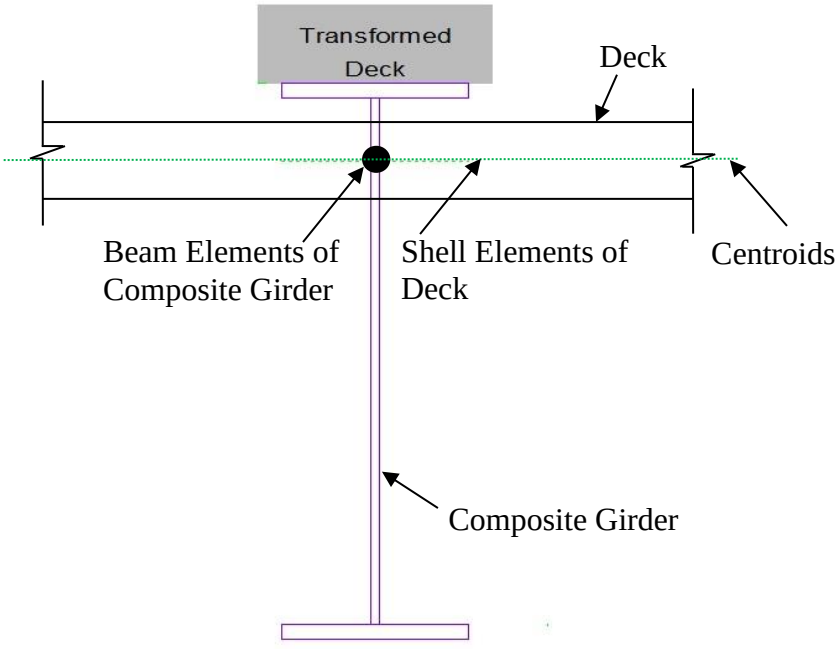

(c) Modeling of girder and deck

Figure 3.1 Details of FE models

The girders were modeled using two-node beam elements, which have three translational and three rotational degrees of freedom at each node. The deck was modeled using four-node quadrilateral shell elements, which have three translational and three rotational degrees of freedom at each node and incorporate bending behavior while ignoring tension membrane behavior. The beam elements share common nodes with the deck shell elements at the centroid location of each as shown in Figure 3.1(c).

To take composite action into account, the composite section of the girder plus the transformed deck (i.e., the deck section was transformed to that with the same elastic modulus as the girder) was utilized to compute the section properties of each beam element. No end restraint at the abutment/pier supports was assumed, and, as a result, simple support conditions were utilized. In all cases, linear elastic material models were used for the concrete and steel. Additional details of the modeling technique can be found in Deng and Phares 2016.

3.3 LDF Results for Steel and Concrete Bridges

3.3.1 Establishment of FE Models and Dual-Lane Loads

Due to the general similarity between the behavior of the steel and concrete girder bridges, the same approach was used to determine their LDFs. In this section, we selected a steel bridge (Bridge 16220) to demonstrate the process of calculating LDFs based on the FE results. Bridge 16220 is a four-girder, three-span, slab-on-steel-girder bridge as shown in Figure 3.2.

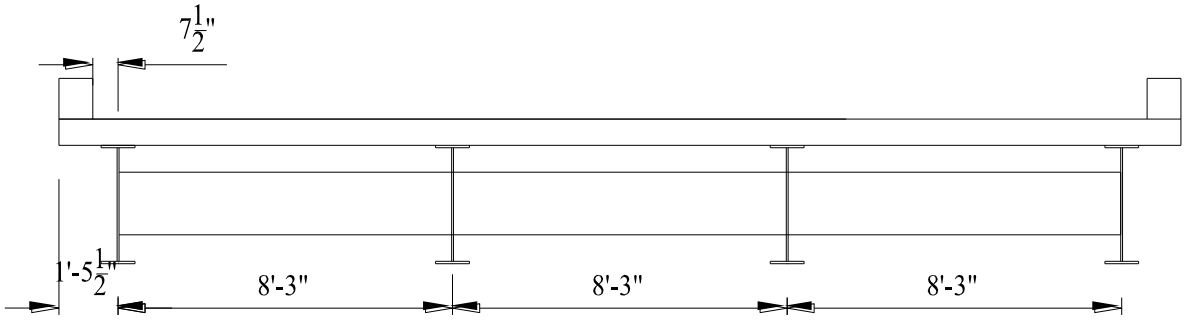

(a) Cross-section

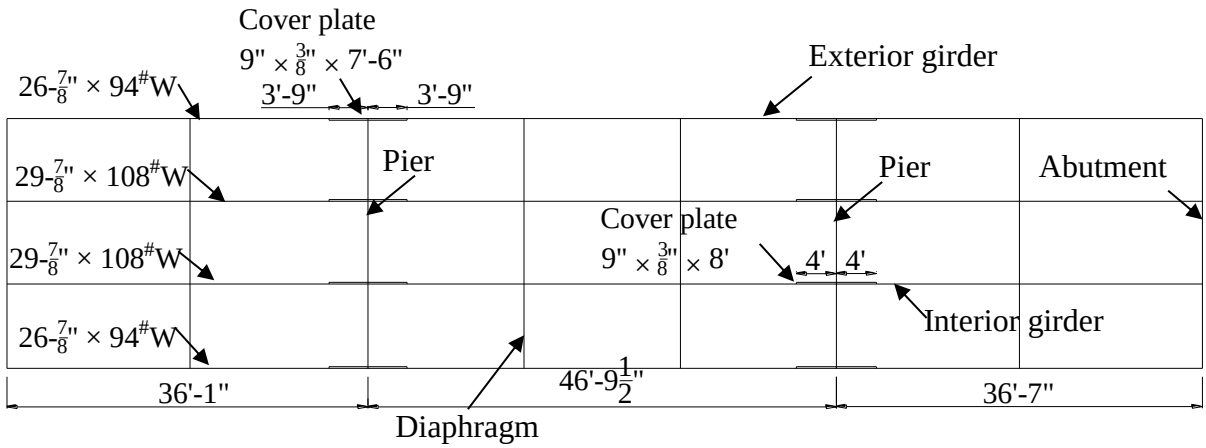

(b) Plan view

Figure 3.2 Details of Bridge 16220

The bridge is simply supported at the pier and abutment locations. The bridge has a deck thickness of 7.75 in., a girder spacing of 8 ft-3 in., and span lengths of 36 ft-1 in., 46 ft-9.5 in. and 36 ft-7 in. The interior and exterior girders are 29 ft-7/8 in. × 108W and 26 ft-7/8 in. × 94W rolled sections, respectively. The dimensions of the flanges and webs are summarized in Table 3.4.

Table 3.4 Dimensions of flanges, webs, and cover plates

	Top Flange (in.)		Bottom Flange (in.)		Web (in.)		Cover Plate (in.)		
	Width	Thickness	Width	Thickness	Width	Thickness	Width	Thickness	Length
Interior Girders	10.5	0.765	0.765	0.765	28.345	0.545	9	0.375	96
Exterior Girders	10.0	0.750	0.750	0.750	25.4	0.490	9	0.375	90

In the negative moment region (pier locations), the interior and exterior girders have cover plates on their top and bottom flanges with dimensions of 9 in. × 3/8 in. × 7 ft-6 in. and 9 in. × 3/8 in. × 8 ft, respectively, as shown in Figure 3.2(b). The distance from the inside edge of the barrier/curb to the centerline of the exterior girder web is 7.5 in.

Based the details of the bridge, the FE model was established as shown in Figure 3.3.

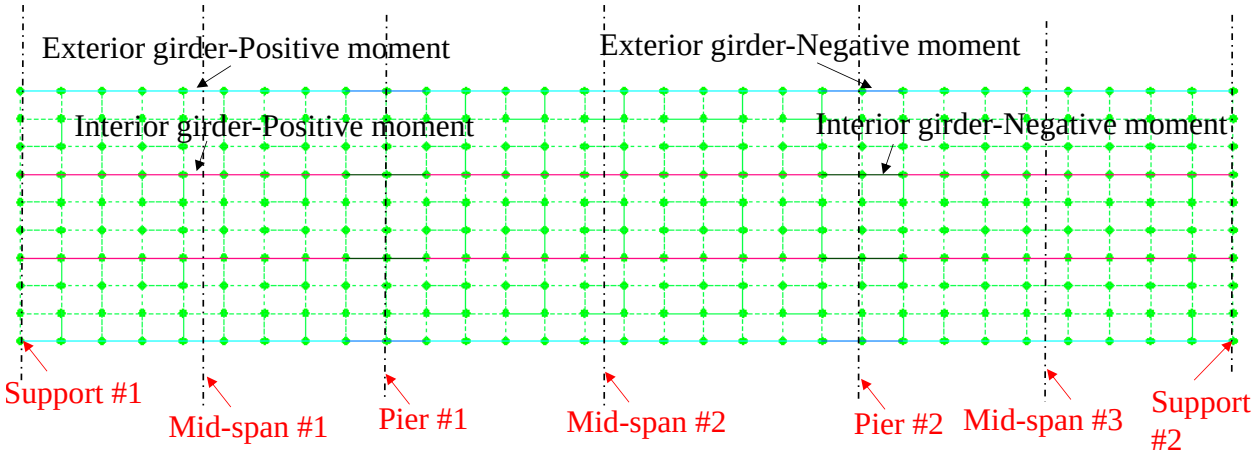

Figure 3.3 FE model of Bridge 16220

The moment LDFs were calculated for the bridge cross-sections at mid-span of all spans and at all piers, while the shear LDFs were calculated for the bridge cross-sections at the abutments and the piers. Based on various geometrical differences, the moment LDFs were further sub-categorized into four regions: (1) interior girders in the positive moment region, (2) interior girders in the negative moment region, (3) exterior girders in the positive moment region, and (4) exterior girders in the negative moment region. For the shear LDFs, the results were categorized into two regions: (1) interior girders and (2) exterior girders. From the calculated results, the largest value was taken as the LDF for each region.

Different adjacent wheel-line spacings for the dual-lane loads were modeled to investigate their effects on the LDF. The loading cases consisted of combinations of the interior wheel-line spacing (2 ft, 2.5 ft, 3 ft, 3.5 ft, 4 ft, 4.5 ft, and 5 ft) and the spacing between the exterior wheel pairs (4, 5, and 6 ft). An additional case with 3 ft spacing between all four wheel lines was investigated. To be conservative, only a single-axle was used to simulate the different loading scenarios as shown in Figure 3.4.

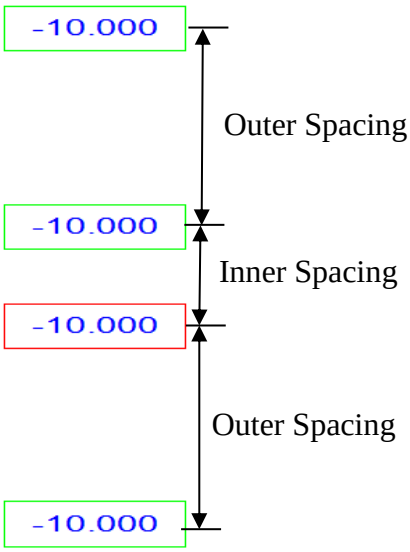

Figure 3.4 Dual-lane load axle example

Taking into account all wheel-line spacing combinations, a total of 22 types of single-axle four-wheel-lines loads were applied to the FE model as summarized in Table 3.5.

Table 3.5 Single-axle four-wheel-lines dual-lane loads

Truck Type	Outer Spacing (ft)	Inner Spacing (ft)
Truck-4-2	4	2
Truck-4-2.5	4	2.5
Truck-4-3	4	3
Truck-4-3.5	4	3.5
Truck-4-4	4	4
Truck-4-4.5	4	4.5
Truck-4-5	4	5
Truck-5-2	5	2
Truck-5-2.5	5	2.5
Truck-5-3	5	3
Truck-5-3.5	5	3.5
Truck-5-4	5	4
Truck-5-4.5	5	4.5
Truck-5-5	5	5
Truck-6-2	6	2
Truck-6-2.5	6	2.5
Truck-6-3	6	3
Truck-6-3.5	6	3.5
Truck-6-4	6	4
Truck-6-4.5	6	4.5
Truck-6-5	6	5
Truck-3-3	3	3

3.3.2 Moment and Shear LDFs

3.3.2.1 Moment LDFs

Various loading cases for each type of dual-lane load with different transverse positions were taken into account in the FE model. These transverse positions were selected by placing the simulated vehicles in various positions across the bridge width, with the outermost wheel line no less than 2 ft away from the inside of the bridge barrier rails. Dual-lane load Truck-4-2 is described below as an example of the LDF calculation process (see also Figure 3.5).

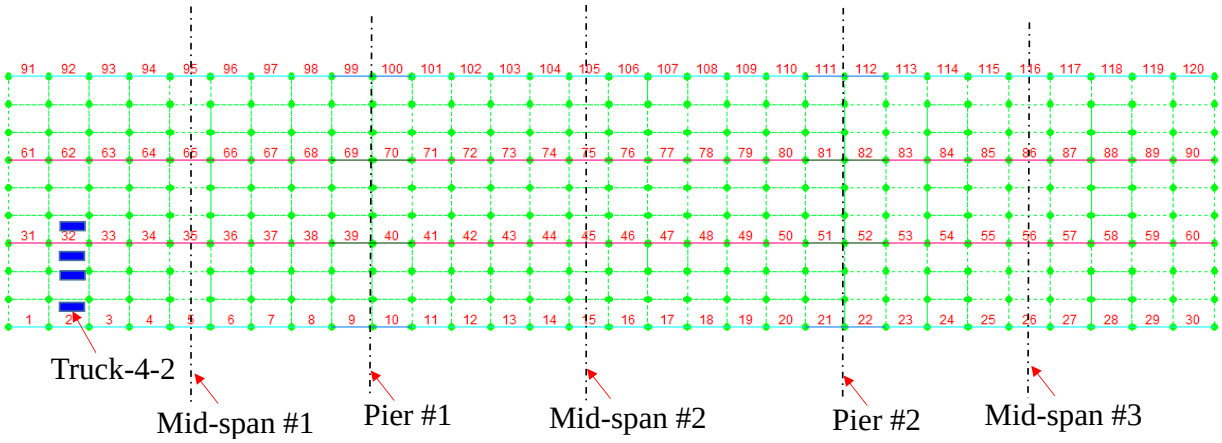

Figure 3.5 Load case with transverse position 2 feet from bridge barrier rails

Truck-4-2 travels across the bridge in a transverse position with the outermost wheel line 2 ft away from the bridge barrier rail and at an incremental longitudinal travel distance of 5 ft. The bridge cross-section mid-span #1 includes beam elements 5, 35, 65, and 95 as shown in Figure 3.5.

The moment-travel position relationships of the beam elements (5, 35, 65, and 95) at mid-span #1 are shown in Figure 3.6.

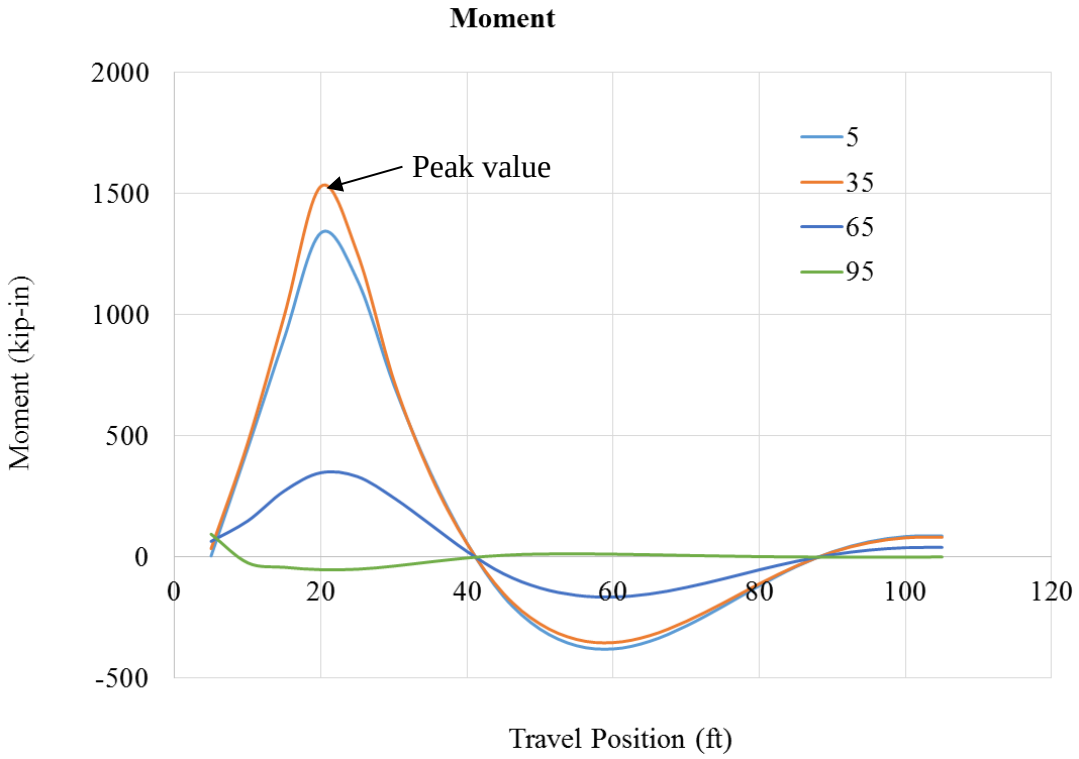

Figure 3.6 Moment-travel position relationships of beam elements at mid-span #1

When the truck had a travel position of 20 ft, the highest moment value was reached for this load case. Note that the LDFs were calculated based on the internal forces of these beam elements at the 20-ft travel position using equation (1):

$$LDF_i = \frac{L_i}{\sum_{i=1}^{n} L_i} \quad \textbf{(1)}$$

where, i = girder number, n = total number of girders, LDF_i = load distribution factor of girder i, and L_i = internal force (moment or shear) in girder i.

For different truck transverse positions, the relationships between moment LDFs with varying transverse positions for mid-span #1 are shown in Figure 3.7.

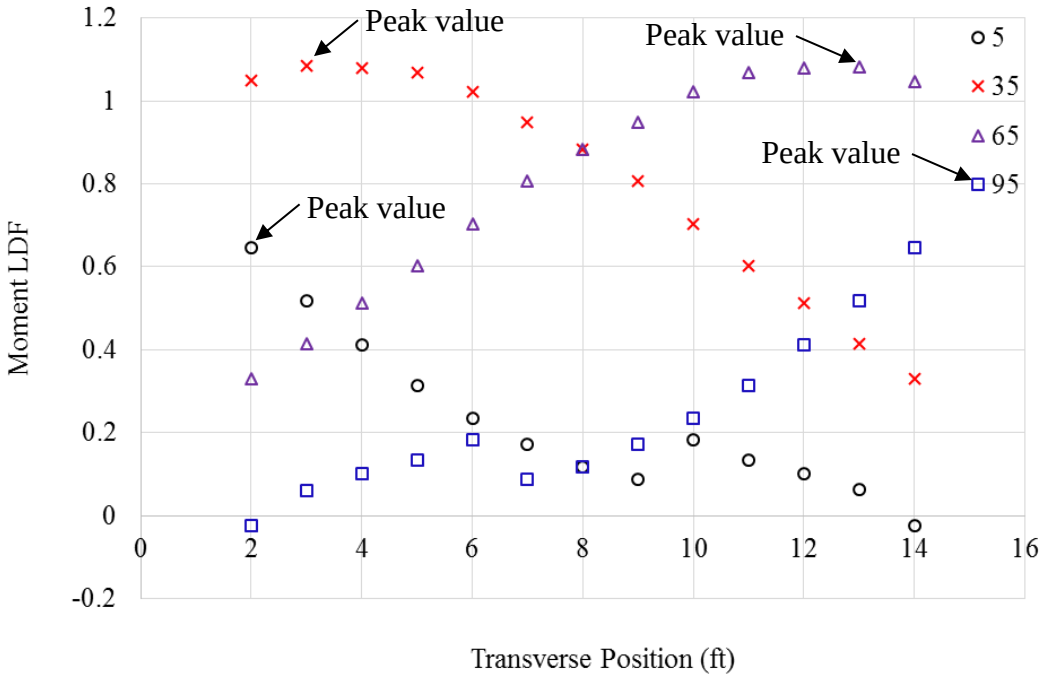

Figure 3.7 Moment-travel position relationships of beam elements at mid-span #1

From this, the peak values (shown in Figure 3.7) were taken as the LDFs of the four elements in the bridge cross-section at mid-span #1.

The moment LDFs for the cross-section at mid-span #1 for different types of truck loads are summarized in Table 3.6.

Table 3.6 Moment LDFs for elements at section mid-span #1 for different types of truck loads

Truck Type	Outer Spacing (ft)	Inner Spacing (ft)	Moment LDFs of Different Elements			
			5	35	65	95
Truck-4-2	4	2	0.646	1.084	1.083	0.647
Truck-4-2.5	4	2.5	0.625	1.056	1.055	0.626
Truck-4-3	4	3	0.607	1.028	1.027	0.607
Truck-4-3.5	4	3.5	0.595	1.001	1.001	0.595
Truck-4-4	4	4	0.583	0.974	0.973	0.583
Truck-4-4.5	4	4.5	0.571	0.947	0.941	0.571
Truck-4-5	4	5	0.56	0.914	0.913	0.561
Truck-5-2	5	2	0.564	1.008	1.007	0.564
Truck-5-2.5	5	2.5	0.552	0.981	0.981	0.553
Truck-5-3	5	3	0.542	0.954	0.953	0.542
Truck-5-3.5	5	3.5	0.532	0.927	0.923	0.532
Truck-5-4	5	4	0.521	0.897	0.896	0.522
Truck-5-4.5	5	4.5	0.511	0.87	0.869	0.511
Truck-5-5	5	5	0.503	0.84	0.84	0.504
Truck-6-2	6	2	0.504	0.931	0.93	0.505
Truck-6-2.5	6	2.5	0.494	0.91	0.904	0.494
Truck-6-3	6	3	0.484	0.886	0.885	0.484
Truck-6-3.5	6	3.5	0.475	0.86	0.857	0.476
Truck-6-4	6	4	0.471	0.834	0.833	0.471
Truck-6-4.5	6	4.5	0.467	0.808	0.807	0.467
Truck-6-5	6	5	0.463	0.782	0.782	0.463
Truck-3-3	3	3	0.906	1.105	1.105	0.907

Likewise, moment LDFs were also derived for the bridge cross-sections at mid-spans #2 and #3 and piers #1 and #2. By categorizing these elements into different regions, moment LDFs were further summarized by the four previously mentioned regions: (1) exterior girders in the positive moment region shown in Table 3.7, (2) exterior girders in the negative moment region shown in Table 3.8, (3) interior girders in the positive moment region shown in Table 3.9, and (4) interior girders in the negative moment region shown in Table 3.10.

Table 3.7 Moment LDFs of exterior girders in positive moment region elements for different types of truck loads

Truck Type	Outer Spacing (ft)	Inner Spacing (ft)	Moment LDFs of Different Elements						
			5	16	26	95	106	116	Maximum
Truck-4-2	4	2	0.646	0.66	0.649	0.647	0.659	0.647	0.66
Truck-4-2.5	4	2.5	0.625	0.639	0.628	0.626	0.639	0.626	0.639
Truck-4-3	4	3	0.607	0.621	0.609	0.607	0.62	0.608	0.621
Truck-4-3.5	4	3.5	0.595	0.609	0.597	0.595	0.608	0.596	0.609
Truck-4-4	4	4	0.583	0.596	0.585	0.583	0.596	0.584	0.596
Truck-4-4.5	4	4.5	0.571	0.584	0.573	0.571	0.584	0.572	0.584
Truck-4-5	4	5	0.56	0.574	0.563	0.561	0.573	0.562	0.574
Truck-5-2	5	2	0.564	0.578	0.566	0.564	0.578	0.565	0.578
Truck-5-2.5	5	2.5	0.552	0.567	0.555	0.553	0.566	0.554	0.567
Truck-5-3	5	3	0.542	0.556	0.544	0.542	0.555	0.543	0.556
Truck-5-3.5	5	3.5	0.532	0.545	0.534	0.532	0.545	0.533	0.545
Truck-5-4	5	4	0.521	0.534	0.524	0.522	0.534	0.523	0.534
Truck-5-4.5	5	4.5	0.511	0.523	0.513	0.511	0.523	0.512	0.523
Truck-5-5	5	5	0.503	0.515	0.506	0.504	0.515	0.505	0.515
Truck-6-2	6	2	0.504	0.518	0.507	0.505	0.518	0.506	0.518
Truck-6-2.5	6	2.5	0.494	0.507	0.496	0.494	0.507	0.495	0.507
Truck-6-3	6	3	0.484	0.496	0.486	0.484	0.496	0.485	0.496
Truck-6-3.5	6	3.5	0.475	0.488	0.478	0.476	0.487	0.477	0.488
Truck-6-4	6	4	0.471	0.482	0.473	0.471	0.482	0.472	0.482
Truck-6-4.5	6	4.5	0.467	0.477	0.469	0.467	0.477	0.468	0.477
Truck-6-5	6	5	0.463	0.473	0.465	0.463	0.473	0.464	0.473
Truck-3-3	3	3	0.906	0.908	0.907	0.907	0.907	0.905	0.908

Table 3.8 Moment LDFs of exterior girders in negative moment region elements for different types of truck loads

Truck Type	Outer Spacing (ft)	Inner Spacing (ft)	Moment LDFs of Different Elements				
			10	22	100	112	Maximum
Truck-4-2	4	2	0.667	0.659	0.666	0.658	0.667
Truck-4-2.5	4	2.5	0.645	0.638	0.644	0.637	0.645
Truck-4-3	4	3	0.625	0.618	0.624	0.617	0.625
Truck-4-3.5	4	3.5	0.61	0.604	0.609	0.603	0.61
Truck-4-4	4	4	0.595	0.589	0.594	0.588	0.595
Truck-4-4.5	4	4.5	0.581	0.575	0.58	0.575	0.581
Truck-4-5	4	5	0.569	0.564	0.569	0.563	0.569
Truck-5-2	5	2	0.58	0.574	0.579	0.573	0.58
Truck-5-2.5	5	2.5	0.566	0.56	0.565	0.56	0.566
Truck-5-3	5	3	0.554	0.549	0.553	0.548	0.554
Truck-5-3.5	5	3.5	0.542	0.537	0.542	0.537	0.542
Truck-5-4	5	4	0.53	0.526	0.53	0.525	0.53
Truck-5-4.5	5	4.5	0.518	0.514	0.518	0.514	0.518
Truck-5-5	5	5	0.51	0.507	0.51	0.506	0.51
Truck-6-2	6	2	0.516	0.512	0.516	0.511	0.516
Truck-6-2.5	6	2.5	0.504	0.5	0.504	0.5	0.504
Truck-6-3	6	3	0.493	0.489	0.492	0.488	0.493
Truck-6-3.5	6	3.5	0.482	0.478	0.481	0.478	0.482
Truck-6-4	6	4	0.475	0.472	0.475	0.471	0.475
Truck-6-4.5	6	4.5	0.47	0.467	0.469	0.466	0.47
Truck-6-5	6	5	0.464	0.462	0.464	0.461	0.464
Truck-3-3	3	3	0.929	0.92	0.928	0.919	0.929

Table 3.9 Moment LDFs of interior girders in positive moment region elements for different types of truck loads

Truck Type	Outer Spacing (ft)	Inner Spacing (ft)	Moment LDFs of Different Elements						
			35	46	56	65	76	86	Maximum
Truck-4-2	4	2	1.084	1.05	1.081	1.083	1.049	1.081	1.084
Truck-4-2.5	4	2.5	1.056	1.024	1.053	1.055	1.023	1.052	1.056
Truck-4-3	4	3	1.028	0.998	1.025	1.027	0.998	1.025	1.028
Truck-4-3.5	4	3.5	1.001	0.972	0.997	1.001	0.971	0.997	1.001
Truck-4-4	4	4	0.974	0.947	0.97	0.973	0.946	0.97	0.974
Truck-4-4.5	4	4.5	0.947	0.921	0.943	0.941	0.918	0.937	0.947
Truck-4-5	4	5	0.914	0.893	0.911	0.913	0.892	0.91	0.914
Truck-5-2	5	2	1.008	0.979	1.005	1.007	0.979	1.004	1.008
Truck-5-2.5	5	2.5	0.981	0.954	0.978	0.981	0.953	0.977	0.981
Truck-5-3	5	3	0.954	0.929	0.951	0.953	0.928	0.95	0.954
Truck-5-3.5	5	3.5	0.927	0.903	0.924	0.923	0.902	0.92	0.927
Truck-5-4	5	4	0.897	0.877	0.894	0.896	0.876	0.893	0.897
Truck-5-4.5	5	4.5	0.87	0.852	0.867	0.869	0.851	0.866	0.87
Truck-5-5	5	5	0.84	0.823	0.837	0.84	0.822	0.836	0.84
Truck-6-2	6	2	0.931	0.91	0.929	0.93	0.909	0.928	0.931
Truck-6-2.5	6	2.5	0.91	0.888	0.907	0.904	0.884	0.901	0.91
Truck-6-3	6	3	0.886	0.866	0.883	0.885	0.865	0.882	0.886
Truck-6-3.5	6	3.5	0.86	0.842	0.857	0.857	0.84	0.854	0.86
Truck-6-4	6	4	0.834	0.818	0.831	0.833	0.818	0.83	0.834
Truck-6-4.5	6	4.5	0.808	0.795	0.805	0.807	0.794	0.804	0.808
Truck-6-5	6	5	0.782	0.771	0.779	0.782	0.77	0.779	0.782
Truck-3-3	3	3	1.105	1.068	1.101	1.105	1.07	1.103	1.105

Table 3.10 Moment LDFs of interior girders in negative moment region elements for different types of truck loads

Truck Type	Outer Spacing (ft)	Inner Spacing (ft)	Moment LDFs of Different Elements				
			40	52	70	82	Maximum
Truck-4-2	4	2	1.134	1.143	1.135	1.143	1.143
Truck-4-2.5	4	2.5	1.106	1.046	1.107	1.046	1.107
Truck-4-3	4	3	1.077	1.023	1.077	1.022	1.077
Truck-4-3.5	4	3.5	1.048	1	1.049	0.999	1.049
Truck-4-4	4	4	1.02	0.976	1.019	0.975	1.02
Truck-4-4.5	4	4.5	0.991	0.952	0.985	0.946	0.991
Truck-4-5	4	5	0.921	0.923	0.921	0.922	0.923
Truck-5-2	5	2	1.052	1.002	1.052	1.001	1.052
Truck-5-2.5	5	2.5	1.024	0.978	1.024	0.977	1.024
Truck-5-3	5	3	0.995	0.954	0.995	0.953	0.995
Truck-5-3.5	5	3.5	0.929	0.93	0.925	0.927	0.93
Truck-5-4	5	4	0.902	0.904	0.902	0.903	0.904
Truck-5-4.5	5	4.5	0.879	0.88	0.879	0.879	0.88
Truck-5-5	5	5	0.851	0.85	0.85	0.85	0.851
Truck-6-2	6	2	0.928	0.93	0.927	0.929	0.93
Truck-6-2.5	6	2.5	0.908	0.909	0.904	0.905	0.909
Truck-6-3	6	3	0.884	0.884	0.883	0.883	0.884
Truck-6-3.5	6	3.5	0.862	0.862	0.861	0.861	0.862
Truck-6-4	6	4	0.837	0.837	0.837	0.836	0.837
Truck-6-4.5	6	4.5	0.811	0.81	0.811	0.81	0.811
Truck-6-5	6	5	0.785	0.784	0.784	0.783	0.785
Truck-3-3	3	3	1.16	1.169	1.161	1.17	1.17

Finally, for each type of dual-lane load, the maximum moment LDF in each region was taken as the moment LDF in this region. The moment LDFs for bridge 16220 are further summarized in Table 3.11.

Table 3.11 Moment LDFs of girders in different regions for different types of truck loads

Truck Type	Outer Spacing (ft)	Inner Spacing (ft)	Moment LDFs			
			Exterior Girder-Positive Region	Exterior Girder-Negative Region	Interior Girder-Positive Region	Interior Girder-Negative Region
Truck-4-2	4	2	0.66	0.667	1.084	1.143
Truck-4-2.5	4	2.5	0.639	0.645	1.056	1.107
Truck-4-3	4	3	0.621	0.625	1.028	1.077
Truck-4-3.5	4	3.5	0.609	0.61	1.001	1.049
Truck-4-4	4	4	0.596	0.595	0.974	1.02
Truck-4-4.5	4	4.5	0.584	0.581	0.947	0.991
Truck-4-5	4	5	0.574	0.569	0.914	0.923
Truck-5-2	5	2	0.578	0.58	1.008	1.052
Truck-5-2.5	5	2.5	0.567	0.566	0.981	1.024
Truck-5-3	5	3	0.556	0.554	0.954	0.995
Truck-5-3.5	5	3.5	0.545	0.542	0.927	0.93
Truck-5-4	5	4	0.534	0.53	0.897	0.904
Truck-5-4.5	5	4.5	0.523	0.518	0.87	0.88
Truck-5-5	5	5	0.515	0.51	0.84	0.851
Truck-6-2	6	2	0.518	0.516	0.931	0.93
Truck-6-2.5	6	2.5	0.507	0.504	0.91	0.909
Truck-6-3	6	3	0.496	0.493	0.886	0.884
Truck-6-3.5	6	3.5	0.488	0.482	0.86	0.862
Truck-6-4	6	4	0.482	0.475	0.834	0.837
Truck-6-4.5	6	4.5	0.477	0.47	0.808	0.811
Truck-6-5	6	5	0.473	0.464	0.782	0.785
Truck-3-3	3	3	0.908	0.929	1.105	1.17
LRFD Equations			0.61	0.60	0.72	0.71
LFD Equations			0.75	0.75	0.75	0.75

The moment LDFs for all of the girder bridges were determined following this procedure.

3.3.2.2 Shear LDFs

Following the procedure used to determine the moment LDFs, the shear LDFs were determined for the interior and exterior girders at supports #1 and #2 and piers #1 and #2. The shear LDFs for bridge 16220 were calculated and are shown in Table 3.12.

Table 3.12 Shear LDFs of girders in different regions for different types of truck loads

Truck Type	Outer Spacing (ft)	Inner Spacing (ft)	Shear LDFs	
			Exterior Positive	Interior Positive
Truck-4-2	4	2	0.659	1.318
Truck-4-2.5	4	2.5	0.637	1.271
Truck-4-3	4	3	0.618	1.22
Truck-4-3.5	4	3.5	0.603	1.177
Truck-4-4	4	4	0.587	1.128
Truck-4-4.5	4	4.5	0.573	1.082
Truck-4-5	4	5	0.56	1.027
Truck-5-2	5	2	0.574	1.185
Truck-5-2.5	5	2.5	0.56	1.144
Truck-5-3	5	3	0.548	1.095
Truck-5-3.5	5	3.5	0.535	1.051
Truck-5-4	5	4	0.523	1.002
Truck-5-4.5	5	4.5	0.51	0.962
Truck-5-5	5	5	0.504	0.926
Truck-6-2	6	2	0.51	1.055
Truck-6-2.5	6	2.5	0.497	1.025
Truck-6-3	6	3	0.485	0.987
Truck-6-3.5	6	3.5	0.473	0.949
Truck-6-4	6	4	0.467	0.912
Truck-6-4.5	6	4.5	0.462	0.873
Truck-6-5	6	5	0.456	0.838
Truck-3-3	3	3	0.899	1.361
LRFD			0.55	0.83
LFD			0.75	0.75

Likewise, the moment and shear LDFs for the other 19 steel bridges were derived following the same procedure. Note that shear LDFs were not calculated for the concrete girder bridges.

3.3.3 LDFs Determined Using LRFD and LFD Equations

3.3.3.1 Moment LDFs

For concrete slab on steel or prestressed-concrete girder bridges, the moment LDFs of dual-lane loads for interior beams can be determined with equation (2) (AASHTO LRFD 2010):

$$LDF_{interior} = 0.075 + \left(\frac{S}{9.5}\right)^{0.6}\left(\frac{S}{L}\right)^{0.2}\left(\frac{K_g}{12.0Lt_s^{\,3}}\right)^{0.1} \quad \textbf{(2)}$$

where, S = girder spacing (ft), L = span length (ft), t_s = deck thickness (in.), and K_g = longitudinal stiffness parameter, which can be expressed by:

$$K_g = n(I + Ae_g^2) \quad \textbf{(3)}$$

where, A = area of beam, I = moment of inertia of beam (in.^{4}), e_g = vertical distance between the centroids of the beam and deck (in.), and n = stiffness ratio, which can be expressed by:

$$n = \frac{E_B}{E_D} \quad \textbf{(4)}$$

where, E_B = modulus of elasticity of beam material (ksi) and E_D= modulus of elasticity of deck concrete (ksi).

And, the moment LDFs of dual-lane loads for exterior beams can be determined with equation (5) (AASHTO LRFD 2010):

$$LDF_{\text{ext}erior} = e \cdot LDF_{\text{int}erior} \quad \textbf{(5)}$$

where, e = correction factor, which can be expressed by:

$$e = 0.77 + \frac{d_e}{9.1} \quad \textbf{(-1.0} \leq \boldsymbol{d_e} \leq \textbf{5.5)} \quad \textbf{(6)}$$

where, d_e = horizontal distance from the centerline of exterior web of exterior beam to the inside surface of barrier.

For the AASHTO LFD standard specifications, the moment LDFs of dual-lane loads for all beams of slab-on-girder bridges can be determined with equation (7) (AASHTO LFD 1996):

$$LDF = \frac{S}{11} \quad \textbf{(7)}$$

For Bridge 16220, the moment LDFs determined using the FE model are compared with those obtained using AASHTO LRFD and LFD equations (as shown in Table 3.11). And, the moment LDFs are further illustrated in Figure 3.8 to demonstrate the relationships between the LDFs and the wheel-line spacing.

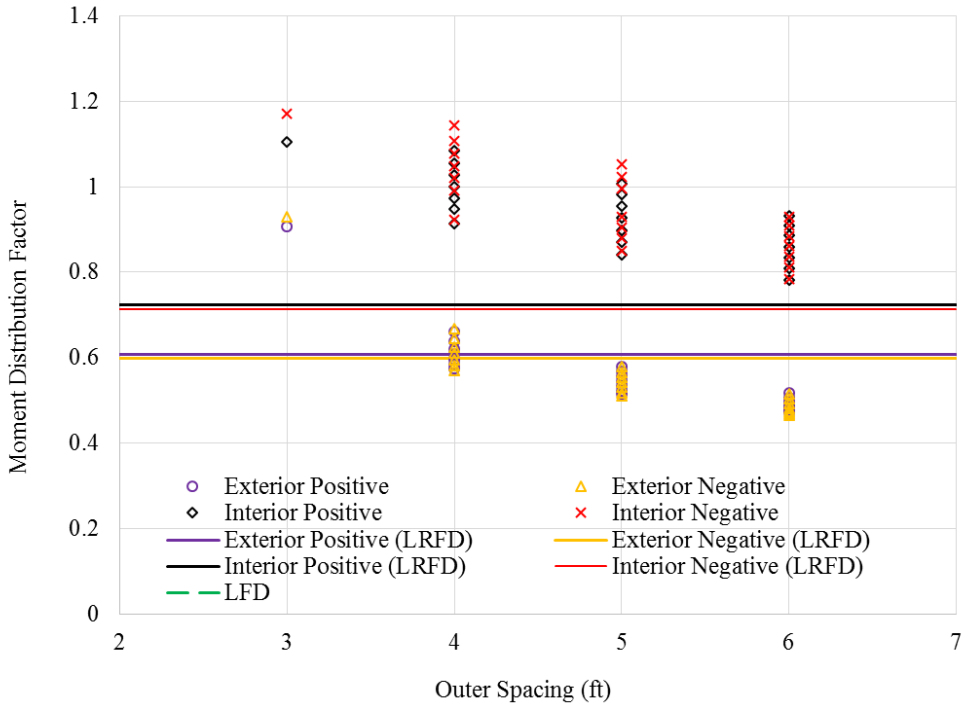

(a) Outer spacing

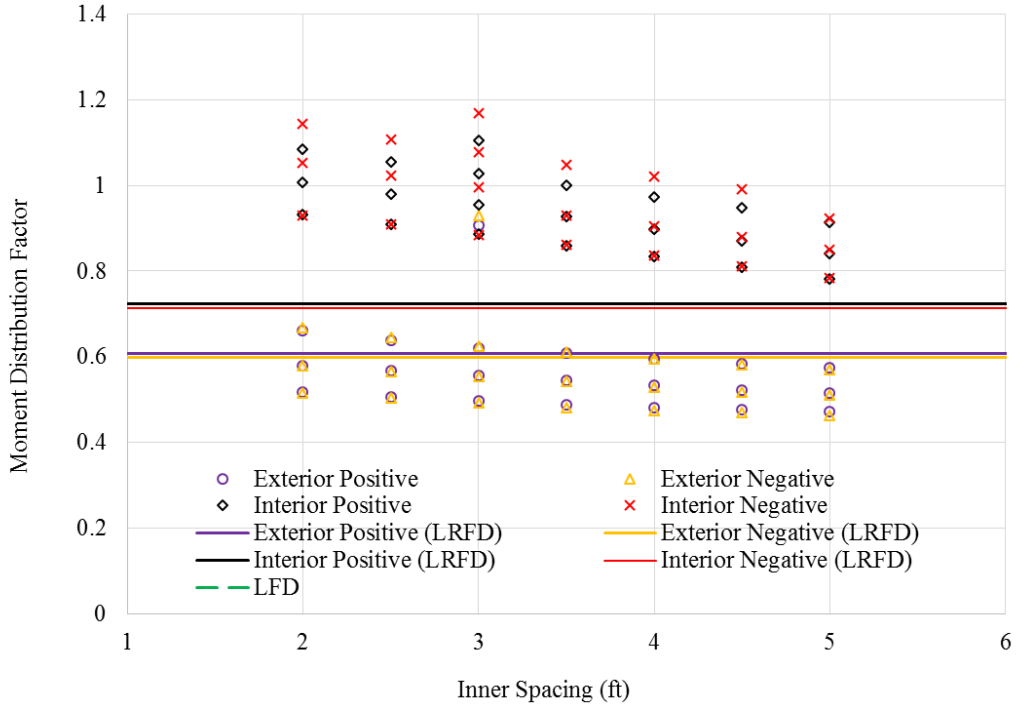

(b) Inner spacing

Figure 3.8 Comparisons of moment LDFs with LRFD and LFD results

Table 3.11 and Figure 3.8 indicate, as expected, that the moment LDF decreases with an increase in outer spacing and inner spacing of dual-lane loads; and, in general, the LRFD and LFD

equations overestimate the moment LDFs for exterior girders but underestimate the moment LDFs for interior girders.

3.3.3.2 Shear LDFs

For concrete slab on steel or prestressed-concrete girder bridges, the shear LDFs for dual-lane loads for interior beams can be determined with equation (10) (AASHTO LRFD 2010):

$$LDF_{interior} = 0.2 + \frac{S}{12} - \left(\frac{S}{35}\right)^{2.0} \quad \textbf{(10)}$$

And, the shear LDFs of dual-lane loads for exterior beams can be determined with equation (8) (AASHTO LRFD 2010):

$$LDF_{exterior} = e \cdot LDF_{interior} \quad \textbf{(8)}$$

where, e = correction factor, which can be expressed by (girder number is more than three):

$$e = 0.6 + \frac{d_e}{10} \quad (-1.0 \le d_e \le 5.5) \quad \textbf{(9)}$$

For AASHTO LFD standard specifications, the shear LDFs of dual-lane loads for all beams of slab-on-girder bridges can be determined with equation (10) (AASHTO LFD 1996):

$$LDF = \frac{S}{11} \quad \textbf{(10)}$$

For Bridge 16220, shear LDFs determined using the FE model were compared with those obtained using the AASHTO LRFD and LFD equations (as summarized in Table 3.12). And, the shear LDFs are further illustrated in Figure 3.9 to demonstrate the relationships between the LDFs and wheel-line spacing.

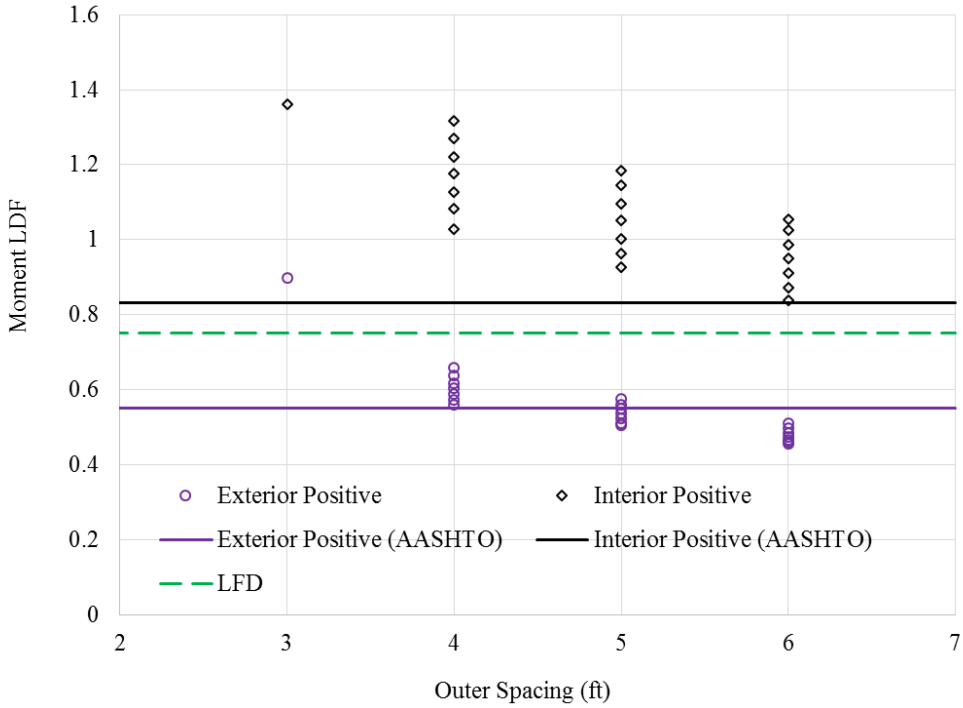

(a) Outer spacing

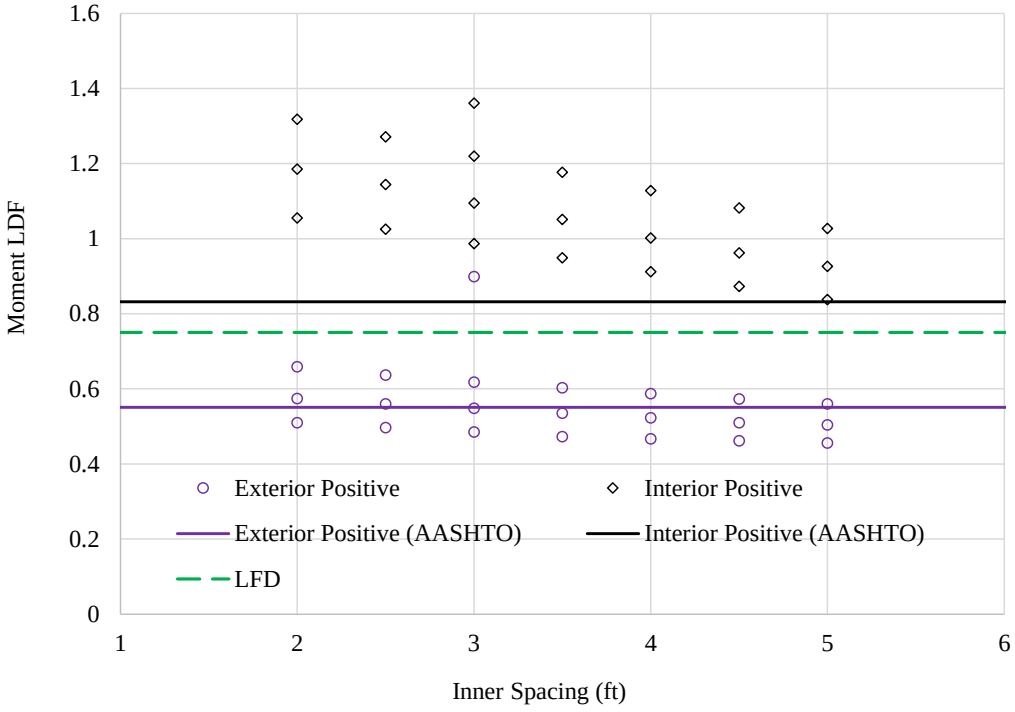

(b) Inner spacing

Figure 3.9 Comparisons of shear LDFs with LRFD and LFD results

Table 3.12 and Figure 3.9 indicate that the moment LDF decreases along with an increase in outer and inner spacing of the dual-lane loads; and, in general, the LRFD and LFD equations overestimate the shear LDFs for exterior girders but underestimate the LDFs for interior girders.

Further comparisons of LDFs obtained using the FE models with those using the AASHTO equations for all of the steel and concrete bridges are presented in Section 3.3.4.

3.3.4 Comparisons of LDFs Obtained Using FE Models with Those Using AASHTO Equations

The so-called Iowa DOT five-foot requirement mandates that the distance between the interior wheel lines of a dual-lane load be no less than 5 ft and, if the distance is less than 5 ft, each axle weight of the truck per lane should be less than 20 kips. To study this requirement, Truck-5-5 and Truck-6-5 were selected for comparison purposes. Since the AASHTO equations were developed for geometries similar to Truck-6-4, Truck-6-4 was also selected for further comparison.

3.3.4.1 Ratios of Moment LDFs

The moment LDFs for the concrete girder bridges determined using the FE models under the three previously mentioned dual-lane loads (i.e., Truck-5-5, Truck-6-5, and Truck-6-4) and the AASHTO equations are summarized in Table 3.13 and Table 3.14.

Table 3.13 Moment LDFs of concrete bridges derived using FE models

Structure Number	FEA (6-4-6)				FEA (6-5-6)				FEA (5-5-5)			
	Exterior Positive	Exterior Negative	Interior Positive	Interior Negative	Exterior Positive	Exterior Negative	Interior Positive	Interior Negative	Exterior Positive	Exterior Negative	Interior Positive	Interior Negative
19811	0.65	0.66	0.89	0.89	0.63	0.64	0.84	0.84	0.69	0.70	0.89	0.89
51111	0.59	0.60	0.67	0.68	0.57	0.57	0.63	0.64	0.63	0.63	0.67	0.69
608435	0.60	0.62	0.72	0.63	0.58	0.60	0.66	0.61	0.63	0.66	0.72	0.64
16611	0.60	0.00	0.64	0.00	0.58	0.00	0.61	0.00	0.63	0.00	0.65	0.00
47851	0.55	0.55	0.63	0.63	0.53	0.53	0.59	0.59	0.59	0.59	0.63	0.63
605525	0.56	0.54	0.72	0.73	0.55	0.53	0.67	0.68	0.60	0.58	0.72	0.74
601925	0.59	0.61	0.70	0.65	0.58	0.59	0.66	0.62	0.63	0.64	0.71	0.66
608560	0.58	0.60	0.75	0.65	0.57	0.58	0.68	0.62	0.62	0.64	0.75	0.66
609185	0.62	0.58	0.68	0.68	0.60	0.56	0.64	0.64	0.66	0.62	0.68	0.69
24171	0.51	0.50	0.61	0.61	0.50	0.49	0.56	0.56	0.55	0.54	0.60	0.61
13040	0.32	0.32	0.50	0.52	0.32	0.31	0.46	0.47	0.34	0.34	0.48	0.51
17301	0.53	0.54	0.68	0.66	0.52	0.52	0.63	0.62	0.57	0.57	0.68	0.66
22451	0.52	0.52	0.68	0.68	0.51	0.50	0.63	0.63	0.56	0.56	0.68	0.69
17571	0.55	0.55	0.68	0.65	0.53	0.53	0.65	0.61	0.59	0.59	0.69	0.66
604250	0.49	0.50	0.68	0.63	0.48	0.49	0.63	0.59	0.53	0.54	0.68	0.64
31190	0.29	0.28	0.54	0.54	0.29	0.28	0.49	0.49	0.31	0.31	0.51	0.52
45430	0.33	0.31	0.48	0.49	0.32	0.31	0.44	0.46	0.35	0.34	0.47	0.49
41430	0.21	0.19	0.44	0.45	0.21	0.19	0.41	0.41	0.22	0.20	0.44	0.45
41231	0.57	0.58	0.79	0.67	0.56	0.56	0.72	0.64	0.61	0.62	0.79	0.68
13170	0.25	0.24	0.43	0.42	0.25	0.24	0.39	0.39	0.27	0.26	0.42	0.42

Table 3.14 Moment LDFs of concrete bridges derived using LRFD and LFD equations

Structure Number	LRFD				LFD			
	Exterior Positive	Exterior Negative	Interior Positive	Interior Negative	Exterior Positive	Exterior Negative	Interior Positive	Interior Negative
19811	0.76	0.72	0.81	0.77	0.84	0.84	0.84	0.84
51111	0.59	0.58	0.63	0.62	0.67	0.67	0.67	0.67
608435	0.67	0.60	0.71	0.63	0.66	0.66	0.66	0.66
16611	0.57	0.00	0.61	0.00	0.67	0.00	0.67	0.00
47851	0.57	0.55	0.60	0.59	0.60	0.60	0.60	0.60
605525	0.61	0.61	0.65	0.65	0.67	0.67	0.67	0.67
601925	0.66	0.60	0.69	0.64	0.66	0.66	0.66	0.66
608560	0.74	0.63	0.78	0.66	0.66	0.66	0.66	0.66
609185	0.59	0.58	0.62	0.62	0.66	0.66	0.66	0.66
24171	0.55	0.53	0.59	0.57	0.56	0.56	0.56	0.56
13040	0.47	0.47	0.51	0.50	0.45	0.45	0.45	0.45
17301	0.61	0.58	0.66	0.62	0.63	0.63	0.63	0.63
22451	0.60	0.58	0.65	0.63	0.63	0.63	0.63	0.63
17571	0.58	0.57	0.62	0.61	0.62	0.62	0.62	0.62
604250	0.59	0.54	0.67	0.61	0.61	0.61	0.61	0.61
31190	0.42	0.41	0.54	0.53	0.45	0.45	0.45	0.45
45430	0.39	0.38	0.49	0.48	0.44	0.44	0.44	0.44
41430	0.34	0.33	0.48	0.48	0.39	0.39	0.39	0.39
41231	0.73	0.63	0.81	0.69	0.68	0.68	0.68	0.68
13170	0.37	0.36	0.48	0.46	0.36	0.36	0.36	0.36

It should be iterated that, for each bridge under each load type, moment LDFs were calculated for four regions as shown in Table 3.13 and Table 3.14: (1) exterior girders in the positive moment regions (exterior positive), (2) exterior girders in the negative moment regions (exterior negative), (3) interior girders in the positive moment regions (interior positive), and (4) interior girders in the negative moment regions (interior negative). For comparison purposes, the ratios of the moment LDFs of the concrete bridges using LRFD and LFD equations to those determined from the FE models were calculated and are summarized in Table 3.15 and Table 3.16.

Likewise, the moment LDFs of the steel bridges determined using the FE models and the AASHTO LRFD and LFD equations under the three types of dual-lane loads were calculated and are summarized in Table 3.17 and Table 3.18.

Table 3.15 Ratios of moment LDFs of concrete bridges using LRFD equations to those derived from FE models

Structure Number	LRFD/FEA (6-4-6)				LRFD/FEA (6-5-6)				LRFD/FEA (5-5-5)			
	Exterior Positive	Exterior Negative	Interior Positive	Interior Negative	Exterior Positive	Exterior Negative	Interior Positive	Interior Negative	Exterior Positive	Exterior Negative	Interior Positive	Interior Negative
19811	1.17	1.09	0.91	0.87	1.21	1.13	0.97	0.91	1.10	1.03	0.91	0.86
51111	1.00	0.97	0.95	0.91	1.03	1.01	1.00	0.96	0.94	0.91	0.94	0.90
608435	1.13	0.97	0.99	1.00	1.16	1.01	1.07	1.05	1.07	0.92	0.99	0.99
16611	0.96	NA	0.95	NA	0.99	NA	1.00	NA	0.91	NA	0.94	NA
47851	1.03	1.01	0.95	0.93	1.06	1.04	1.02	1.00	0.96	0.94	0.96	0.93
605525	1.10	1.13	0.91	0.89	1.12	1.15	0.98	0.96	1.03	1.05	0.91	0.88
601925	1.11	0.99	0.99	0.98	1.15	1.03	1.06	1.03	1.05	0.94	0.98	0.96
608560	1.27	1.05	1.04	1.02	1.31	1.09	1.14	1.07	1.19	0.99	1.04	1.00
609185	0.95	1.01	0.93	0.91	0.98	1.05	0.98	0.96	0.90	0.95	0.91	0.90
24171	1.08	1.06	0.96	0.94	1.11	1.09	1.06	1.02	1.01	0.99	0.97	0.93
13040	1.47	1.48	1.01	0.97	1.51	1.51	1.10	1.06	1.38	1.37	1.05	0.99
17301	1.15	1.08	0.97	0.95	1.18	1.11	1.04	1.01	1.07	1.00	0.97	0.94
22451	1.15	1.12	0.96	0.92	1.18	1.16	1.03	0.99	1.07	1.04	0.96	0.92
17571	1.05	1.03	0.90	0.93	1.08	1.07	0.96	0.99	0.98	0.96	0.90	0.92
604250	1.19	1.07	0.98	0.97	1.23	1.10	1.06	1.03	1.11	1.00	0.98	0.95
31190	1.43	1.46	1.00	0.98	1.45	1.45	1.12	1.08	1.35	1.33	1.06	1.01
45430	1.19	1.23	1.02	0.99	1.22	1.25	1.11	1.07	1.11	1.14	1.05	1.00
41430	1.64	1.75	1.09	1.05	1.63	1.73	1.18	1.15	1.54	1.65	1.10	1.05
41231	1.28	1.07	1.02	1.04	1.31	1.12	1.13	1.09	1.20	1.01	1.03	1.02
13170	1.47	1.48	1.11	1.09	1.47	1.46	1.22	1.20	1.38	1.37	1.14	1.11

Table 3.16 Ratios of moment LDFs of concrete bridges using LFD equations to those derived from FE models

Structure Number	LFD/FEA (6-4-6)				LFD/FEA (6-5-6)				LFD/FEA (5-5-5)			
	Exterior Positive	Exterior Negative	Interior Positive	Interior Negative	Exterior Positive	Exterior Negative	Interior Positive	Interior Negative	Exterior Positive	Exterior Negative	Interior Positive	Interior Negative
19811	1.30	1.28	0.95	0.95	1.35	1.32	1.00	1.00	1.22	1.20	0.94	0.94
51111	1.14	1.13	1.01	1.00	1.17	1.17	1.07	1.05	1.07	1.06	1.00	0.98
608435	1.10	1.06	0.92	1.04	1.13	1.10	0.99	1.08	1.04	1.00	0.91	1.02
16611	1.13	NA	1.05	NA	1.16	NA	1.10	NA	1.07	NA	1.04	NA
47851	1.09	1.09	0.95	0.95	1.12	1.13	1.02	1.02	1.02	1.02	0.96	0.95
605525	1.21	1.24	0.93	0.92	1.23	1.27	1.01	0.99	1.13	1.16	0.93	0.91
601925	1.11	1.08	0.93	1.01	1.14	1.12	1.00	1.06	1.04	1.02	0.92	1.00
608560	1.13	1.09	0.87	1.01	1.16	1.13	0.96	1.06	1.06	1.02	0.87	0.99
609185	1.06	1.14	0.97	0.97	1.09	1.18	1.03	1.02	1.00	1.06	0.96	0.95
24171	1.10	1.12	0.92	0.92	1.13	1.15	1.01	1.01	1.03	1.04	0.93	0.92
13040	1.41	1.43	0.91	0.88	1.44	1.46	0.98	0.96	1.33	1.33	0.94	0.89
17301	1.18	1.17	0.92	0.95	1.21	1.21	0.99	1.01	1.10	1.09	0.92	0.94
22451	1.20	1.21	0.93	0.92	1.24	1.25	0.99	0.99	1.12	1.12	0.93	0.91
17571	1.13	1.13	0.91	0.96	1.17	1.17	0.96	1.02	1.06	1.06	0.91	0.95
604250	1.25	1.22	0.91	0.97	1.28	1.26	0.98	1.03	1.16	1.14	0.90	0.95
31190	1.56	1.63	0.84	0.84	1.57	1.62	0.94	0.93	1.47	1.49	0.89	0.87
45430	1.35	1.41	0.91	0.90	1.39	1.44	0.99	0.97	1.27	1.31	0.94	0.90
41430	1.88	2.03	0.87	0.85	1.87	2.00	0.95	0.94	1.76	1.91	0.88	0.85
41231	1.19	1.17	0.86	1.02	1.22	1.22	0.95	1.07	1.12	1.10	0.87	1.01
13170	1.46	1.51	0.85	0.86	1.46	1.50	0.93	0.94	1.37	1.40	0.87	0.87

Table 3.17 Moment LDFs of steel bridges derived from FE models

Structure Number	FEA (6-4-6)				FEA (6-5-6)				FEA (5-5-5)			
	Exterior Positive	Exterior Negative	Interior Positive	Interior Negative	Exterior Positive	Exterior Negative	Interior Positive	Interior Negative	Exterior Positive	Exterior Negative	Interior Positive	Interior Negative
22520	0.51	0.53	0.84	0.79	0.50	0.50	0.80	0.75	0.54	0.55	0.85	0.80
16220	0.48	0.48	0.83	0.84	0.47	0.46	0.78	0.79	0.52	0.51	0.84	0.85
46730	0.53	0.54	0.75	0.78	0.51	0.51	0.72	0.73	0.56	0.58	0.76	0.79
46750	0.54	0.54	0.75	0.77	0.52	0.52	0.71	0.73	0.57	0.58	0.76	0.78
37570	0.60	0.62	0.84	0.86	0.58	0.59	0.81	0.81	0.64	0.65	0.86	0.87
25140	0.59	0.53	0.81	0.86	0.57	0.51	0.77	0.82	0.62	0.56	0.82	0.88
29110	0.48	0.47	0.83	0.84	0.47	0.46	0.78	0.79	0.51	0.51	0.84	0.85
15750	0.54	0.54	0.75	0.77	0.52	0.52	0.71	0.73	0.57	0.58	0.76	0.78
43370	0.54	0.00	0.92	0.00	0.52	0.00	0.87	0.00	0.57	0.00	0.93	0.00
50910	0.55	0.58	0.78	0.77	0.53	0.56	0.75	0.75	0.58	0.61	0.79	0.78
43880	0.57	0.52	0.89	0.89	0.55	0.50	0.85	0.84	0.60	0.55	0.91	0.91
606320	0.78	0.81	0.82	0.82	0.76	0.79	0.78	0.76	0.81	0.85	0.82	0.82
50995	0.79	0.77	0.72	0.69	0.77	0.74	0.69	0.66	0.83	0.80	0.72	0.70
22930	0.68	0.72	0.74	0.76	0.66	0.69	0.72	0.71	0.71	0.75	0.75	0.77
364700	0.78	0.82	0.76	0.76	0.76	0.79	0.74	0.74	0.82	0.85	0.77	0.76
19011	0.61	0.63	0.62	0.62	0.59	0.61	0.59	0.60	0.64	0.67	0.63	0.63
40521	0.71	0.75	0.71	0.71	0.69	0.72	0.69	0.69	0.75	0.78	0.72	0.72
13330	0.33	0.00	0.48	0.00	0.32	0.00	0.45	0.00	0.35	0.00	0.47	0.00
601356	0.74	0.76	0.85	0.75	0.72	0.74	0.81	0.73	0.78	0.80	0.85	0.75
609280	0.69	0.73	0.68	0.66	0.67	0.70	0.65	0.65	0.72	0.76	0.69	0.67

Table 3.18 Moment LDFs of steel bridges derived from LRFD and LFD equations

Structure Number	LRFD				LFD			
	Exterior Positive	Exterior Negative	Interior Positive	Interior Negative	Exterior Positive	Exterior Negative	Interior Positive	Interior Negative
22520	0.59	0.60	0.67	0.67	0.75	0.75	0.75	0.75
16220	0.61	0.60	0.72	0.71	0.75	0.75	0.75	0.75
46730	0.56	0.62	0.63	0.71	0.75	0.75	0.75	0.75
46750	0.54	0.56	0.65	0.66	0.75	0.75	0.75	0.75
37570	0.65	0.66	0.74	0.75	0.88	0.88	0.88	0.88
25140	0.63	0.65	0.72	0.73	0.81	0.81	0.81	0.81
29110	0.64	0.63	0.72	0.71	0.75	0.75	0.75	0.75
15750	0.57	0.61	0.65	0.69	0.75	0.75	0.75	0.75
43370	0.72	0.00	0.82	0.00	0.88	0.00	0.88	0.00
50910	0.56	0.59	0.63	0.67	0.81	0.81	0.81	0.81
43880	0.65	0.70	0.73	0.79	0.81	0.81	0.81	0.81
606320	0.71	0.73	0.69	0.71	0.89	0.89	0.89	0.89
50995	0.65	0.65	0.64	0.64	0.81	0.81	0.81	0.81
22930	0.60	0.61	0.71	0.72	0.88	0.88	0.88	0.88
364700	0.73	0.75	0.74	0.76	0.93	0.93	0.93	0.93
19011	0.54	0.52	0.58	0.56	0.67	0.67	0.67	0.67
40521	0.63	0.66	0.66	0.69	0.84	0.84	0.84	0.84
13330	0.37	0.00	0.48	0.00	0.45	0.00	0.45	0.00
601356	0.78	0.71	0.80	0.72	0.88	0.88	0.88	0.88
609280	0.59	0.62	0.63	0.67	0.82	0.82	0.82	0.82

And, the ratios of the moment LDFs of the steel bridges using the LRFD and LFD equations to those determined from the FE Models were calculated and are summarized in Table 3.19 and Table 3.20.

Table 3.19 Ratios of moment LDFs of steel bridges using LRFD equations to those derived from FE models

Structure Number	LRFD/FEA (6-4-6)				LRFD/FEA (6-5-6)				LRFD/FEA (5-5-5)			
	Exterior Positive	Exterior Negative	Interior Positive	Interior Negative	Exterior Positive	Exterior Negative	Interior Positive	Interior Negative	Exterior Positive	Exterior Negative	Interior Positive	Interior Negative
22520	1.17	1.13	0.80	0.85	1.20	1.20	0.84	0.89	1.10	1.08	0.79	0.84
16220	1.26	1.26	0.87	0.85	1.28	1.29	0.93	0.91	1.18	1.17	0.86	0.84
46730	1.06	1.15	0.85	0.91	1.10	1.22	0.89	0.96	1.00	1.08	0.84	0.89
46750	1.01	1.03	0.87	0.87	1.04	1.07	0.91	0.91	0.95	0.97	0.85	0.85
37570	1.08	1.07	0.87	0.87	1.12	1.12	0.91	0.93	1.02	1.02	0.86	0.86
25140	1.08	1.23	0.89	0.85	1.12	1.27	0.93	0.89	1.02	1.15	0.87	0.83
29110	1.32	1.33	0.87	0.85	1.35	1.36	0.92	0.91	1.24	1.24	0.86	0.83
15750	1.06	1.13	0.87	0.90	1.10	1.18	0.91	0.94	1.00	1.06	0.86	0.89
43370	1.35	NA	0.89	NA	1.40	NA	0.94	NA	1.27	NA	0.88	NA
50910	1.01	1.01	0.81	0.87	1.05	1.06	0.84	0.89	0.97	0.97	0.79	0.86
43880	1.14	1.35	0.82	0.90	1.17	1.40	0.86	0.94	1.07	1.27	0.80	0.87
606320	0.92	0.90	0.85	0.87	0.94	0.93	0.89	0.93	0.88	0.86	0.84	0.87
50995	0.82	0.85	0.89	0.93	0.85	0.88	0.93	0.97	0.79	0.82	0.88	0.93
22930	0.89	0.85	0.95	0.94	0.92	0.88	0.98	1.00	0.85	0.81	0.94	0.93
364700	0.94	0.92	0.97	1.00	0.96	0.95	1.00	1.02	0.90	0.88	0.97	1.00
19011	0.89	0.82	0.93	0.90	0.91	0.85	0.97	0.93	0.85	0.78	0.92	0.89
40521	0.88	0.88	0.93	0.97	0.91	0.91	0.96	1.00	0.84	0.84	0.92	0.96
13330	1.12	NA	0.99	NA	1.16	NA	1.07	NA	1.06	NA	1.01	NA
601356	1.05	0.93	0.94	0.97	1.08	0.96	0.99	1.00	1.00	0.89	0.94	0.97
609280	0.85	0.86	0.93	1.01	0.88	0.89	0.96	1.03	0.82	0.82	0.91	1.00

Table 3.20 Ratios of moment LDFs of steel bridges using LFD equations to those derived from FE models

Structure Number	LFD/FEA (6-4-6)				LFD/FEA (6-5-6)				LFD/FEA (5-5-5)			
	Exterior Positive	Exterior Negative	Interior Positive	Interior Negative	Exterior Positive	Exterior Negative	Interior Positive	Interior Negative	Exterior Positive	Exterior Negative	Interior Positive	Interior Negative
22520	1.47	1.42	0.90	0.95	1.52	1.51	0.94	1.00	1.38	1.36	0.88	0.93
16220	1.56	1.58	0.90	0.90	1.59	1.62	0.96	0.96	1.46	1.47	0.89	0.88
46730	1.42	1.38	1.00	0.97	1.46	1.46	1.05	1.02	1.34	1.30	0.99	0.95
46750	1.39	1.38	1.00	0.98	1.44	1.45	1.05	1.02	1.31	1.30	0.99	0.96
37570	1.46	1.42	1.04	1.02	1.51	1.48	1.09	1.09	1.38	1.35	1.03	1.01
25140	1.39	1.54	1.00	0.94	1.44	1.60	1.06	0.99	1.31	1.45	0.99	0.92
29110	1.56	1.58	0.90	0.89	1.59	1.62	0.96	0.95	1.46	1.47	0.90	0.88
15750	1.39	1.38	1.00	0.98	1.44	1.45	1.05	1.02	1.31	1.30	0.99	0.96
43370	1.65	NA	0.96	NA	1.70	NA	1.01	NA	1.55	NA	0.94	NA
50910	1.48	1.39	1.04	1.06	1.53	1.46	1.08	1.08	1.41	1.32	1.02	1.04
43880	1.43	1.56	0.91	0.92	1.47	1.62	0.96	0.97	1.35	1.46	0.89	0.90
606320	1.15	1.10	1.09	1.09	1.18	1.14	1.14	1.17	1.10	1.06	1.09	1.09
50995	1.02	1.05	1.12	1.16	1.05	1.09	1.17	1.21	0.98	1.01	1.11	1.16
22930	1.29	1.22	1.18	1.15	1.33	1.26	1.22	1.23	1.24	1.17	1.16	1.14
364700	1.19	1.14	1.22	1.23	1.23	1.19	1.26	1.26	1.14	1.09	1.22	1.23
19011	1.10	1.06	1.08	1.09	1.13	1.10	1.13	1.13	1.05	1.01	1.07	1.07
40521	1.18	1.13	1.18	1.18	1.22	1.17	1.22	1.21	1.13	1.08	1.17	1.17
13330	1.39	NA	0.95	NA	1.43	NA	1.02	NA	1.31	NA	0.96	NA
601356	1.19	1.15	1.03	1.17	1.22	1.19	1.09	1.21	1.12	1.09	1.03	1.17
609280	1.19	1.12	1.21	1.23	1.23	1.17	1.25	1.26	1.14	1.08	1.19	1.22

Table 3.15, Table 3.16, Table 3.19, and Table 3.20 indicate that the LDFs in the negative moment regions are almost the same as those in the positive moment regions for both exterior and interior girders.

Accordingly, only the LDFs in the positive moment regions were selected for further analysis. Five bridge parameters utilized in the AASHTO LRFD equations for calculating LDFs are number of girders, span length, girder spacing, longitudinal stiffness parameter (k_g), and deck thickness (or depth). The relationships between the ratios of the moment LDFs and the five parameters for the interior girder positive moment regions and the exterior girder positive moment regions of the concrete bridges are illustrated in Figure 3.10 and Figure 3.11, respectively.

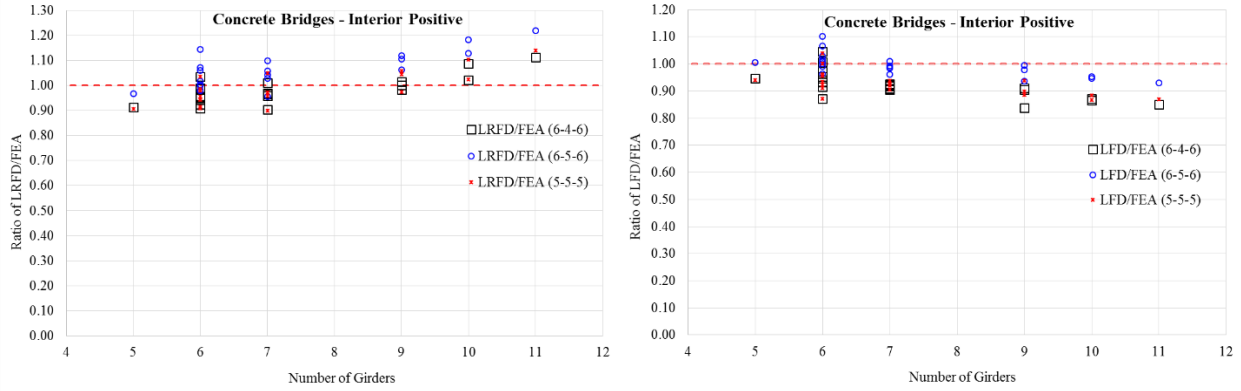

(a) Number of girders

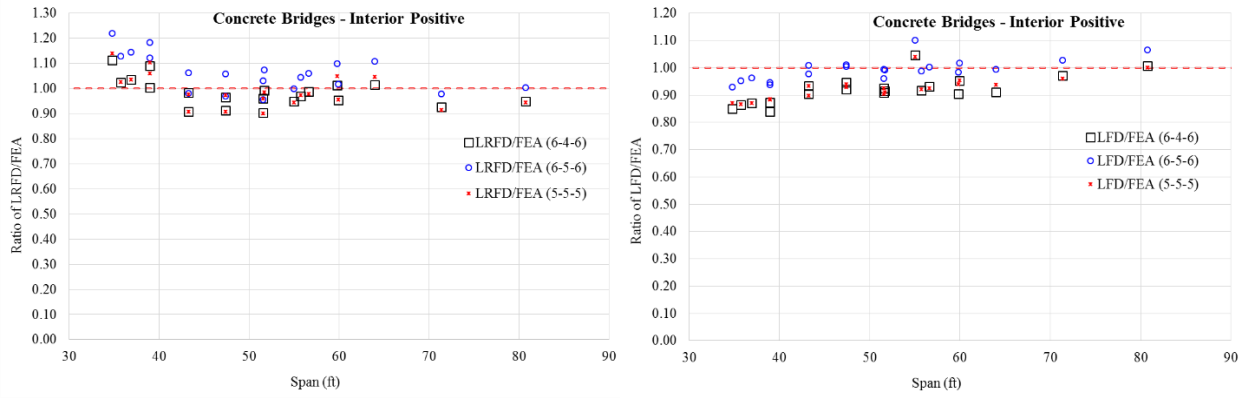

(b) Span length

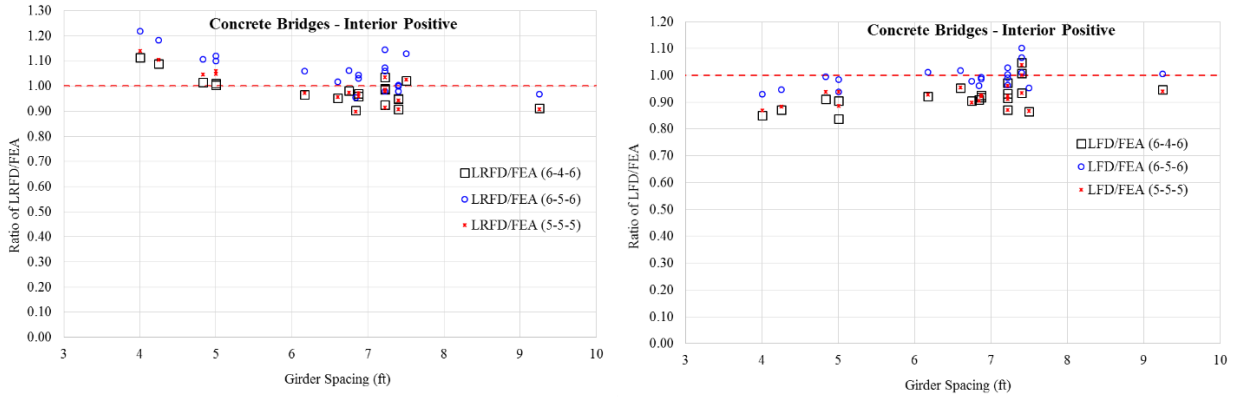

(c) Girder spacing

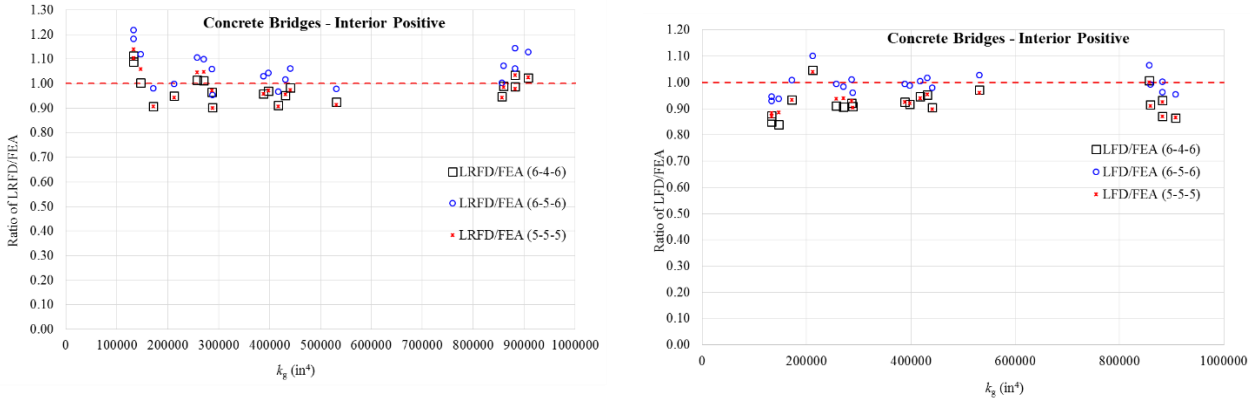

(d) Longitudinal stiffness parameter (k_g)

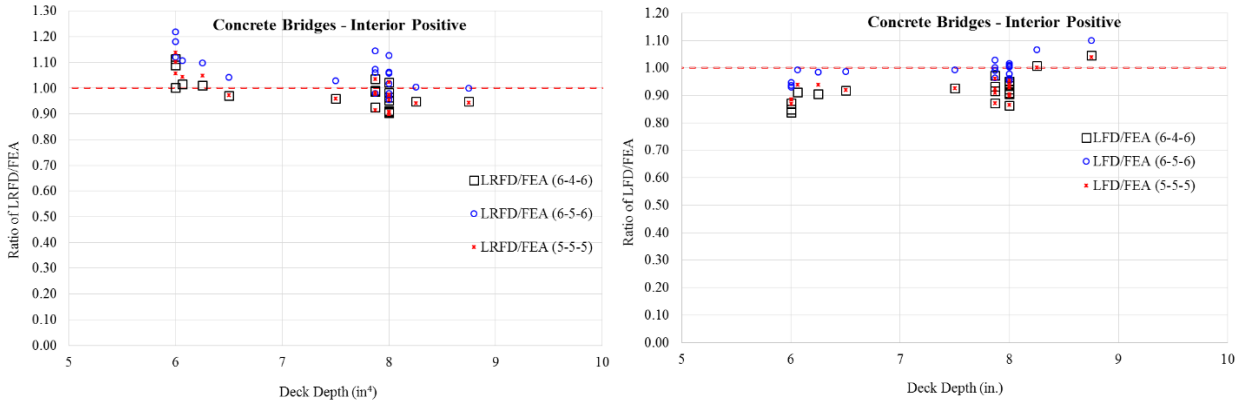

(e) Deck thickness

Figure 3.10 Relationships between the ratios of moment LDFs with LRFD and LFD results for concrete bridges – interior girder positive moment regions

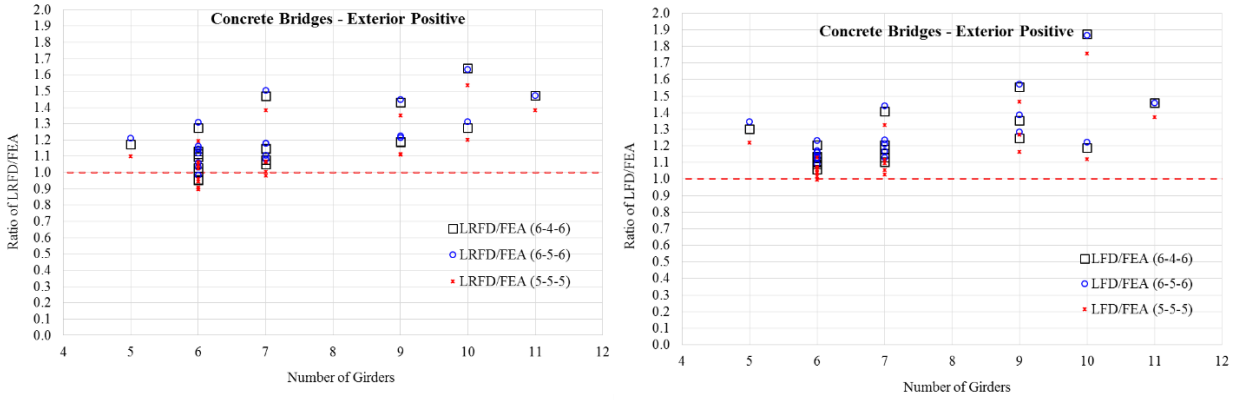

(a) Number of girders

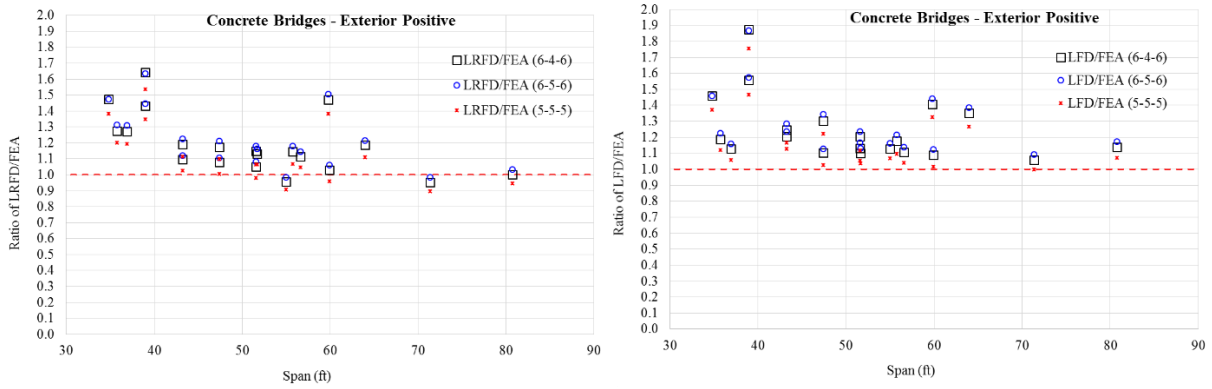

(b) Span length

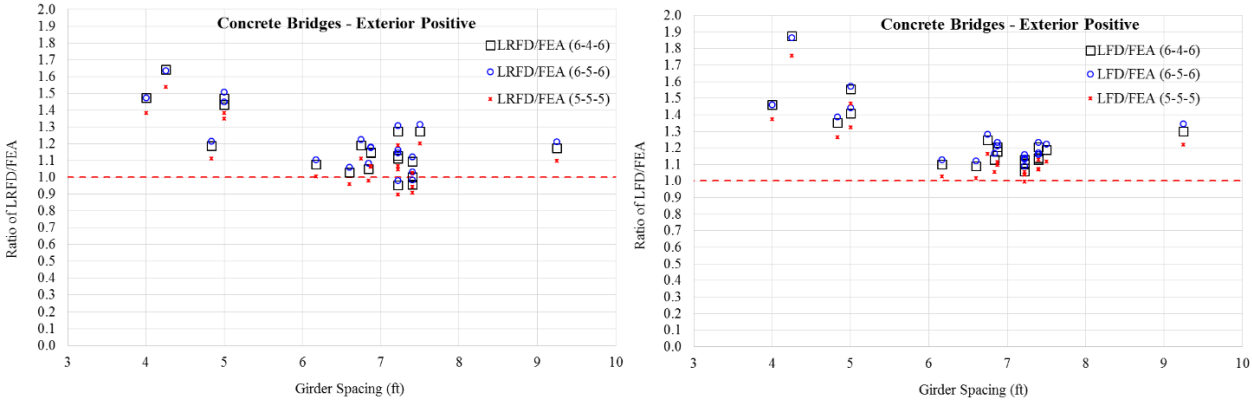

(c) Girder spacing

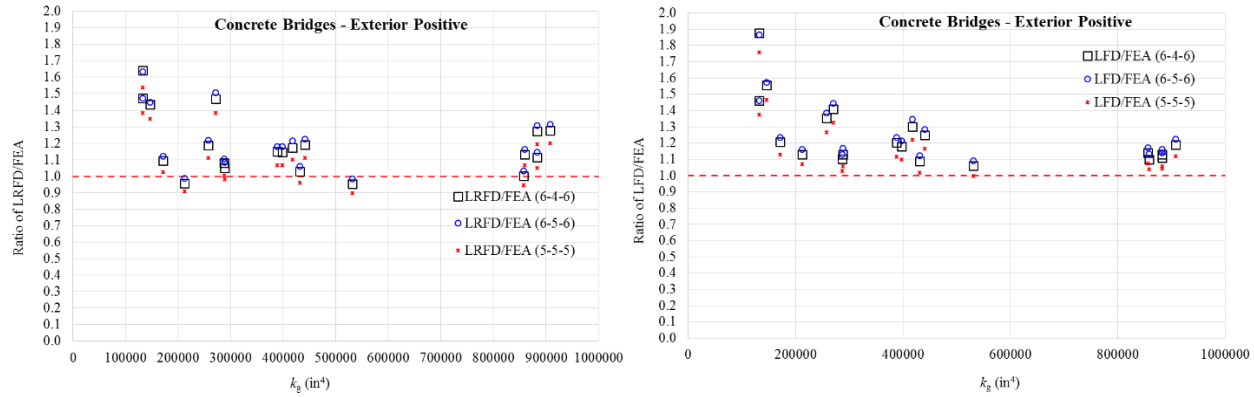

(d) Longitudinal stiffness parameter (k_g)

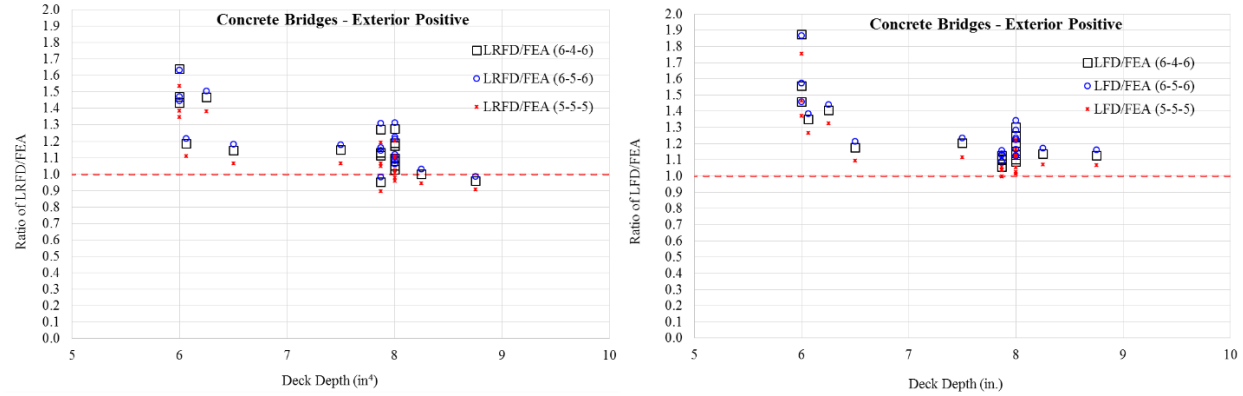

(e) Deck thickness

Figure 3.11 Relationships between the ratios of moment LDFs and bridge parameters for concrete bridges – exterior girder positive moment regions

The relationships between the ratios of the moment LDFs and the five parameters for the interior girder positive moment regions and the exterior girder positive moment regions of the steel bridges are illustrated in Figure 3.12 and Figure 3.13, respectively.

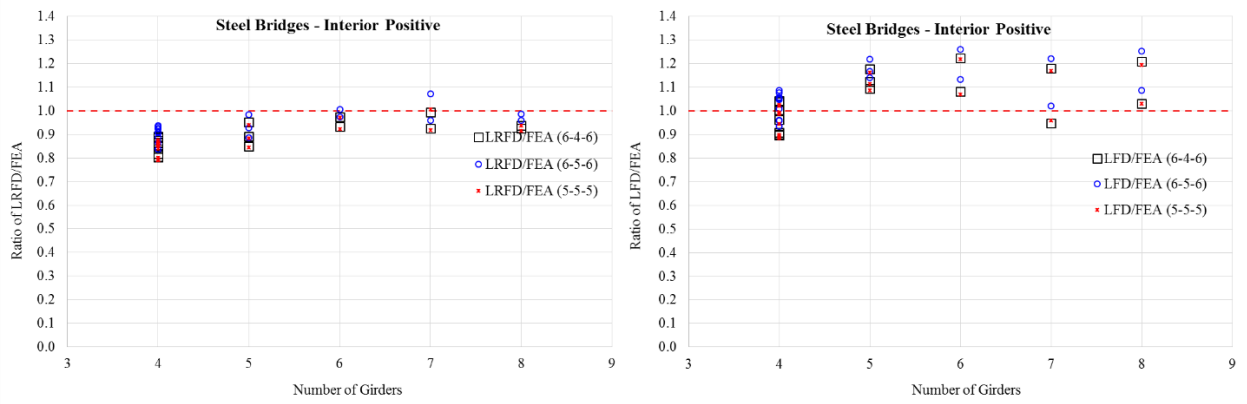

(a) Number of girders

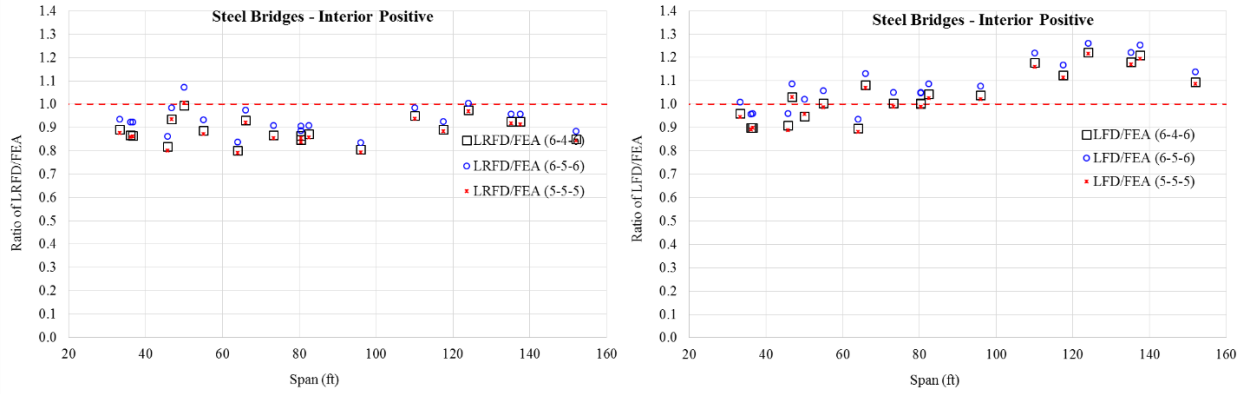

(b) Span length

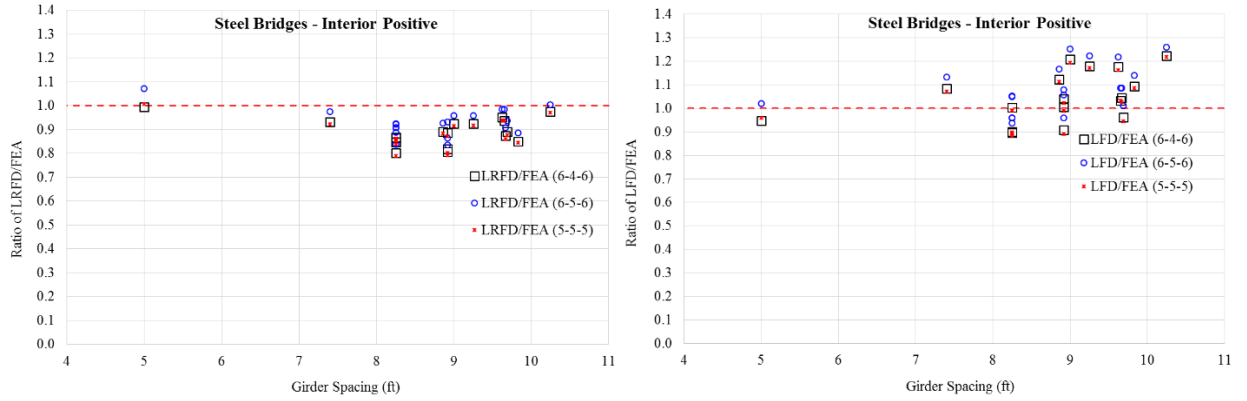

(c) Girder spacing

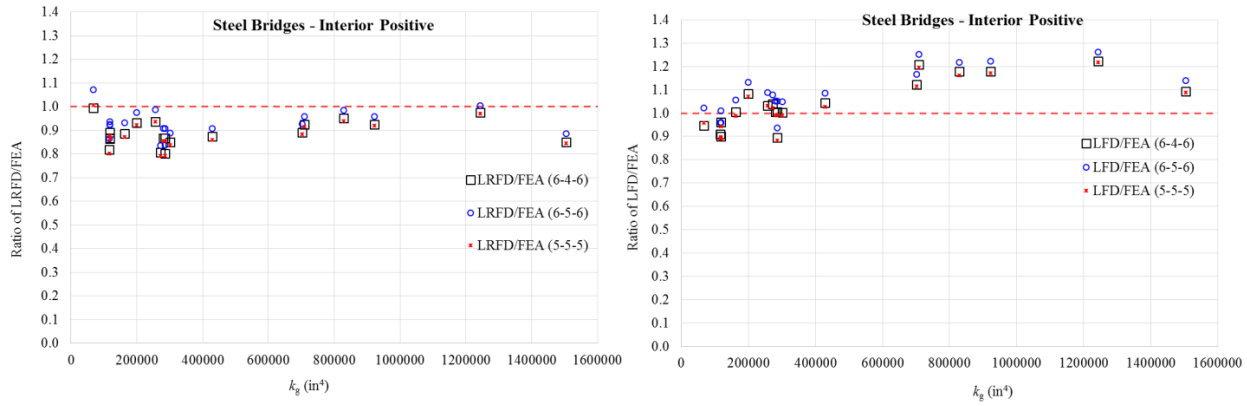

(d) Longitudinal stiffness parameter (k_g)

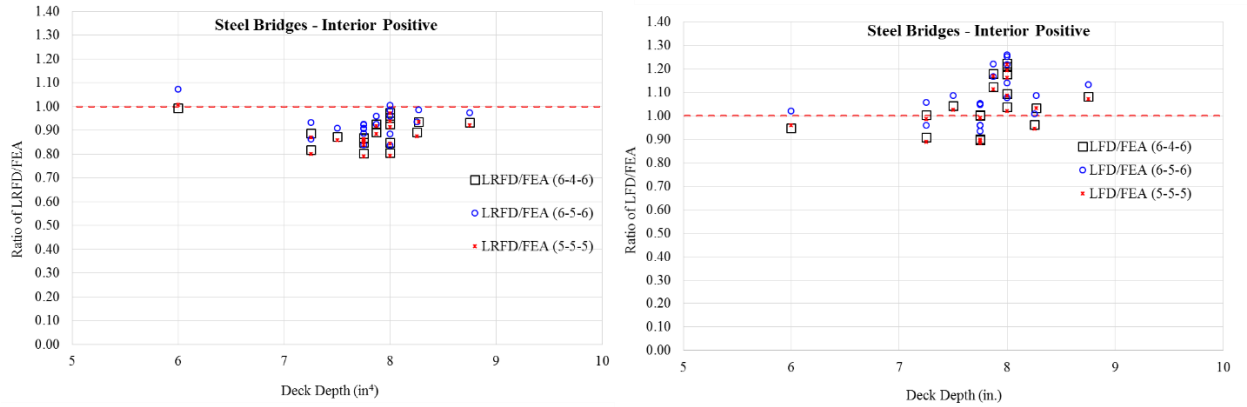

(e) Deck thickness

Figure 3.12 Relationships between the ratios of moment LDFs and bridge parameters for steel bridges – interior girder positive moment regions

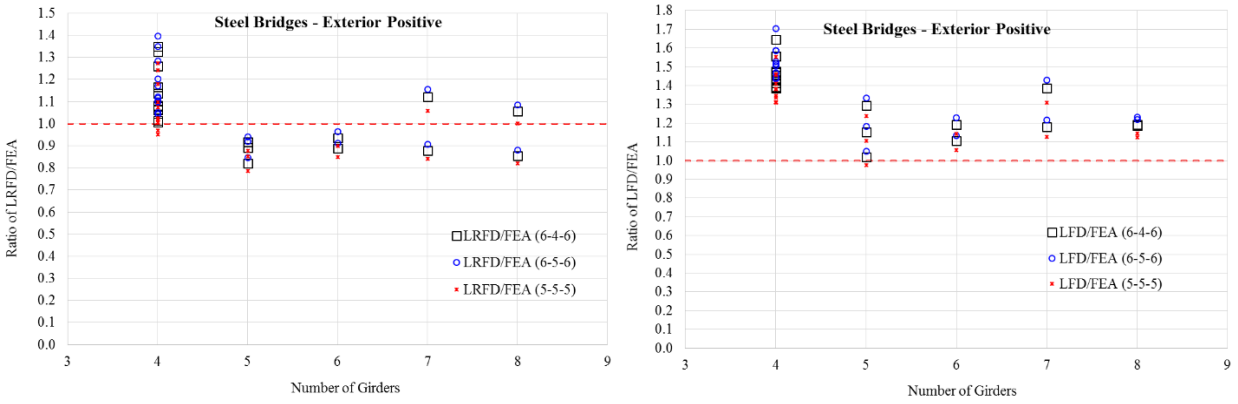

(a) Number of girders

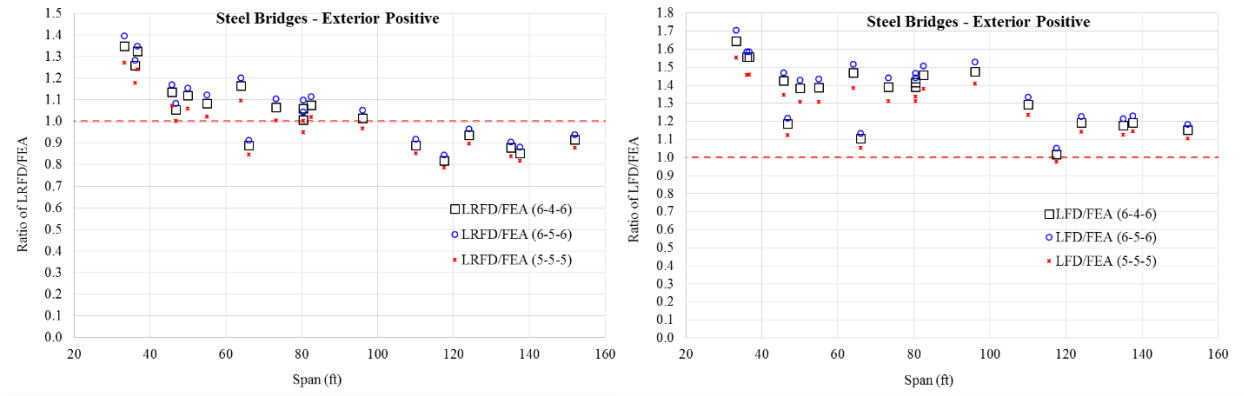

(b) Span length

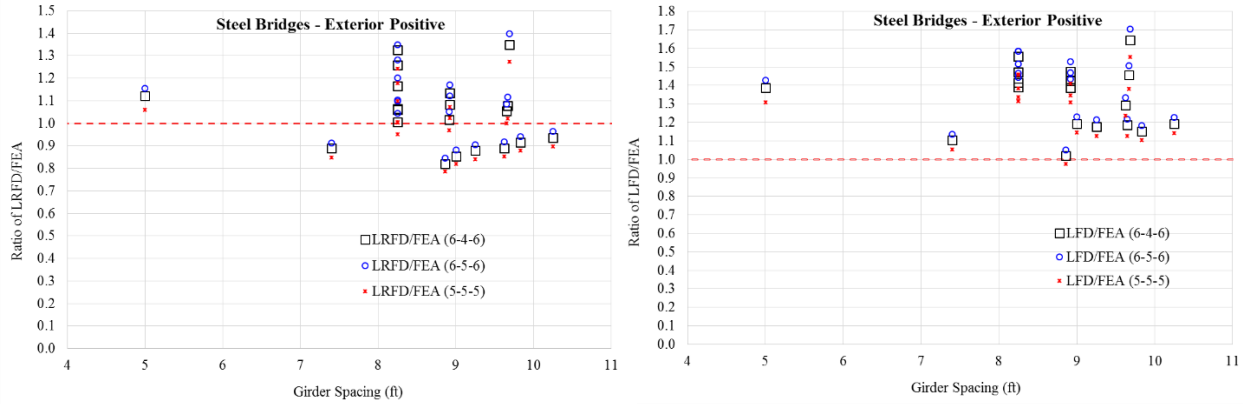

(c) Girder spacing

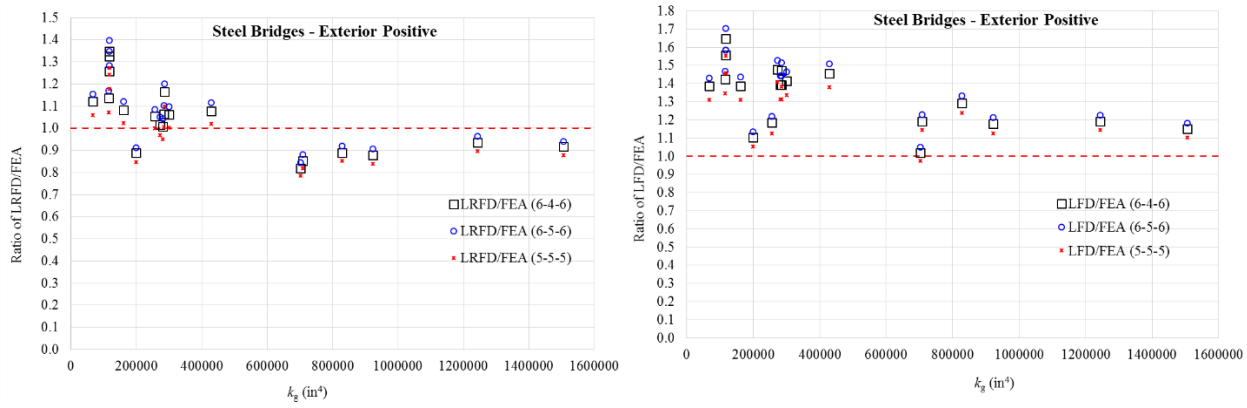

(d) Longitudinal stiffness parameter (k_g)

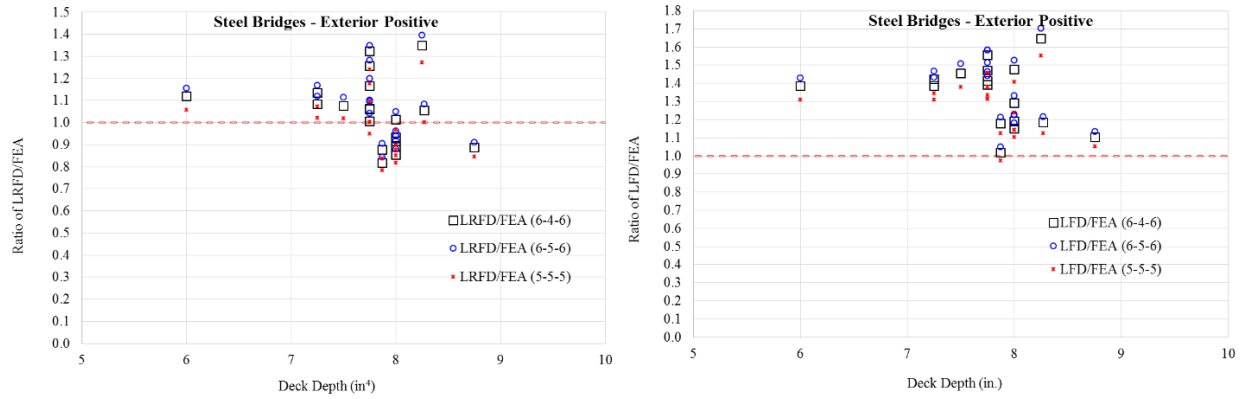

(e) Deck thickness

Figure 3.13 Relationships between the ratios of moment LDFs and bridge parameters for steel bridges – exterior girder positive moment regions

For the concrete girder bridges, Figure 3.10 indicates that the LRFD equations provide good estimations of the moment LDFs for the interior girders and the ratios of the moment LDFs range from 0.9 to 1.1; also, the LFD equations underestimate the moment LDFs of the interior girders with the ratios of the moment LDFs mostly less than 1.0. Figure 3.11 indicates that the LRFD equations overestimate the moment LDFs for the exterior girders and the ratios of the moment LDFs range from 0.9 to 1.7; also, the LFD equations overestimate the moment LDFs of the exterior girders and the ratios of the moment LDFs are mostly larger than 1.0.

For the steel girder bridges, Figure 3.12 indicates that the LRFD equations underestimate the moment LDFs of the interior girders and the ratios of the moment LDFs range from 0.8 to 1.0; also, the LFD equations overestimate the moment LDFs of interior girders with the ratios of the moment LDFs mostly larger than 1.0. Figure 3.13 indicates that the LRFD equations sometimes underestimate the moment LDFs for the exterior girders with the ratios of the moment LDFs ranging from 0.8 to 1.4; and, the LFD equations overestimate the moment LDFs of the exterior girders and the ratios of the moment LDFs are mostly larger than 1.0.

Figure 3.10 through Figure 3.13 indicate that the LRFD equations give more consistent predictions compared to the LFD equations. From Figure 3.10 through Figure 3.13, good relationships between the important bridge parameters and the ratios of the moment LDFs were not always found, but still some general trends were observed. For instance, the LRFD equations are less conservative for the interior girders when the number of girders is less than or equal to 5 (see Figure 3.12); the LRFD equations are less conservative for the exterior girders when the number of girders is more than 4 and the span length is loger than 100 ft (see Figure 3.13).

Figure 3.10 through Figure 3.13 also demonstrate that the results associated with Truck-5-5 and Truck-6-5 compare well with those associated with Truck-6-4 and those predicted using the FE models; and, the results associated with Truck-6-5 are the lower bound of the moment LDFs among all types of dual-lane loads. Consequently, the Iowa DOT current practice of moment LDFs associated with Truck-5-5 and Truck-6-5 appears reasonable and adequate.

3.3.4.2 Ratios of Shear LDFs

Following the same procedure of determining ratios of moment LDFs, the relationships between the ratios of shear LDFs with the three parameters used in the AASHTO equations for interior girders and exterior girders of steel girder bridges are illustrated in Figure 3.14 and Figure 3.15, respectively.

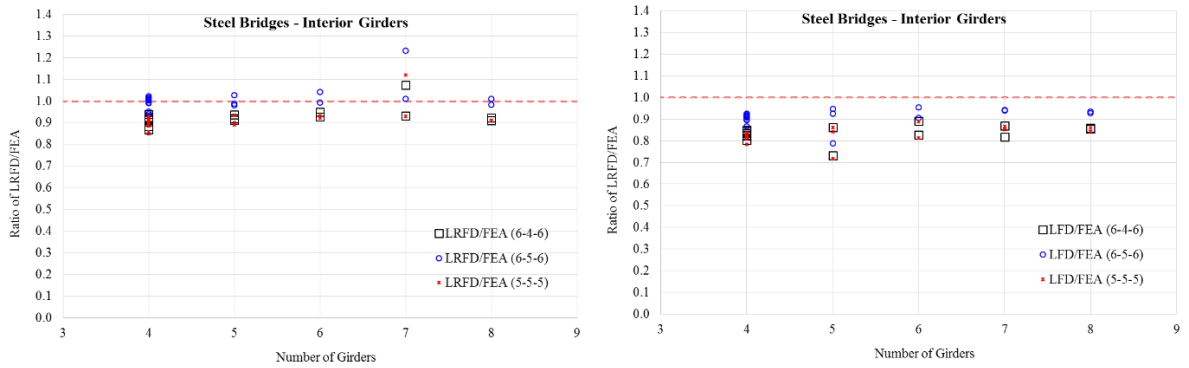

(a) Number of girders

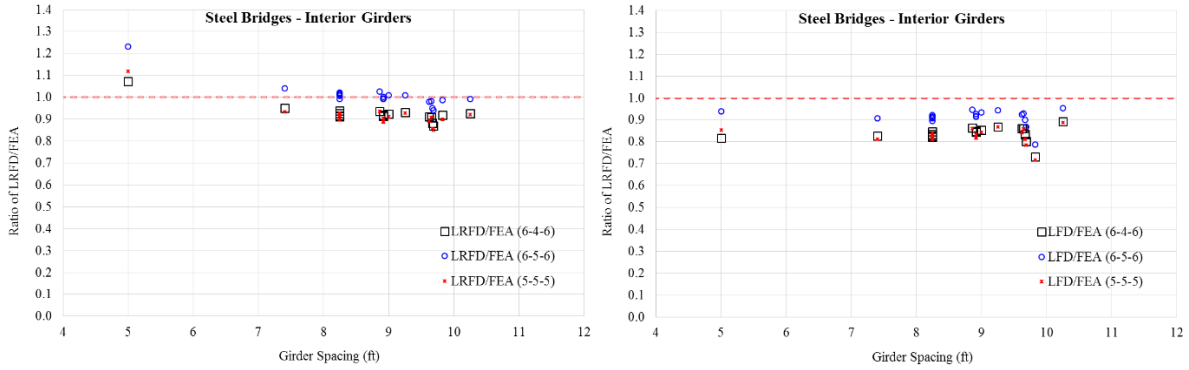

(b) Girder spacing

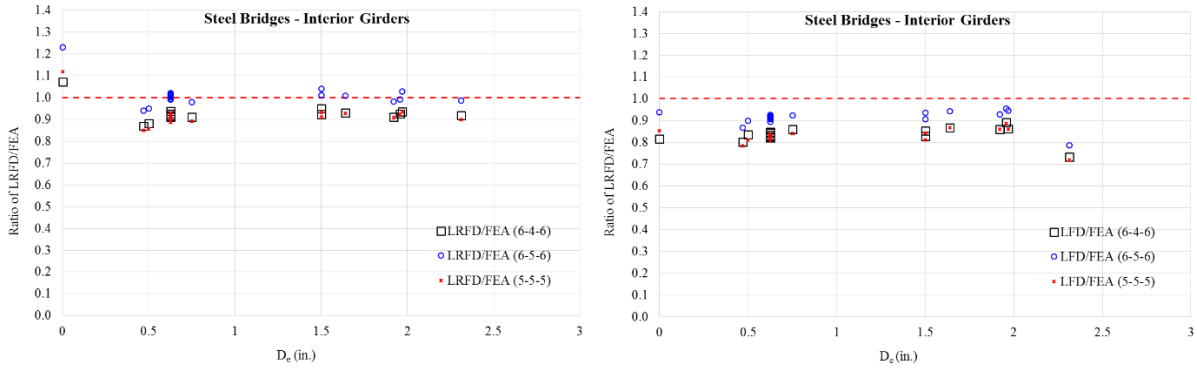

(c) D_e

Figure 3.14 Relationships between the ratios of shear LDFs and bridge parameters for steel bridges – interior girders

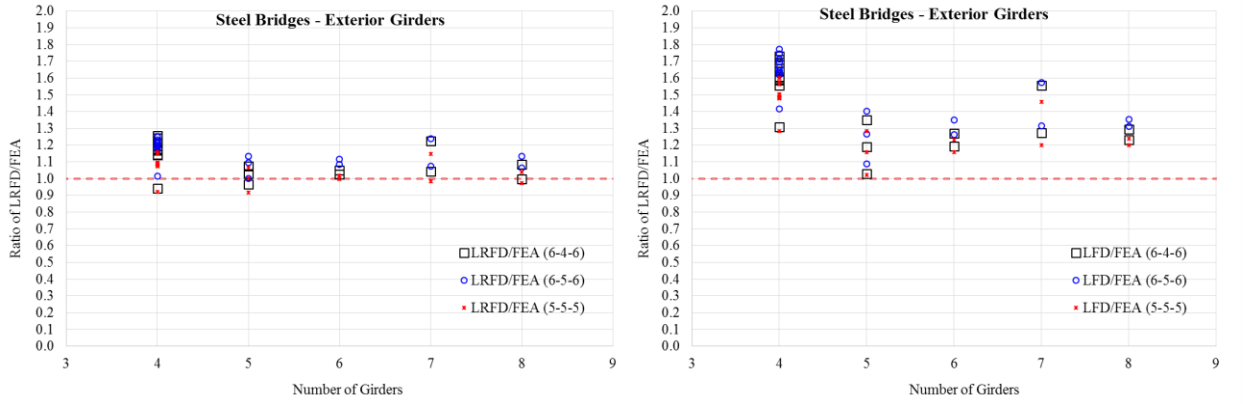

(a) Number of girders

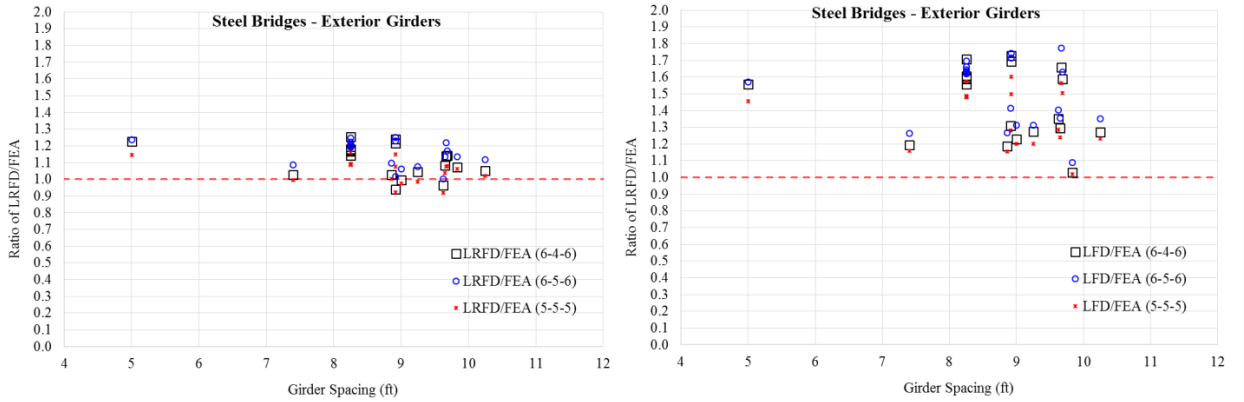

(b) Girder spacing

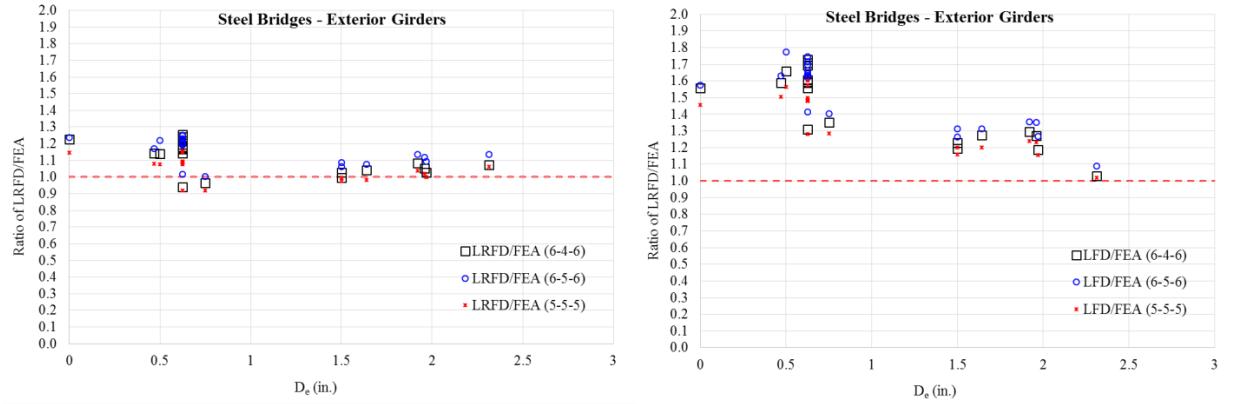

(c) D_e

Figure 3.15 Relationships between the ratios of shear LDFs and bridge parameters for steel bridges – exterior girders

For the steel girder bridges, Figure 3.14 indicates that the LRFD equations underestimate the shear LDFs for the interior girders and that the ratios of the shear LDFs range from 0.85 to 1.1; and the LFD equations underestimate shear LDFs for the interior girders with the ratios of the moment LDFs ranging from 0.75 to 0.95. Figure 3.15 indicates that the LRFD equations

overestimate the shear LDFs of the exterior girders and the ratios of the shear LDFs range from 0.9 to 1.3; also, the LFD equations overestimate the moment LDFs for the exterior girders and the ratios of the shear LDFs mostly larger than 1.0.

Figure 3.14 and Figure 3.15 also indicate that the LRFD equations give more consistent predictions than the LFD equations. Some general trends relating the shear LDFs with the bridge parameters were found and can be observed in Figure 3.14 and Figure 3.15. For instance, the LRFD equations are less conservative for interior girders when the number of girders is less than 5 and when larger girder spacing is present (see Figure 3.14); the LRFD equations are less conservative for exterior girders when the number of girders is less than 5 (see Figure 3.15).

Figure 3.14 and Figure 3.15 also demonstrate that the results associated with Truck-5-5 and Truck-6-5 compare well with those associated with Truck-6-4 and those predicted using the FE models; additionally, the results associated with Truck-6-5 are the lower bound of the shear LDFs among all types of dual-lane loads. Consequently, the Iowa DOT current practice on shear LDFs associated with Truck-5-5 and Truck-6-5 is reasonable and adequate.

3.4 Results of Equivalent Width Factor for Slab Bridges

3.4.1 Demonstration of Equivalent Width Derivation Based on FE Models

In this section, slab Bridge 608740 is used to demonstrate the process of calculating the equivalent deck width from FE results. Bridge 608740 is a three-span slab bridge with its cross-section as shown in Figure 3.16.

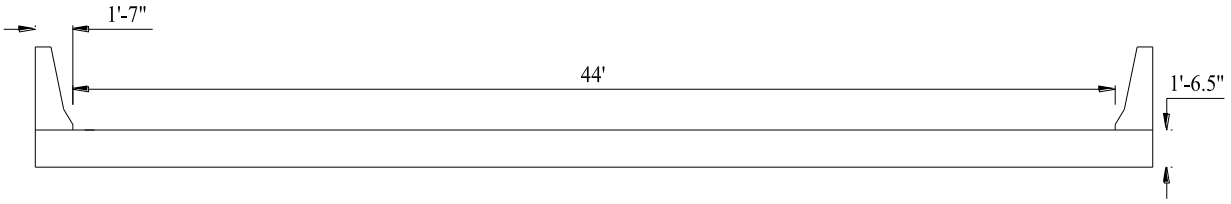

Figure 3.16 Cross-section of Bridge 608740

The bridge is simply supported at the pier and abutment locations. The bridge has a deck thickness of 1 ft-6.5 in., a deck width of 47 ft-2 in., a roadway width of 44 ft, and span lengths of 33 ft-6 in., 43 ft, and 33 ft-6 in. The distance from the inside edge of the barrier rail to the deck edge is 1 ft-7 in.

Based on the details and dimensions of the bridge, the FE model was established as shown in Figure 3.17.

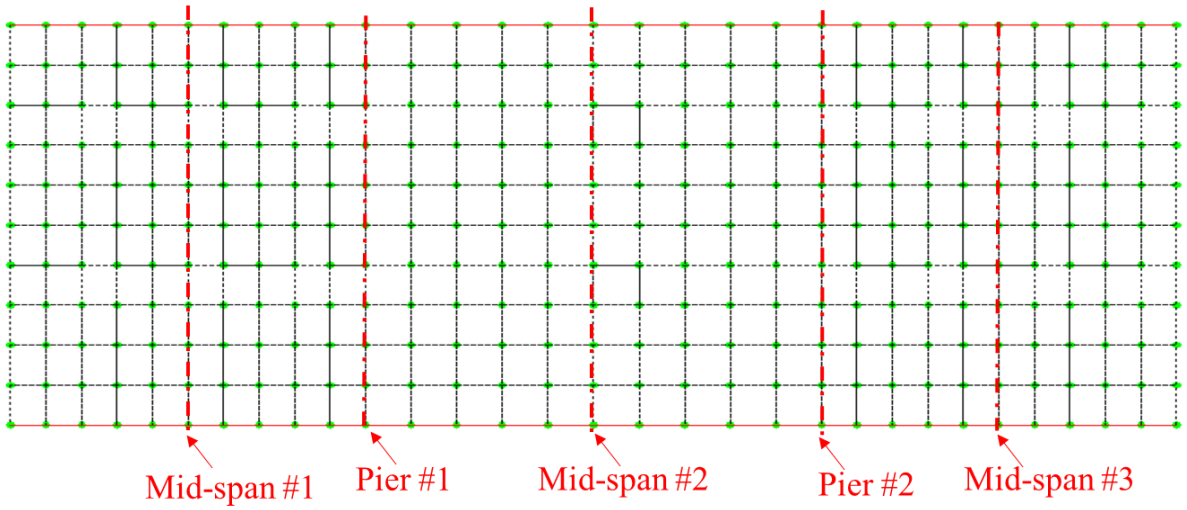

Figure 3.17 FE model of Bridge 608740

For consistency with other processes, the deck equivalent widths were determined for the bridge cross-sections at mid-spans #1, #2, and #3 and piers #1 and #2. Also, the equivalent widths were further categorized as: (1) the positive moment region (mid-spans #1, #2, and #3) and (2) the negative moment region (piers #1 and #2). From the calculated results, the largest value was taken as the equivalent width for each region.

Similar to the concrete and steel girder bridges, the same dual-lane loads were utilized to investigate their effects on equivalent width. That is, a total of 22 types of single-axle four-wheel-line loads were applied to the established bridge model as summarized earlier in Table 3.5 and as shown in Figure 3.18.

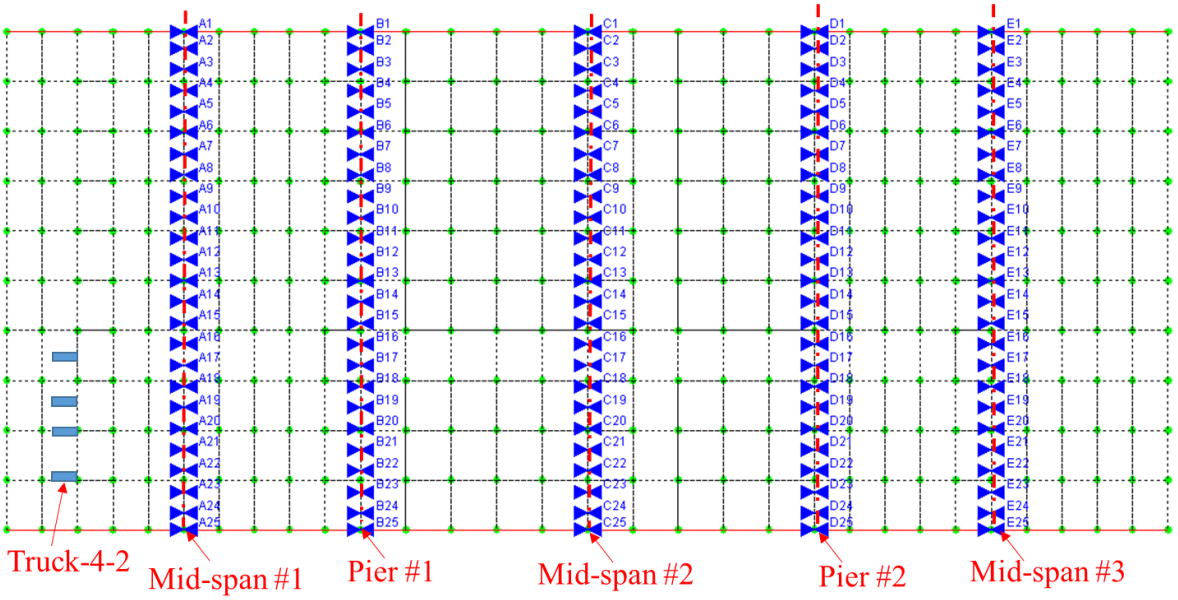

Figure 3.18 FE model of Bridge 16220

For each truck type, various loading cases with different transverse positions were taken into account for the dual-lane truck traveling across the bridge. These transverse positions extended from one side of the bridge to the other side with the outermost wheel lines located no less than 2 ft away from the bridge barrier rails.

Take, for example, the dual-lane load Truck-4-2, which will be used to illustrate the equivalent width calculation process. Truck-4-2 travels across the bridge in a transverse position with an outermost wheel line 2 ft away from the bridge barrier rail and at an incremental longitudinal travel position of every 5 ft from one end of the bridge to the other end. The bridge cross-sections at mid-spans #1, #2, and #3 and piers #1 and #2 (designated as sections A, B, C, D, and E, respectively) have "simulated strain gauges" transversely spaced at 2 ft to determine the response at the bottom of the deck at these location. The gauges are numbered from one edge to the other edge of the deck, from 1 through 25.

Section A will be used as an example to determine the deck equivalent width. The strain profiles determined for the 25 simulated gauges at Section A for different travel positions are shown in Figure 3.19(a).

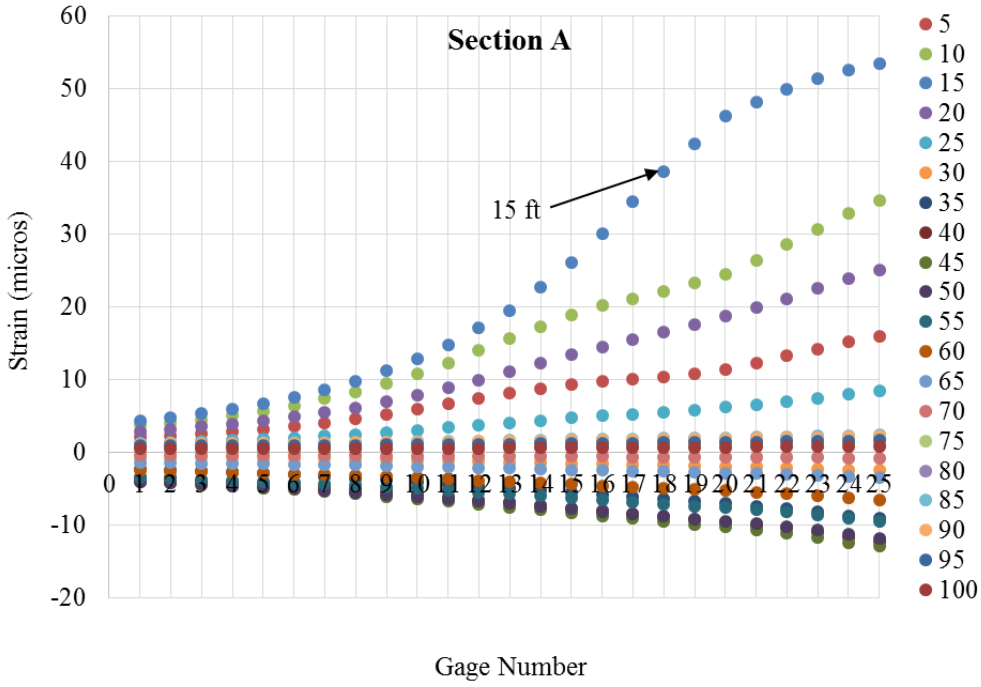

(a) Different longitudinal travel positions

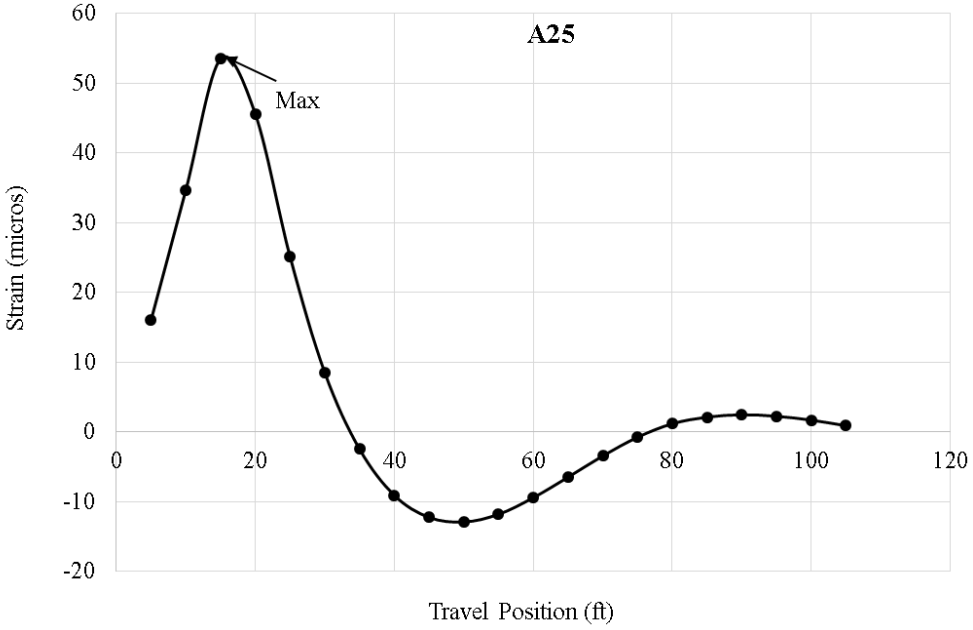

(b) Gauge A25

Figure 3.19 Strain in gauges of Section A for different travel positions

Figure 3.19(a) indicates that the maximum strain was reached when the truck had a longitudinal position of 15 ft and the maximum strain occurred at location A25. The strain-travel position relationship of gauge A25 is illustrated in Figure 3.19(b). Accordingly, the strain profile at the travel position of 15 ft was utilized to determine the equivalent width shown in Figure 3.20.

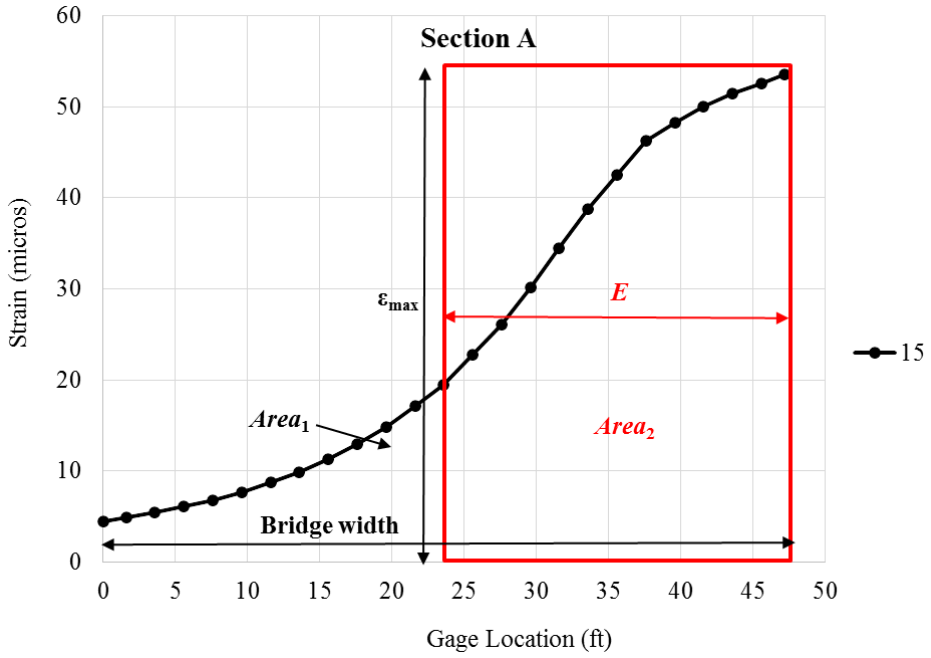

Figure 3.20 Calculation of equivalent width based on strain profile in Section A

The area below the strain curve is defined as $Area_1$ and the area consisting of the maximum strain (ε_{max}) multiplied by the equivalent width (E) is defined as $Area_2$, as illustrated in Figure 3.20.

Determining the equivalent width is as simple as determining the equivalent width required to ensure that $Area_1$ is equal to $Area_2$. Once the equivalent width was calculated for Section A, the equivalent widths for other four sections were also determined using the same approach with the results as summarized in Table 3.21.

Table 3.21 Equivalent widths of different sections

	Section A	**Section B**	**Section C**	**Section D**	**Section E**
Equivalent width	10.94	10.53	11.19	8.65	10.86

Likewise, the equivalent widths were determined for different transverse positions of Truck-4-2, and the smallest of the equivalent widths corresponding to each transverse position was taken as the final equivalent width for each section. Following the same procedure, the equivalent widths at different sections due to different types of dual-lane loads were derived and are summarized in Table 3.22.

Table 3.22 Equivalent widths at different sections due to different dual-lane loads

Truck Type	Outer Spacing (ft)	Inner Spacing (ft)	Equivalent Width (ft)				
			Section A	Section B	Section C	Section D	Section E
Truck-4-2	4	2	10.94	10.53	11.19	8.65	10.86
Truck-4-2.5	4	2.5	11.11	10.7	11.34	8.84	11.03
Truck-4-3	4	3	11.26	10.85	11.48	9	11.17
Truck-4-3.5	4	3.5	11.4	11.01	11.61	9.17	11.31
Truck-4-4	4	4	11.55	11.17	11.74	9.33	11.46
Truck-4-4.5	4	4.5	11.71	11.34	11.88	9.51	11.61
Truck-4-5	4	5	11.87	11.51	12.02	9.69	11.76
Truck-5-2	5	2	11.66	11.19	11.93	9.45	11.6
Truck-5-2.5	5	2.5	11.82	11.36	12.07	9.63	11.75
Truck-5-3	5	3	11.98	11.53	12.22	9.81	11.91
Truck-5-3.5	5	3.5	12.15	11.71	12.37	10.01	12.07
Truck-5-4	5	4	12.32	11.89	12.52	10.21	12.23
Truck-5-4.5	5	4.5	12.5	12.08	12.68	10.42	12.4
Truck-5-5	5	5	12.68	12.27	12.84	10.64	12.58
Truck-6-2	6	2	12.43	11.91	12.7	10.33	12.37
Truck-6-2.5	6	2.5	12.61	12.1	12.86	10.55	12.54
Truck-6-3	6	3	12.79	12.29	13.03	10.77	12.72
Truck-6-3.5	6	3.5	12.97	12.48	13.19	10.99	12.9
Truck-6-4	6	4	13.14	12.66	13.35	11.19	13.06
Truck-6-4.5	6	4.5	13.32	12.84	13.51	11.4	13.24
Truck-6-5	6	5	13.46	13.01	13.64	11.55	13.37
Truck-3-3	3	3	7.79	4.99	7.11	5.06	7.35

Also, as previously discussed, the equivalent widths at different sections in the negative and positive regions due to different configurations of dual-lane loads were determined and are summarized in Table 3.23.

Table 3.23 Equivalent widths at different regions due to different dual-lane loads

Truck Type	Outer Spacing (ft)	Inner Spacing (ft)	Equivalent Width (ft)	
			Positive Moment Region	Negative Moment Region
Truck-4-2	4	2	10.9	8.7
Truck-4-2.5	4	2.5	11.0	8.8
Truck-4-3	4	3	11.2	9.0
Truck-4-3.5	4	3.5	11.3	9.2
Truck-4-4	4	4	11.5	9.3
Truck-4-4.5	4	4.5	11.6	9.5
Truck-4-5	4	5	11.8	9.7
Truck-5-2	5	2	11.6	9.5
Truck-5-2.5	5	2.5	11.8	9.6
Truck-5-3	5	3	11.9	9.8
Truck-5-3.5	5	3.5	12.1	10.0
Truck-5-4	5	4	12.2	10.2
Truck-5-4.5	5	4.5	12.4	10.4
Truck-5-5	5	5	12.6	10.6
Truck-6-2	6	2	12.4	10.3
Truck-6-2.5	6	2.5	12.5	10.6
Truck-6-3	6	3	12.7	10.8
Truck-6-3.5	6	3.5	12.9	11.0
Truck-6-4	6	4	13.1	11.2
Truck-6-4.5	6	4.5	13.2	11.4
Truck-6-5	6	5	13.4	11.6
Truck-3-3	3	3	7.1	5.0
LRFD			11.8	11.8

3.4.2 Equivalent Widths Derived Using LRFD Equations

For slab-type bridges, equivalent widths (also named equivalent strip widths) of longitudinal strips per lane due to dual-lane loads can be calculated with (AASHTO LRFD 2010):

$$E = 84 + 1.44\sqrt{L_1 W_1} \le \frac{12W}{N_L} \quad \textbf{(10)}$$

where, E = equivalent width (in.), L_1 = modified span length taken equal to the lesser of the actual span or 60 (ft, W_1 = modified edge-to-edge width of the actual width or 60 for multilane loading (ft), and W = physical edge-to-edge width of bridge (ft).

For Bridge 608470, equivalent widths determined using the FE model were compared with those obtained using the AASHTO LRFD equations (as shown in Table 3.23). The equivalent widths are further illustrated in Figure 3.21 to demonstrate the relationships between the LDFs and wheel-line spacing.

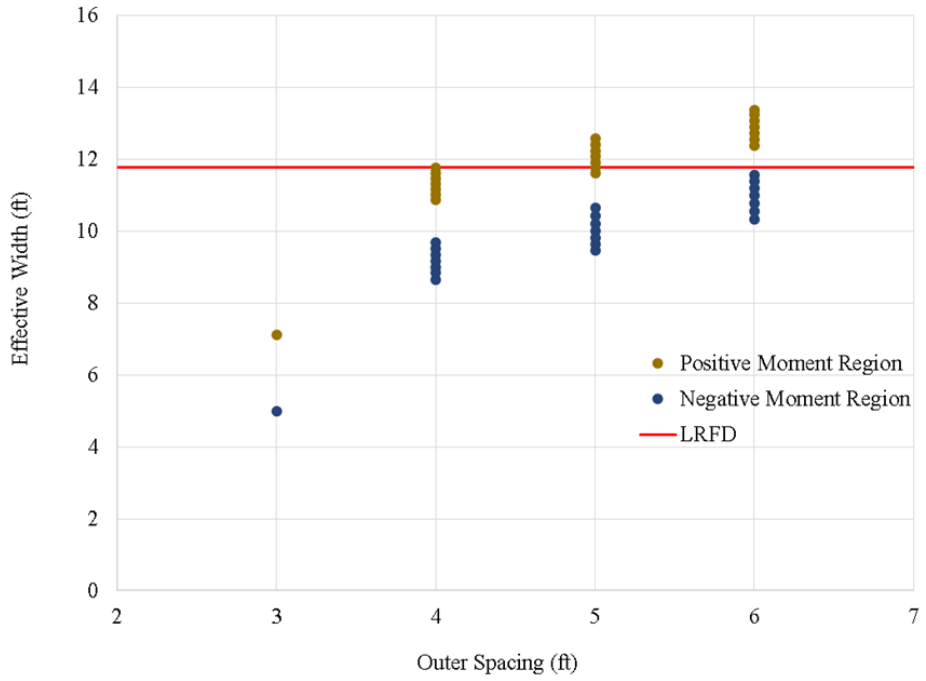

(a) Outer spacing

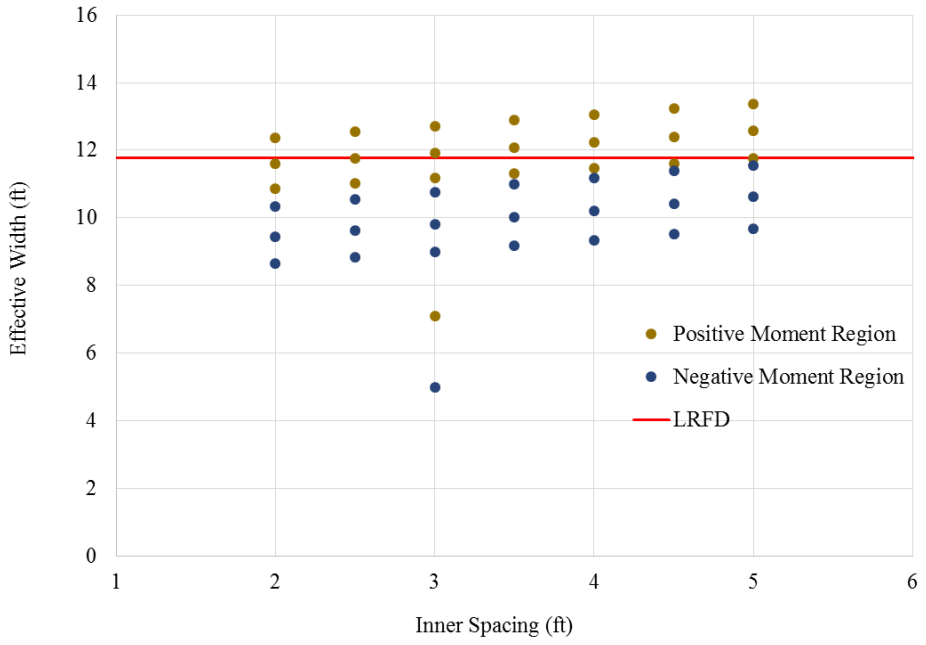

(b) Inner spacing

Figure 3.21 Comparisons of equivalent widths from FE model with LRFD results

Table 3.23 and Figure 3.21 indicate the equivalent width increases with an increase in the outer and inner spacing of a dual-lane load; also, the LRFD equations overestimate the equivalent width for the positive moment region but underestimate the equivalent width for the negative moment region.

3.4.3 Comparisons of Effective Widths Obtained Using FE Models with Those Using AASHTO Equations

Similar to the LDF evaluation, the Iowa DOT five-foot requirement and AASHTO equations were also evaluated for the equivalent width evaluation. And, Truck-5-5, Truck-6-4, and Truck-6-5 were selected for comparison purposes. The equivalent widths of the slab bridges derived using the FE models under the three types of dual-lane loads (i.e., Truck-5-5, Truck-6-5, and Truck-6-4) and the AASHTO LRFD equations are summarized in Table 3.24.

Table 3.24 Equivalent widths of slab bridges derived using FE models and AASHTO LRFD equations

Structure Number	FEA (6-4-6)		FEA (6-5-6)		FEA (5-5-5)		LFRD	
	Positive Moment	Negative Moment	Positive Moment	Negative Moment	Positive Moment	Negative Moment	Positive Moment	Negative Moment
15280	13.3	NA	13.5	NA	12.9	NA	11.3	11.3
46391	13.6	11.2	13.9	11.6	13.3	10.8	12.0	12.0
36210	12.2	11.8	12.6	12.2	11.8	11.3	10.9	10.9
53360	12.0	10.3	12.2	10.7	11.7	9.8	11.0	11.0
28670	12.8	11.5	13.2	11.9	12.4	10.9	11.5	11.5
14070	13.7	12.8	14.1	13.4	13.2	12.3	10.4	10.4
26780	12.1	11.2	12.4	11.6	11.6	10.7	10.4	10.4
36541	13.2	11.1	13.5	11.4	12.8	10.6	12.0	12.0
605755	12.9	11.0	13.2	11.3	12.5	10.5	11.7	11.7
23710	13.3	11.2	13.6	11.5	12.9	10.7	12.0	12.0
39441	12.2	0.0	12.5	NA	11.8	NA	10.9	10.9
49980	12.9	11.0	13.1	11.4	12.5	10.5	11.3	11.3
26860	11.5	0.0	11.7	NA	11.1	NA	9.7	9.7
29571	12.7	11.4	13.0	11.8	12.2	10.7	11.3	11.3
14371	13.0	10.9	13.2	11.2	12.6	10.4	11.4	11.4
608740	13.1	11.2	13.4	11.6	12.6	10.6	11.8	11.8
17990	12.4	10.3	12.7	10.6	12.0	9.9	11.8	11.8
39501	13.1	0.0	13.4	NA	12.8	NA	11.3	11.3
44290	12.2	10.4	12.4	10.7	11.8	9.9	11.3	11.3
28760	12.3	10.9	12.6	12.2	11.8	11.1	10.2	10.2

Note that for each bridge under each type of dual-lane load, equivalent widths were calculated for the positive and negative moment regions as shown in Table 3.24.

For comparison purposes, the ratios of equivalent widths for the slab bridges determined from the FE models to those determined using the LRFD equations were calculated and are summarized in Table 3.25.

Table 3.25 Ratios of equivalent widths of slab bridges using LRFD equations to those derived from FE models

Structure Number	FEA/LRFD (6-4-6)		FEA/LRFD (6-5-6)		FEA/LRFD (5-5-5)	
	Positive Moment	Negative Moment	Positive Moment	Negative Moment	Positive Moment	Negative Moment
15280	1.17	NA	1.20	NA	1.14	NA
46391	1.14	0.94	1.16	0.97	1.11	0.90
36210	1.12	1.08	1.15	1.12	1.08	1.04
53360	1.09	0.94	1.11	0.97	1.06	0.89
28670	1.11	1.00	1.15	1.03	1.07	0.95
14070	1.31	1.23	1.35	1.28	1.26	1.17
26780	1.16	1.08	1.19	1.11	1.12	1.03
36541	1.10	0.93	1.13	0.96	1.07	0.88
605755	1.10	0.94	1.13	0.97	1.07	0.90
23710	1.11	0.93	1.14	0.96	1.07	0.89
39441	1.11	0.00	1.14	NA	1.08	NA
49980	1.14	0.98	1.16	1.01	1.11	0.93
26860	1.18	0.00	1.21	NA	1.13	NA
29571	1.12	1.01	1.15	1.04	1.07	0.95
14371	1.14	0.96	1.16	0.98	1.11	0.91
608740	1.11	0.95	1.14	0.98	1.07	0.90
17990	1.05	0.87	1.08	0.90	1.02	0.84
39501	1.16	0.00	1.18	NA	1.13	NA
44290	1.07	0.91	1.10	0.94	1.04	0.87
28760	1.20	1.07	1.23	1.19	1.15	1.08

Two bridge parameters related to the AASHTO LRFD equations for calculating LDFs are modified span length and modified deck width. The relationships between the ratios of equivalent widths and the two parameters for the positive moment regions and negative moment regions of the slab bridges are illustrated in Figure 3.22 and Figure 3.23, respectively.

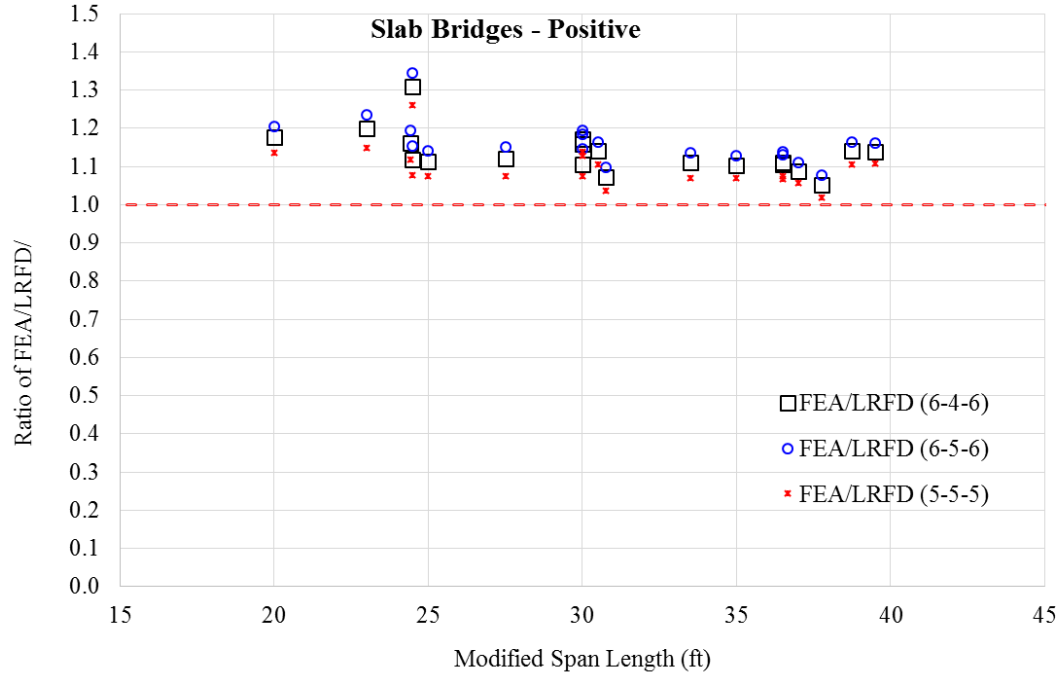

(a) Modified span length

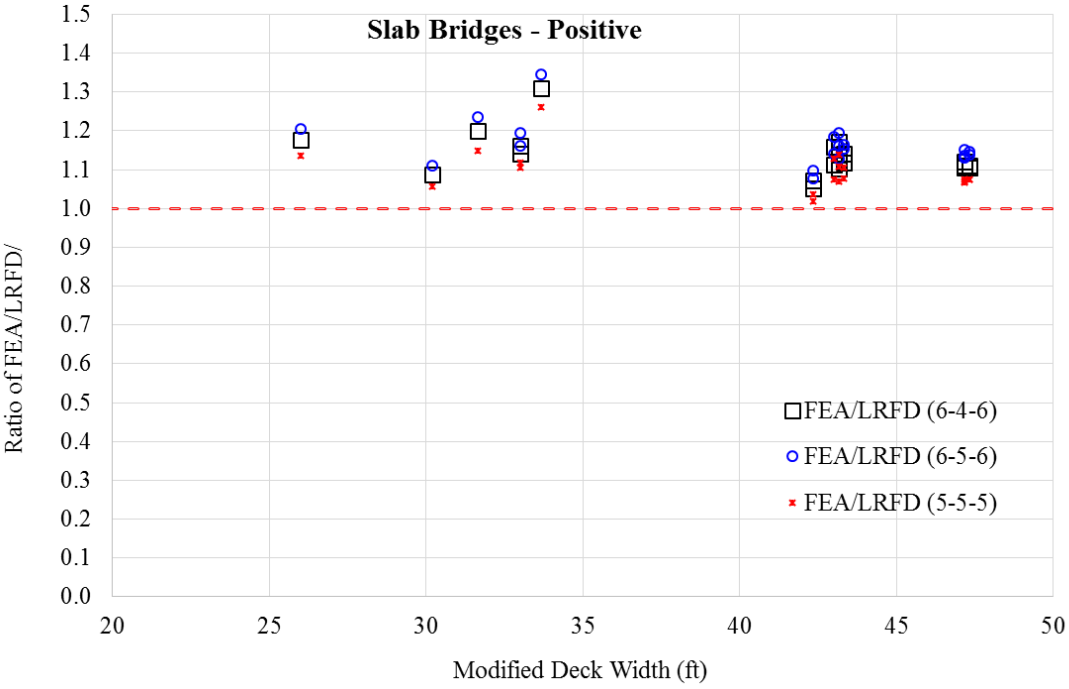

(b) Modified deck width

Figure 3.22 Relationships between the ratios of equivalent widths and bridge parameters for slab bridges – positive moment regions

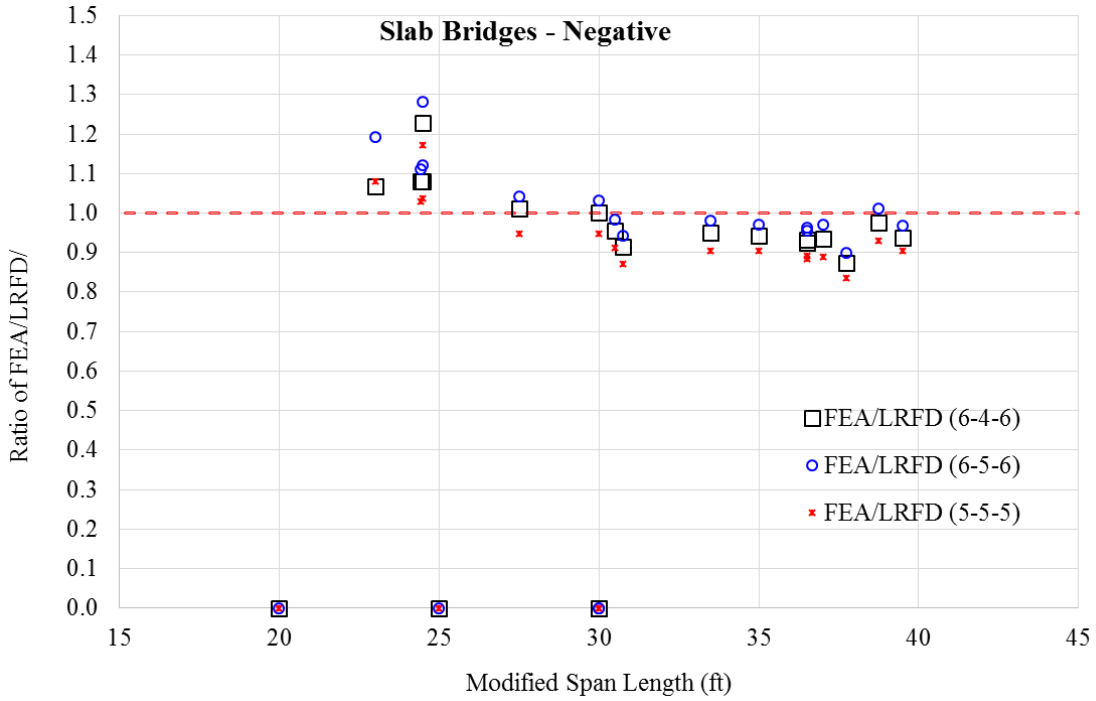

(a) Modified span length

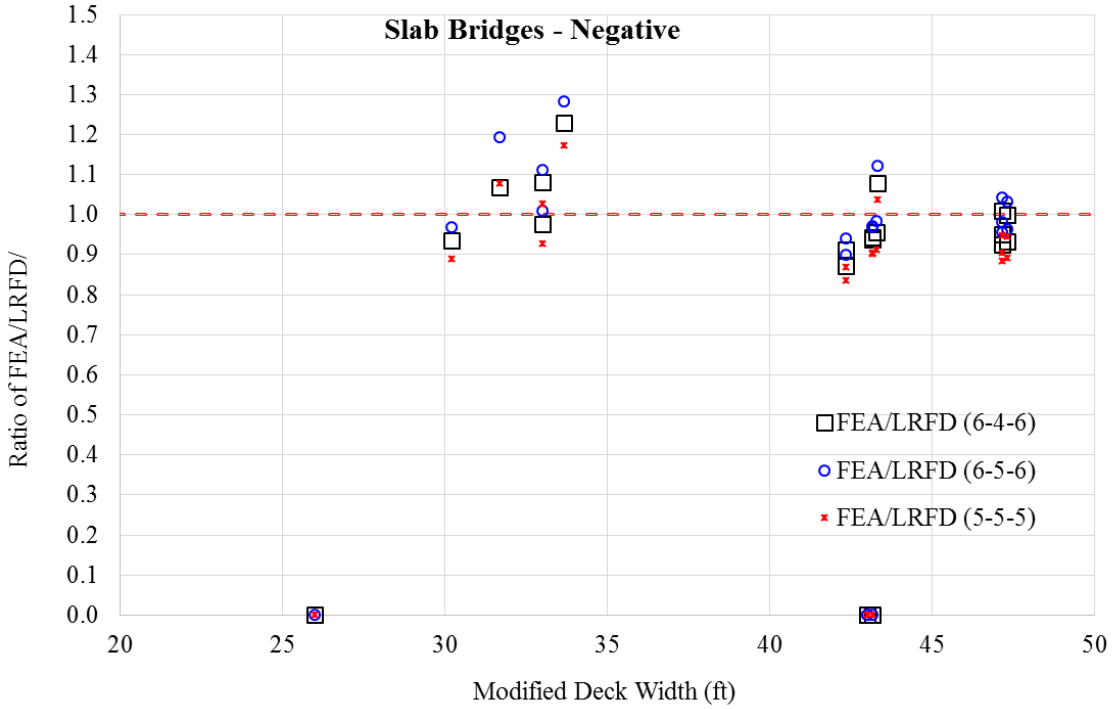

(b) Modified deck width

Figure 3.23 Relationships between the ratios of equivalent widths and bridge parameters for slab bridges – negative moment regions

Figure 3.22 indicates that the LRFD equations slightly overestimate the equivalent width in the positive moment region and that the ratios of the equivalent widths range from 1.0 to 1.35. Figure 3.23 indicates that the LRFD equations slightly underestimate the equivalent width in the negative moment region and that the ratios of the equivalent widths range from 0.8 to 1.0.

No significant relationships between the important bridge parameters and the ratios of equivalent widths were found. As shown in both Figure 3.22 and Figure 3.23, the equivalent widths predicted using the LRFD equations are less conservative when the modified span length is longer than 30 ft.

However, in general, the results associated with Truck-5-5 and Truck-6-5 compare well with those associated with Truck-6-4 and those predicted using the FE models; and, the results associated with Truck-6-5 are the lower bound of the equivalent widths among all of the types of dual-lane loads.

3.5 Axle Weight Limits for Different Dual-Lane Loads

As concluded from previous sections, the Iowa DOT current practice of the moment and shear LDFs and the equivalent widths associated with Truck-5-5 and Truck-6-5 appear adequate, based on the comparisons against the results associated with Truck-6-4 using the AASHTO equations. The so-called five-foot requirement specifies that dual-lane trucks with greater than five-foot interior-wheel-line spacing are allowed to have an axle weight up to 20 kips per lane. For practical needs, it is also desirable to know the allowable axle weights for other truck types to complement the current Iowa DOT policy.

The moment and shear LDFs and the equivalent widths for different truck types were calculated for the bridges investigated. From design and rating perspectives, a higher moment LDF, a higher shear LDF, or a lower equivalent width due to a dual-lane load should result in a lower allowable axle weight for the dual-lane load. As mentioned previously, the results associated with Truck-6-5 were, based on the FE results, the lower bound of the moment and shear LDFs and the equivalent widths. Accordingly, Truck-6-5 was selected as the baseline and assumed to have an axle weight of 20 kips per lane. To determine the axle weight limits for other truck types, the ratios of moment and shear LDFs of Truck-6-5 to those of other truck types and the ratios of equivalent lengths of other truck types to those of Truck-6-5 were calculated. For instance, for the 20 steel girder bridges, the ratios associated with Truck-6-4 and Truck-5-5 were calculated and are shown in Table 3.26.

Table 3.26 Ratios of moment LDFs associated to Truck-6-5 to those associated with Truck-6-4 and Truck-5-5 derived from FE models

Structure Number	Number of Girders	Ratio FEA (6-5-6/6-4-6)				Ratio FEA (6-5-6/5-5-5)			
		Exterior Positive	Exterior Negative	Interior Positive	Interior Negative	Exterior Positive	Exterior Negative	Interior Positive	Interior Negative
22520	4	0.97	0.94	0.96	0.96	0.91	0.90	0.94	0.94
16220	4	0.98	0.98	0.94	0.94	0.92	0.91	0.93	0.92
46730	4	0.97	0.94	0.96	0.94	0.91	0.89	0.94	0.93
46750	4	0.96	0.96	0.95	0.96	0.91	0.90	0.94	0.94
37570	4	0.97	0.96	0.96	0.94	0.92	0.91	0.95	0.92
25140	4	0.97	0.96	0.95	0.95	0.91	0.90	0.93	0.93
29110	4	0.98	0.98	0.94	0.94	0.92	0.91	0.94	0.92
15750	4	0.96	0.96	0.95	0.96	0.91	0.90	0.94	0.94
43370	4	0.97	NA	0.95	NA	0.91	NA	0.94	NA
50910	4	0.97	0.95	0.96	0.98	0.92	0.91	0.95	0.96
43880	4	0.97	0.97	0.95	0.95	0.92	0.91	0.93	0.93
606320	5	0.97	0.97	0.96	0.94	0.93	0.93	0.95	0.93
50995	5	0.97	0.96	0.96	0.96	0.93	0.93	0.95	0.95
22930	5	0.97	0.96	0.97	0.94	0.93	0.92	0.95	0.93
364700	6	0.97	0.96	0.97	0.98	0.93	0.92	0.97	0.98
19011	6	0.97	0.96	0.96	0.97	0.93	0.92	0.95	0.95
40521	7	0.97	0.96	0.96	0.98	0.93	0.92	0.96	0.97
13330	7	0.97	NA	0.93	NA	0.92	NA	0.94	NA
601356	8	0.97	0.97	0.95	0.97	0.92	0.92	0.95	0.97
609280	8	0.97	0.96	0.96	0.98	0.93	0.92	0.95	0.97
Mean		0.97	0.96	0.95	0.96	0.92	0.91	0.95	0.94
Std. Dev		0.00	0.01	0.01	0.02	0.01	0.01	0.01	0.02
Minimum		0.96	0.94	0.93	0.94	0.91	0.89	0.93	0.92
Maximum		0.98	0.98	0.97	0.98	0.93	0.93	0.97	0.98

Figure 3.24 also shows the relationships of moment LDF ratios associated with Truck-6-4 and Truck-5-5 and bridge parameters.

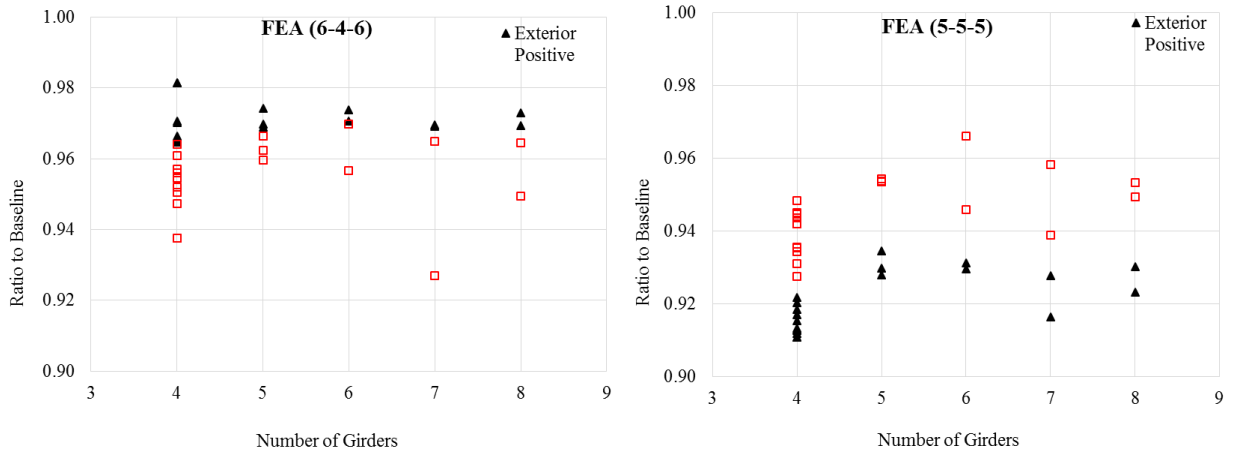

(a) Number of girders

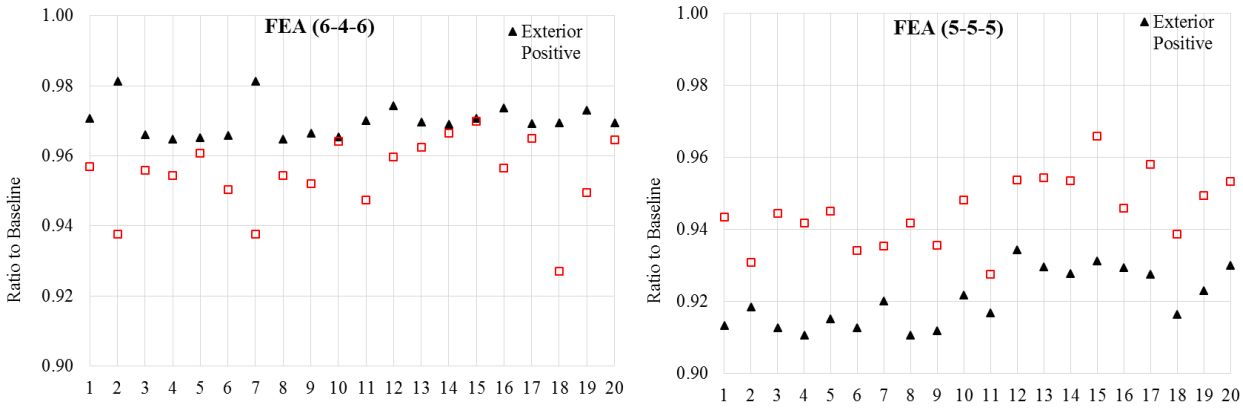

(b) Bridge

Figure 3.24 Relationships of moment LDF ratios associated with Truck-6-4 and Truck-5-5 and bridge parameters

It is indicated from Table 3.26 that the moment LDF ratios slightly vary along with the number of girders and different bridges.

To further investigate the variability, several statistical parameters including mean, standard deviation, maximum value, and minimum moment LDF ratios for the 20 steel bridges were calculated for each dual-lane load as shown in Table 3.27.

Table 3.27 Ratios of moment LDFs to baseline 6-5-6 and recommended axle weight limits for steel bridges

Dual-Lane Load Type	Ratio to Baseline 6-5-6								
	Girder Type	Region	Mean	Standard Deviation	Maximum	Minimum	Maximum in Girder Type	Recommended	Recommended Weight Limit per Lane (kips)
3-3-3	Interior	Positive	0.61	0.09	0.74	0.45	0.45	0.45	9.0
		Negative	0.61	0.09	0.75	0.50			
	Exterior	Positive	0.82	0.08	0.96	0.66	0.66		
		Negative	0.83	0.09	0.97	0.67			
4-2-4	Interior	Positive	0.74	0.02	0.78	0.71	0.69	0.69	13.8
		Negative	0.72	0.03	0.78	0.69			
	Exterior	Positive	0.82	0.06	0.95	0.72	0.70		
		Negative	0.82	0.06	0.95	0.70			
4-2.5-4	Interior	Positive	0.76	0.02	0.79	0.73	0.70	0.70	13.9
		Negative	0.74	0.03	0.79	0.70			
	Exterior	Positive	0.83	0.06	0.94	0.74	0.71		
		Negative	0.83	0.07	0.97	0.71			
4-3-4	Interior	Positive	0.78	0.02	0.81	0.75	0.72	0.72	14.3
		Negative	0.76	0.03	0.80	0.72			
	Exterior	Positive	0.84	0.05	0.94	0.76	0.73		
		Negative	0.84	0.06	0.97	0.73			
4-3.5-4	Interior	Positive	0.79	0.02	0.82	0.77	0.73	0.73	14.7
		Negative	0.78	0.03	0.82	0.73			
	Exterior	Positive	0.85	0.04	0.95	0.78	0.75		
		Negative	0.86	0.06	0.97	0.75			
4-4-4	Interior	Positive	0.81	0.02	0.84	0.79	0.75	0.75	15.1
		Negative	0.79	0.02	0.83	0.75			
	Exterior	Positive	0.86	0.04	0.95	0.80	0.77		
		Negative	0.87	0.05	0.97	0.77			
4-4.5-4	Interior	Positive	0.83	0.02	0.85	0.81	0.77	0.77	15.5
		Negative	0.81	0.02	0.85	0.77			
	Exterior	Positive	0.88	0.03	0.95	0.83	0.79		
		Negative	0.89	0.04	0.97	0.79			
4-5-4	Interior	Positive	0.84	0.02	0.87	0.82	0.79	0.79	15.9
		Negative	0.83	0.02	0.86	0.79			
	Exterior	Positive	0.90	0.03	0.95	0.85	0.85		
		Negative	0.90	0.03	0.97	0.85			
5-2-5	Interior	Positive	0.82	0.02	0.87	0.80	0.76	0.76	15.2
		Negative	0.80	0.02	0.84	0.76			
	Exterior	Positive	0.85	0.04	0.94	0.77	0.75		
		Negative	0.85	0.06	0.96	0.75			
5-2.5-5	Interior	Positive	0.84	0.02	0.89	0.82	0.78	0.78	15.6
		Negative	0.82	0.02	0.85	0.78			
	Exterior	Positive	0.86	0.04	0.94	0.80	0.77		
		Negative	0.87	0.05	0.96	0.77			
5-3-5	Interior	Positive	0.86	0.02	0.91	0.84	0.80	0.80	16.0
		Negative	0.84	0.02	0.87	0.80			
	Exterior	Positive	0.87	0.03	0.94	0.82	0.79		
		Negative	0.88	0.04	0.96	0.79			

Dual-Lane Load Type	Ratio to Baseline 6-5-6								
	Girder Type	Region	Mean	Standard Deviation	Maximum	Minimum	Maximum in Girder Type	Recommended	Recommended Weight Limit per Lane (kips)
5-3.5-5	Interior	Positive	0.87	0.01	0.89	0.86	0.82	0.82	16.4
		Negative	0.86	0.02	0.88	0.82			
	Exterior	Positive	0.89	0.03	0.95	0.84	0.84		
		Negative	0.89	0.03	0.96	0.84			
5-4-5	Interior	Positive	0.89	0.01	0.90	0.87	0.84	0.84	16.8
		Negative	0.87	0.02	0.90	0.84			
	Exterior	Positive	0.91	0.02	0.95	0.87	0.87		
		Negative	0.91	0.03	0.97	0.87			
5-4.5-5	Interior	Positive	0.91	0.01	0.92	0.89	0.86	0.86	17.3
		Negative	0.89	0.01	0.91	0.86			
	Exterior	Positive	0.92	0.02	0.96	0.90	0.89		
		Negative	0.92	0.02	0.97	0.89			
5-5-5	Interior	Positive	0.92	0.01	0.93	0.91	0.89	0.89	17.7
		Negative	0.91	0.01	0.93	0.89			
	Exterior	Positive	0.95	0.01	0.97	0.93	0.92		
		Negative	0.94	0.02	0.98	0.92			
6-2-6	Interior	Positive	0.90	0.02	0.97	0.89	0.85	0.85	17.0
		Negative	0.88	0.02	0.90	0.85			
	Exterior	Positive	0.89	0.03	0.94	0.83	0.83		
		Negative	0.90	0.03	0.96	0.84			
6-2.5-6	Interior	Positive	0.92	0.01	0.94	0.91	0.87	0.87	17.4
		Negative	0.90	0.01	0.92	0.87			
	Exterior	Positive	0.90	0.02	0.95	0.86	0.86		
		Negative	0.91	0.03	0.96	0.86			
6-3-6	Interior	Positive	0.94	0.01	0.96	0.93	0.90	0.90	17.9
		Negative	0.92	0.01	0.94	0.90			
	Exterior	Positive	0.92	0.02	0.96	0.88	0.88		
		Negative	0.92	0.02	0.97	0.89			
6-3.5-6	Interior	Positive	0.95	0.01	0.97	0.95	0.92	0.92	18.4
		Negative	0.94	0.01	0.96	0.92			
	Exterior	Positive	0.93	0.02	0.96	0.90	0.90		
		Negative	0.94	0.02	0.98	0.91			
6-4-6	Interior	Positive	0.97	0.00	0.98	0.96	0.94	0.94	18.8
		Negative	0.96	0.01	0.98	0.94			
	Exterior	Positive	0.95	0.01	0.97	0.93	0.93		
		Negative	0.96	0.02	0.98	0.94			
6-4.5-6	Interior	Positive	0.99	0.00	0.99	0.98	0.96	0.96	19.2
		Negative	0.98	0.01	0.99	0.96			
	Exterior	Positive	0.98	0.01	0.98	0.96	0.95		
		Negative	0.98	0.01	0.99	0.95			

The minimum values for the interior and exterior girders were also determined based on the smaller values of negative and positive moment regions shown in Table 3.27. Then, recommended moment LDF ratios were determined based on the minimum values for interior girders due to the fact that the interior girders commonly control designs and the exterior girders are commonly designed using the same cross-sections as the interior girders. Then, the

recommended axle weight limits were determined by the baseline axle weight limit of 20 kips multiplied by the recommended moment LDF ratios shown in Table 3.27.

Following the same procedure, the shear LDF ratios and recommended axle weight limits for the steel bridges, the moment LDF ratios and recommended axle weight limits for the concrete bridges, and the equivalent width ratios and recommended axle weight limits for the slab bridges were determined as summarized in Table 3.28, Table 3.29, and Table 3.30, respectively.

Table 3.28 Ratios of shear LDFs to baseline 6-5-6 and recommended axle weight limits for steel bridges

Dual-Lane Load Type	Ratio to Baseline 6-5-6						
	Girder Type	Mean	Standard Deviation	Maximum	Minimum	Maximum in Girder Type	Recommended Axle Weight Limit per Lane (kips)
3-3-3	Exterior	0.56	0.08	0.68	0.43	0.58	11.7
	Interior	0.67	0.09	0.91	0.58		
4-2-4	Exterior	0.70	0.02	0.74	0.65	0.61	12.1
	Interior	0.69	0.07	0.88	0.61		
4-2.5-4	Exterior	0.72	0.03	0.77	0.67	0.63	12.7
	Interior	0.71	0.07	0.89	0.63		
4-3-4	Exterior	0.74	0.03	0.79	0.69	0.65	13.0
	Interior	0.72	0.06	0.89	0.65		
4-3.5-4	Exterior	0.77	0.02	0.81	0.72	0.68	13.7
	Interior	0.74	0.05	0.89	0.68		
4-4-4	Exterior	0.78	0.02	0.82	0.74	0.73	14.6
	Interior	0.77	0.04	0.90	0.73		
4-4.5-4	Exterior	0.80	0.02	0.84	0.76	0.76	15.3
	Interior	0.79	0.03	0.90	0.76		
4-5-4	Exterior	0.82	0.02	0.85	0.78	0.80	15.9
	Interior	0.83	0.03	0.91	0.80		
5-2-5	Exterior	0.79	0.03	0.86	0.72	0.67	13.5
	Interior	0.74	0.05	0.87	0.67		
5-2.5-5	Exterior	0.81	0.04	0.88	0.74	0.70	14.1
	Interior	0.76	0.05	0.88	0.70		
5-3-5	Exterior	0.83	0.03	0.89	0.78	0.74	14.7
	Interior	0.78	0.04	0.88	0.74		
5-3.5-5	Exterior	0.85	0.03	0.91	0.81	0.78	15.5
	Interior	0.81	0.03	0.89	0.78		
5-4-5	Exterior	0.87	0.02	0.91	0.84	0.81	16.2
	Interior	0.84	0.02	0.90	0.81		
5-4.5-5	Exterior	0.89	0.02	0.92	0.86	0.86	17.1
	Interior	0.87	0.01	0.92	0.86		
5-5-5	Exterior	0.91	0.01	0.94	0.87	0.89	17.9
	Interior	0.91	0.01	0.93	0.89		
6-2-6	Exterior	0.88	0.04	0.95	0.81	0.73	14.5
	Interior	0.80	0.04	0.88	0.73		
6-2.5-6	Exterior	0.90	0.03	0.97	0.85	0.76	15.3
	Interior	0.82	0.03	0.89	0.76		
6-3-6	Exterior	0.92	0.03	0.98	0.88	0.79	15.9
	Interior	0.85	0.02	0.91	0.79		
6-3.5-6	Exterior	0.94	0.03	1.00	0.90	0.82	16.4
	Interior	0.88	0.02	0.92	0.82		
6-4-6	Exterior	0.96	0.02	1.01	0.93	0.87	17.4
	Interior	0.92	0.01	0.93	0.87		
6-4.5-6	Exterior	0.98	0.02	1.00	0.95	0.93	18.7
	Interior	0.96	0.01	0.96	0.93		

Table 3.29 Ratios of moment LDFs to baseline 6-5-6 and recommended axle weight limits for concrete bridges

Dual-Lane Load Type	Ratio to Baseline 6-5-6								
	Girder Type	Region	Mean	Standard Deviation	Maximum	Minimum	Minimum in Girder Type	Recommended	Recommended Axle Weight Limit per Lane (kips)
3-3-3	Exterior	Positive	0.56	0.10	0.65	0.32	0.30	0.57	11.4
		Negative	0.54	0.10	0.64	0.30			
	Interior	Positive	0.70	0.08	0.91	0.60	0.57		
		Negative	0.71	0.08	0.92	0.57			
4-2-4	Exterior	Positive	0.73	0.02	0.80	0.70	0.68	0.61	12.1
		Negative	0.71	0.03	0.79	0.68			
	Interior	Positive	0.71	0.06	0.85	0.63	0.61		
		Negative	0.72	0.06	0.86	0.61			
4-2.5-4	Exterior	Positive	0.75	0.02	0.82	0.72	0.71	0.63	12.7
		Negative	0.73	0.04	0.88	0.71			
	Interior	Positive	0.73	0.05	0.85	0.65	0.63		
		Negative	0.74	0.06	0.86	0.63			
4-3-4	Exterior	Positive	0.77	0.02	0.83	0.74	0.73	0.66	13.3
		Negative	0.75	0.04	0.89	0.73			
	Interior	Positive	0.75	0.05	0.85	0.67	0.66		
		Negative	0.76	0.05	0.86	0.66			
4-3.5-4	Exterior	Positive	0.78	0.02	0.85	0.76	0.75	0.70	14.0
		Negative	0.77	0.04	0.89	0.75			
	Interior	Positive	0.77	0.04	0.85	0.71	0.70		
		Negative	0.78	0.04	0.86	0.70			
4-4-4	Exterior	Positive	0.80	0.02	0.86	0.79	0.77	0.74	14.7
		Negative	0.79	0.03	0.89	0.77			
	Interior	Positive	0.80	0.03	0.86	0.74	0.74		
		Negative	0.81	0.03	0.87	0.74			
4-4.5-4	Exterior	Positive	0.82	0.02	0.87	0.80	0.78	0.77	15.4
		Negative	0.81	0.03	0.89	0.78			
	Interior	Positive	0.83	0.03	0.87	0.77	0.77		
		Negative	0.83	0.03	0.88	0.78			
4-5-4	Exterior	Positive	0.83	0.01	0.87	0.82	0.80	0.81	16.2
		Negative	0.82	0.02	0.89	0.80			
	Interior	Positive	0.86	0.02	0.89	0.81	0.81		
		Negative	0.86	0.02	0.89	0.82			
5-2-5	Exterior	Positive	0.82	0.03	0.91	0.80	0.78	0.66	13.3
		Negative	0.81	0.05	0.97	0.78			
	Interior	Positive	0.76	0.05	0.84	0.67	0.66		
		Negative	0.77	0.05	0.85	0.66			
5-2.5-5	Exterior	Positive	0.84	0.03	0.92	0.82	0.80	0.69	13.9
		Negative	0.83	0.05	0.98	0.80			
	Interior	Positive	0.78	0.04	0.85	0.70	0.69		
		Negative	0.79	0.04	0.86	0.69			
5-3-5	Exterior	Positive	0.86	0.02	0.93	0.84	0.82	0.73	14.7
		Negative	0.85	0.04	0.97	0.82			
	Interior	Positive	0.81	0.04	0.86	0.74	0.73		
		Negative	0.82	0.04	0.87	0.73			

Dual-Lane Load Type	Ratio to Baseline 6-5-6								
	Girder Type	Region	Mean	Standard Deviation	Maximum	Minimum	Minimum in Girder Type	Recommended	Recommended Axle Weight Limit per Lane (kips)
5-3.5-5	Exterior	Positive	0.87	0.02	0.94	0.86	0.84	0.77	15.5
		Negative	0.87	0.04	0.97	0.84			
	Interior	Positive	0.83	0.03	0.88	0.78	0.77		
		Negative	0.84	0.03	0.88	0.77			
5-4-5	Exterior	Positive	0.89	0.02	0.94	0.88	0.86	0.82	16.4
		Negative	0.88	0.03	0.97	0.86			
	Interior	Positive	0.86	0.02	0.90	0.82	0.82		
		Negative	0.87	0.02	0.90	0.82			
5-4.5-5	Exterior	Positive	0.90	0.01	0.94	0.89	0.88	0.86	17.2
		Negative	0.90	0.02	0.97	0.88			
	Interior	Positive	0.90	0.02	0.92	0.86	0.86		
		Negative	0.90	0.01	0.92	0.87			
5-5-5	Exterior	Positive	0.92	0.01	0.94	0.90	0.90	0.90	18.1
		Negative	0.91	0.01	0.96	0.90			
	Interior	Positive	0.93	0.01	0.95	0.90	0.90		
		Negative	0.93	0.01	0.94	0.91			
6-2-6	Exterior	Positive	0.91	0.03	0.99	0.89	0.87	0.72	14.5
		Negative	0.91	0.05	1.04	0.87			
	Interior	Positive	0.81	0.04	0.87	0.72	0.72		
		Negative	0.83	0.04	0.88	0.73			
6-2.5-6	Exterior	Positive	0.93	0.02	1.00	0.92	0.89	0.76	15.3
		Negative	0.93	0.04	1.04	0.89			
	Interior	Positive	0.84	0.03	0.89	0.76	0.76		
		Negative	0.85	0.04	0.90	0.77			
6-3-6	Exterior	Positive	0.95	0.02	1.00	0.94	0.92	0.81	16.2
		Negative	0.94	0.03	1.03	0.92			
	Interior	Positive	0.86	0.03	0.91	0.81	0.81		
		Negative	0.88	0.03	0.91	0.81			
6-3.5-6	Exterior	Positive	0.96	0.01	1.00	0.95	0.94	0.85	17.1
		Negative	0.96	0.02	1.03	0.94			
	Interior	Positive	0.89	0.02	0.93	0.85	0.85		
		Negative	0.90	0.02	0.93	0.86			
6-4-6	Exterior	Positive	0.98	0.01	1.00	0.97	0.96	0.89	17.9
		Negative	0.97	0.02	1.02	0.96			
	Interior	Positive	0.93	0.02	0.95	0.89	0.89		
		Negative	0.94	0.02	0.96	0.90			
6-4.5-6	Exterior	Positive	0.99	0.00	1.00	0.98	0.98	0.95	18.9
		Negative	0.99	0.01	1.01	0.98			
	Interior	Positive	0.96	0.01	0.97	0.95	0.95		
		Negative	0.97	0.01	0.98	0.95			

Table 3.30 Ratios of equivalent lengths to baseline 6-5-6 and recommended axle weight limits for slab bridges

Dual-Lane Load Type	Ratio to Baseline 6-5-6						
	Region	Mean	Standard Deviation	Maximum	Minimum	Recommended	Reccomended Axle Weight Limit Per Lane (kips)
3-3-3	Positive	0.52	0.04	0.45	0.58	0.45	9.0
	Negative	0.40	0.04	0.31	0.45		
4-2-4	Positive	0.81	0.02	0.84	0.77	0.70	13.9
	Negative	0.73	0.01	0.75	0.70		
4-2.5-4	Positive	0.82	0.02	0.85	0.79	0.71	14.2
	Negative	0.75	0.02	0.79	0.71		
4-3-4	Positive	0.83	0.02	0.86	0.80	0.73	14.5
	Negative	0.77	0.02	0.80	0.73		
4-3.5-4	Positive	0.84	0.02	0.87	0.82	0.74	14.9
	Negative	0.79	0.02	0.82	0.74		
4-4-4	Positive	0.86	0.01	0.88	0.84	0.76	15.2
	Negative	0.80	0.02	0.83	0.76		
4-4.5-4	Positive	0.87	0.01	0.89	0.85	0.78	15.5
	Negative	0.82	0.02	0.85	0.78		
4-5-4	Positive	0.88	0.01	0.90	0.86	0.79	15.9
	Negative	0.84	0.02	0.86	0.79		
5-2-5	Positive	0.86	0.04	0.89	0.71	0.71	14.3
	Negative	0.81	0.01	0.84	0.77		
5-2.5-5	Positive	0.88	0.01	0.90	0.85	0.79	15.8
	Negative	0.83	0.01	0.85	0.79		
5-3-5	Positive	0.89	0.01	0.91	0.87	0.81	16.1
	Negative	0.85	0.02	0.87	0.81		
5-3.5-5	Positive	0.91	0.01	0.92	0.89	0.83	16.5
	Negative	0.87	0.01	0.89	0.83		
5-4-5	Positive	0.92	0.01	0.93	0.90	0.87	17.4
	Negative	0.89	0.01	0.90	0.87		
5-4.5-5	Positive	0.93	0.01	0.95	0.92	0.89	17.8
	Negative	0.91	0.01	0.92	0.89		
5-5-5	Positive	0.94	0.01	0.95	0.93	0.90	18.1
	Negative	0.92	0.01	0.93	0.90		
6-2-6	Positive	0.92	0.01	0.94	0.88	0.84	16.7
	Negative	0.89	0.02	0.91	0.84		
6-2.5-6	Positive	0.94	0.01	0.95	0.90	0.85	17.1
	Negative	0.91	0.02	0.92	0.85		
6-3-6	Positive	0.95	0.01	0.96	0.92	0.87	17.5
	Negative	0.93	0.02	0.94	0.87		
6-3.5-6	Positive	0.96	0.01	0.97	0.94	0.89	17.7
	Negative	0.95	0.02	0.96	0.89		
6-4-6	Positive	0.98	0.00	0.98	0.96	0.90	17.9
	Negative	0.96	0.02	0.97	0.90		
6-4.5-6	Positive	0.99	0.00	0.99	0.98	0.98	19.6
	Negative	0.98	0.00	0.99	0.98		

The final recommended axle weight limits for different bridge types and all bridge types are summarized in Table 3.31.

Table 3.31 Recommended axle weight limits for different types of bridges

Dual-Lane Load Type	Recommended Axle Weight Limit per Lane (kips)				
	Steel Bridges_Moment	Steel Bridges_Shear	Concrete Bridges	Slab Bridges	All Bridge Types
3-3-3	9.0	11.7	11.4	9.0	9.0
4-2-4	13.8	12.1	12.1	13.9	12.1
4-2.5-4	13.9	12.7	12.7	14.2	12.7
4-3-4	14.3	13.0	13.3	14.5	13.0
4-3.5-4	14.7	13.7	14.0	14.9	13.7
4-4-4	15.1	14.6	14.7	15.2	14.6
4-4.5-4	15.5	15.3	15.4	15.5	15.3
4-5-4	15.9	15.9	16.2	15.9	15.9
5-2-5	15.2	13.5	13.3	14.3	13.3
5-2.5-5	15.6	14.1	13.9	15.8	13.9
5-3-5	16.0	14.7	14.7	16.1	14.7
5-3.5-5	16.4	15.5	15.5	16.5	15.5
5-4-5	16.8	16.2	16.4	17.4	16.2
5-4.5-5	17.3	17.1	17.2	17.8	17.1
5-5-5	17.7	17.9	18.1	18.1	17.7
6-2-6	17.0	14.5	14.5	16.7	14.5
6-2.5-6	17.4	15.3	15.3	17.1	15.3
6-3-6	17.9	15.9	16.2	17.5	15.9
6-3.5-6	18.4	16.4	17.1	17.7	16.4
6-4-6	18.8	17.4	17.9	17.9	17.4
6-4.5-6	19.2	18.7	18.9	19.6	18.7
6-5-6	20.0	20.0	20.0	20.0	20.0

Note that the recommended axle weight limits for all bridge types were determined through selection of the smallest values of the investigated bridge types for each dual-lane load type. As indicated in Table 3.31, the smaller axle weight limit should be used for narrower wheel-line spacing.

CHAPTER 4 SUMMARY, CONCLUSIONS, AND RECOMMENDATIONS

4.1 Summary and Conclusions

The researchers randomly sampled 20 prestressed-concrete girder bridges, 20 steel girder bridges, and 20 slab bridges from the Iowa bridge database to study the lateral load distribution on bridges under variable wheel spacing for multiple dual-lane loadings. Two-dimensional linear elastic FE models of the selected bridges were established to determine the LDFs for the concrete and steel girder bridges and the equivalent deck widths for the slab bridges.

To study the variations of LDFs, 22 types of single-axle, four-wheel-line loads were considered. These load configurations consisted of combinations of the spacing between the interior wheel lines (2 ft, 2.5 ft, 3 ft, 3.5 ft, 4 ft, 4.5 ft, and 5 ft) and the spacing between the exterior wheel pairs (4, 5, and 6 ft). A special case also considered had 3 ft spacing between all four wheel lines.

To calculate moment and shear LDFs for both the steel and concrete girder bridges, the internal forces in the girders at critical cross-sections were extracted from the FE models. Moment LDFs were calculated at all applicable bridge cross-sections: (1) interior girders in the positive moment region, (2) interior girders in the negative moment region, (3) exterior girders in the positive moment region, and (4) exterior girders in the negative moment region. Shear LDFs were calculated for two regions: (1) interior girders and (2) exterior girders. Then, the largest value was taken as the LDF for each region. The equivalent widths of the slab bridges were calculated based on the strain distributions in the deck at critical bridge cross-sections in two regions: (1) the positive moment region and (2) the negative moment region. From the calculated results, the smallest value was taken as the equivalent width for each region.

Based on the FE results, the moment LDFs for the 20 steel girder bridges and 20 concrete girder bridges, the shear LDFs for the 20 steel bridges, and the equivalent widths for the 20 slab bridges were determined. For comparison purposes, the corresponding moment and shear LDFs and equivalent widths were also determined using the AASHTO equations.

To evaluate the adequacy of the Iowa DOT five-foot requirement, the LDFs and equivalent widths obtained using the FE models were compared with those using the AASHTO equations for all of the investigated bridges. Conclusions were as follows:

- The moment LDFs in the negative moment regions were almost the same as those in the positive moment regions for both exterior and interior girders of the steel and concrete girder bridges.

- The AASHTO LRFD and LFD equations sometimes overestimated and sometimes underestimated moment LDFs based on the FE results. For the interior girders of the concrete girder bridges, the LRFD equations provided good estimations of the moment LDFs and the LFD equations underestimated the moment LDFs. For the exterior girders of the concrete girder bridges, both the LRFD equations and the LFD equations overestimated the moment LDFs. For the interior girders of the steel girder bridges, the LRFD equations underestimated

the moment LDFs and the LFD equations overestimated the moment LDFs. For the exterior girders of the steel girder bridges, the LRFD equations underestimated the moment LDFs of the exterior girders and the LFD equations overestimated the moment LDFs.

- The AASHTO LRFD and LFD equations also either overestimated or underestimated shear LDFs based on the FE results. For interior girders of the steel girder bridges, both the LRFD equations and the LFD equations underestimated the shear LDFs. For the exterior girders of the steel bridges, both the LRFD and LFD equations overestimated the shear LDFs.

- The LRFD equations slightly overestimated the equivalent widths in the positive moment regions and slightly underestimated the equivalent widths in the negative moment regions.

- The LRFD equations gave more consistent predictions than the LFD equations. For the most part, no significant relationships were found between the important bridge parameters and the accuracy of AASHTO equations in the prediction of LDFs and equivalent widths, although some general trends were found. For instance, the LRFD equations were less conservative for both moment and shear LDFs when the number of girders was no more than five, and the equivalent widths predicted using LRFD equations were less conservative when the modified span length was longer than 30 ft.

- The Iowa DOT current practice on the moment and shear LDFs and equivalent widths for dual-lane loads is reasonable and adequate.

Based on the derived LDFs and equivalent lengths, the axle weight limits per lane for other dual-lane load types were further investigated and could be used to complement the current Iowa DOT policy. The axle weight limits per lane for different dual-lane load types were determined based on a baseline axle weight limit of 20 kips times the final LDF or equivalent length ratio. The final recommended axle weight limit for each dual-lane load type was also determined through selection of the lowest values for all of the investigated bridge types as shown in Table 4.1.

Table 4.1 Recommended axle weight limits for different types of bridges

Dual-Lane Load Type	Recommended Axle Weight Limit per Lane (kips)				
	Steel Bridges_Moment	Steel Bridges_Shear	Concrete Bridges	Slab Bridges	All Bridge Types
3-3-3	9.0	11.7	11.4	9.0	9.0
4-2-4	13.8	12.1	12.1	13.9	12.1
4-2.5-4	13.9	12.7	12.7	14.2	12.7
4-3-4	14.3	13.0	13.3	14.5	13.0
4-3.5-4	14.7	13.7	14.0	14.9	13.7
4-4-4	15.1	14.6	14.7	15.2	14.6
4-4.5-4	15.5	15.3	15.4	15.5	15.3
4-5-4	15.9	15.9	16.2	15.9	15.9
5-2-5	15.2	13.5	13.3	14.3	13.3
5-2.5-5	15.6	14.1	13.9	15.8	13.9
5-3-5	16.0	14.7	14.7	16.1	14.7
5-3.5-5	16.4	15.5	15.5	16.5	15.5
5-4-5	16.8	16.2	16.4	17.4	16.2
5-4.5-5	17.3	17.1	17.2	17.8	17.1
5-5-5	17.7	17.9	18.1	18.1	17.7
6-2-6	17.0	14.5	14.5	16.7	14.5
6-2.5-6	17.4	15.3	15.3	17.1	15.3
6-3-6	17.9	15.9	16.2	17.5	15.9
6-3.5-6	18.4	16.4	17.1	17.7	16.4
6-4-6	18.8	17.4	17.9	17.9	17.4
6-4.5-6	19.2	18.7	18.9	19.6	18.7
6-5-6	20.0	20.0	20.0	20.0	20.0

The research team found that a lighter axle weight limit should be used for dual-lane loads with narrower wheel-line spacing.

4.2 Future Work

The results from the FE simulations in this study indicate that the LDFs for the investigated four-girder steel and concrete bridges are underestimated using the AASHTO LRFD equations. For improvement purposes, future work can be focused on development of more accurate equations for estimating LDFs for four-girder steel and concrete bridges.

REFERENCES

AASHTO LRFD. 2010. *AASHTO LRFD Bridge Design Specifications, Customary U.S. Units.* 5th Edition, with 2010 Interim Revisions. American Association of State Highway and Transportation Officials, Washington, DC.

AASHTO LFD. 1996. *AASHTO Standard Specifications for Highway Bridges.* American Association of State Highway and Transportation Officials, Washington, DC.

Bae, H. U. and M. G. Oliva. 2011. Moment and shear load distribution factors for multigirder bridges subjected to overloads. *Journal of Bridge Engineering*. *17*(3), 519-527.

Deng, Y. and B. Phares. 2016. Automated Load Rating Determination of Continuous Steel I-Girder Bridges using Ambient Traffic. *Engineering Structures*. 117, 101-117.

Goodrich, B. and J. Puckett. 2000.Simplified load distribution for vehicles with nonstandard axle gauges. *Transportation Research Record: Journal of the Transportation Research Board.* No. 1696, 158-170.

Jones, B. P. and H. W. Shenton. 2012. *Effective Width of Concrete Slab Bridges in Delaware*. Delaware Center for Transportation, University of Delaware, Newark, DE.

Mabsout, M., K. Tarhini, R. Jabakhanji, and E. Awwad. 2004. Wheel Load Distribution in Simply Supported Concrete Slab Bridges. *Journal of Bridge Engineering*. 9(2), 147-155.

Tabsh, S. W., and Tabatabai, M. 2001. Live Load Distribution in Girder Bridges Subject to Oversized Trucks. *Journal of Bridge Engineering*. 6(1), 9-16.